UNIVERSITA' DEGLI STUDI DI VERONA

DIPARTIMENTO DI
Medicina

SCUOLA DI DOTTORATO DI
Scienze della Vita e della Salute

DOTTORATO DI RICERCA IN
Medicina Biomolecolare

Con il contributo di Centro di Riferimento Oncologico di Aviano

CICLO XXX /2014-2017

LONG NON-CODING RNAs IN CANCER

S.S.D. BIO/10

Coordinatore: Prof.ssa Lucia De Fransceschi

Firma _____

Tutor: Prof.ssa Marta Palmieri

Firma _____

Prof. Massimo Donadelli

Firma _____

Dr. Riccardo Spizzo

Firma _____

Dr.ssa Milena Sabrina Nicoloso

Firma _____

Dottorando: Dott.ssa Michela Coan

Firma _____

Table of Contents

Sommario

Mutazioni somatiche nel gene *TP53* si verificano in più del 50% di tutti i tumori umani, tra questi, il carcinoma ovarico sieroso di alto grado (HGSOC) e il carcinoma mammario basale (BC) sono tra i tumori più frequentemente mutati. Le mutazioni di *TP53* sono prevalentemente di tipo missenso, cioè codificano per forme mutate della proteina p53, causando sia una perdita della funzione *wild-type* di p53 (wt_p53) che un guadagno di caratteristiche pro-tumorigeniche al mutante p53 (mut_p53), la cosiddetta *gain of function* (GOF). Diversi studi hanno dimostrato che la GOF di mut_p53 promuove l'invasività e la metastasi del tumore. Tuttavia, i meccanismi molecolari sottostanti non sono stati completamente caratterizzati. Gli RNA non codificanti, in particolare i lncRNA (*long non-coding RNA*), sono attori centrali della regolazione genica, inclusa la via di *wt_p53*, ma fino ad oggi non ci sono studi che indaghino il ruolo degli lncRNA nel fenotipo pro-invasivo di mut_p53. Pertanto, l'obiettivo di questa Tesi di dottorato è indagare, nei modelli cellulari HGSOC e BC, se i lncRNA abbiano un ruolo nellla GOF di mut_p53.

A questo scopo, abbiamo valutato i cambiamenti fenotipici utilizzando saggi di invasività *in vitro* (*mesothelial clearance* e *3D colony assay*) nelle linee cellulari HGSOC e BC silenziate per *TP53*. Per delineare l'espressione dei lncRNA nelle cellule silenziate per *TP53*, abbiamo utilizzato un'analisi di sequenziamento dell'RNA di lunghi RNA nucleari. Successivamente, abbiamo convalidato i risultati dell'analisi di *deep-sequencing* in modelli cellulari mut_p53 e wt_p53.

Abbiamo osservato che mut_p53 migliora la capacità delle cellule di HGSOC di invadere il peritoneo e delle cellule di BC basale di invadere la matrice extracellulare. Dall'analisi dei dati di *deep-sequencing* delle cellule silenziate per *TP53*, abbiamo individuato 806 e 1820 lncRNA differenzialmente espressi nelle linee cellulari BC e HGSOC, rispettivamente. Usando la tecnica qRT-PCR, abbiamo studiato i 10 geni più differenzialmente espressi sia nelle linee cellulari mut_p53 che wt_p53.

Per riassumere, abbiamo osservato che mut_p53 ha un ruolo nel fenotipo metastatico sia nel HGSOC che nel BC e abbiamo identificato alcuni lncRNA (ad esempio *LINC00704*) che potrebbero essere responsabili di questo effetto. Tra i nostri obiettivi futuri c'è quello di attivare o reprimere l'espressione di questi geni candidati e valutarne l'impatto sulla biologia delle cellule tumorali.

Abstract

Somatic mutations in *TP53* gene occur in more than 50% of all human cancers, being of high grade serous ovarian carcinoma (HGSOC) and basal breast cancer (BC) among the most frequently mutated cancers. *TP53* mutations are predominantly missense, thus encoding for mutated forms of p53 protein that cause both a loss of wild-type p53 (wt_p53) function and a gain of pro-tumorigenic features to mutant p53 (mut_p53), so called gain of function (GOF). Several studies demonstrated that mut_p53 GOF promotes tumor invasiveness and metastasis. However, the molecular mechanisms underneath are not fully characterized. Non-coding RNAs, particularly lncRNAs (long non-coding RNAs), are central players of gene regulation including wt_p53 pathway, but up today there are not reports that investigate the role of lncRNAs in the pro-invasive phenotype of mut_p53. Therefore, to better understand the mechanism of mut_p53 oncogenic functions, in this PhD thesis, we aim to investigate whether lncRNAs participate to mut_p53 gain of function, precisely in HGSOC and BC cell models.

To do this, we evaluated changes in *in vitro* invasiveness assays (mesothelial clearance and 3D colony assay) in *TP53*_silenced HGSOC and BC cell lines. To profile the expression of lncRNAs in *TP53*_silenced cells, we used a RNA deep-sequencing analysis of nuclear long RNAs. Next, we validated deep-sequencing results in mut_p53 and wt_p53 cell models.

We observed that mut_p53 enhances the ability of HGSOC to invade the peritoneum and of basal BC cells to invade extracellular matrix. From NGS data analysis of *TP53*_silenced cells, we discovered 806 and 1820 lncRNAs differentially expressed in BC and HGSOC cell lines, respectively. Using qRT-PCR, we investigated the 10 gene most differentially expressed both in mut_p53 and wt_p53 cell lines.

To sum up, we report a role of mut_p53 both in HGSOC and BC metastatic phenotype, and we identify some lncRNAs (e.g. *LINC00704*) which could be accountable of this effect. Our future plan is to activate or repress the expression of these candidate genes and evaluate the impact on tumor cell biology.

List of abbreviations

BC: breast cancer
CBP: CREB-binding protein
CK: cytokeratin
CTC: circulating tumor cell
CTD: C-terminal domain
DBD: DNA-binding domain
DCIS: ductal carcinoma *in situ*
DTC: disseminated tumor cell
DNE: dominant negative effect
ECM: extracellular matrix
EMT: epithelial-to-mesenchymal transition
EOC: Epithelial Ovarian Cancer
ER: estrogen receptor
GOF: gain of function
GWAS: genome-wide association studies
HGSOC: high grade serous ovarian cancer
HOX: homeobox transcription factors
IDC: infiltrating ductal carcinoma
LCIS: lobular carcinoma *in situ*
LGSOC: low grade serous ovarian cancer
lincRNA: long intergenic non-coding RNA
lncRNA: long non-coding RNA
miRNA: micro-RNA
mut_p53: mutant p53
ncRNA: non-coding RNA
NES: nuclear export signal
NGS: next generation sequencing
NLS: nuclear localization signal
nt: nucleotides
OvCa: ovarian cancer
OD: oligomerization domain
PRC1/2: Polycomb repressive complex 1/2
piRNA: piwo-interacting RNA
piRISC: piRNA-induced silencing complex
PR: progesterone receptor
pri-miRNA: primary miRNA
PRR: proline-rich region
RE: response element
RISC: RNA-induced silencing complex
rRNA: ribosomal RNA
shRNA: short hairpin RNA

siRNA: small interfering RNA
snRNA: small nuclear RNA
snoRNA: small nucleolar RNA
SNP: single nucleotide polymorphism
STIC: serous tubal intraepithelial carcinoma
TAD: transactivation domain
TAF: TBP-associated factor
TBP: TATA-binding protein
TE: transposon element
TF: transcription factor
tRNA: transfer RNA
WB: Western blotting
wt_p53: wild-type p53

1. Introduction

1.1. TP53

TP53 gene, the so-called "guardian of the genome" [1], encodes for a tumor suppressor transcription factor that is activated in response to stress stimuli and governs an anti-proliferative and pro-apoptotic transcriptional program [2,3]. When *TP53* was discovered in 1979 [4,5], it was described as an oncogene, based on the evidences that p53 was frequently overexpressed in cancers and, when ectopically expressed in primary cells, induced cellular immortalization and transformation. It was later discovered that the *TP53* gene first cloned was the mutant form, which contained a missense mutation; whereas, the wild type form of *TP53* behaved like a tumor suppressor gene showing opposite effects compared to the mutant one [6].

1.1.1. The structure

p53 is a 393 amino acids nuclear phosphoprotein with a complex structure that consists of five modular domains (Figure 1) [7,8]:

- two N-terminal transactivation domains (TAD) (amino acids 1-62),
- a conserved proline-rich region (PRR) (amino acids 63-94),
- a central DNA-binding domain (DBD) (amino acids 94-292),
- an oligomerization domain (OD) (amino acids 325-356), which is included in
- a C-terminal domain (CTD) (amino acids 311-393).

The TADs are fundamental for p53 function because they interact with the components of the transcription machinery, (i.e. TATA-binding protein - TBP and the TBP-associated factors - TAFs) [9–13], and with the acetyltransferases (i.e. p300 and the CREB-binding protein - CBP) that eventually acetylate the CTD of p53 and regulate its function [14–16]. However, TADs bind also negative regulators (e.g. Mdm2 and Mdmx) proteins that induce p53 degradation through the ubiquitin-dependent proteasome pathway [17–19].

The PRR consists of five PXXP repeats (P is proline and X any amino acid), its function is still not completely understood, but it seems to have a negative regulatory role on p53 DNA binding activity [20].

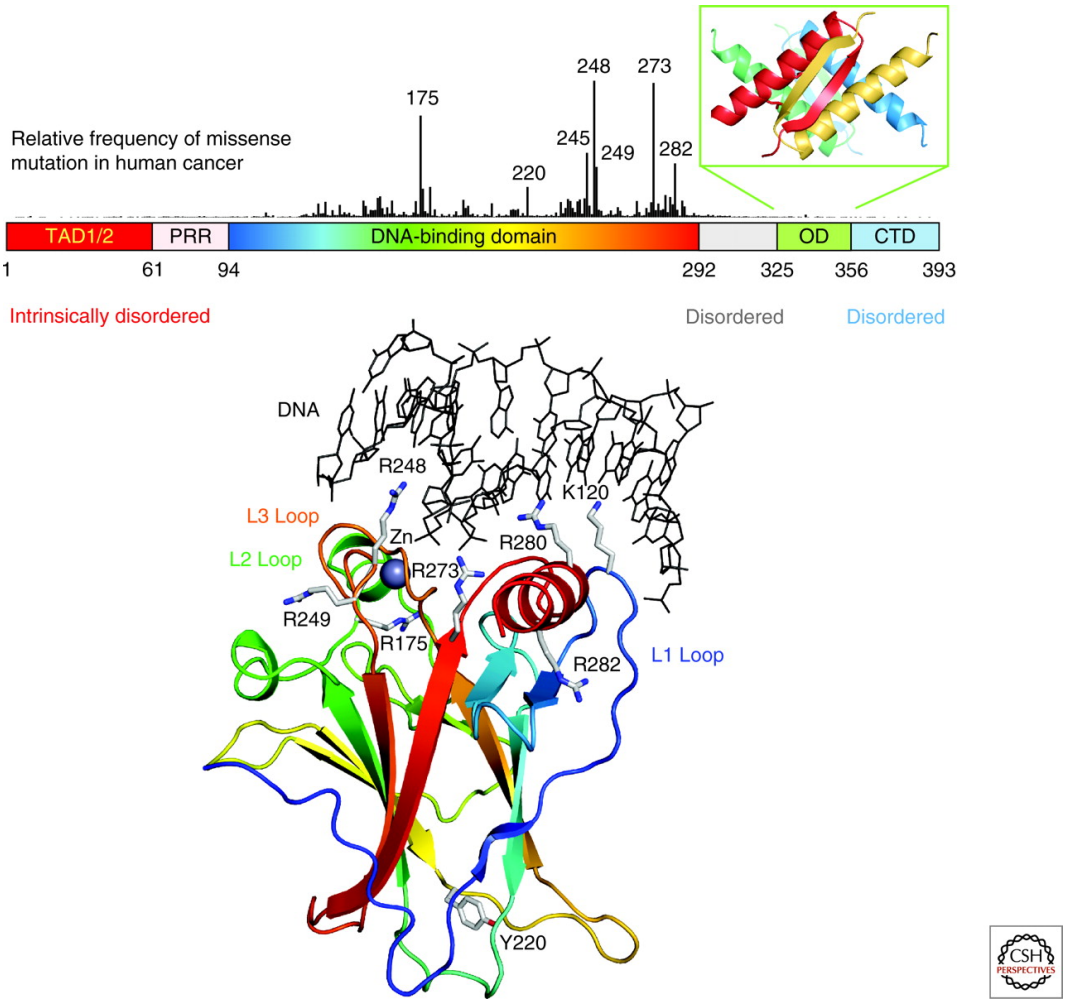

Figure 1 : ***p53 structure****. p53 contains an unfolded amino-terminal transactivation domain (TAD) subdivided into two subdomains (TAD1 and TAD2), followed by a proline-rich region (PRR). The central part is the structured DNA-binding (DBD) and tetramerization domains (OD). Likewise the TAD, there is a disordered regulatory domain at the extreme carboxyl terminus (CTD). Based on the TP53 Mutation Database of IARC [21], the vertical bars indicate the relative missense-mutation frequency in human cancer for each residue, suggesting that most of the cancer mutations are in the DBD. The picture below represents the structure of the DBD, in which is evidenced sites of cancer hotspot mutations and essential DNA contacts. Adapted from [7].*

The DBD is the core of p53 protein, because it contains the DNA binding activity. It has an immunoglobulin-like β-sandwich scaffold and other structural elements (i.e. a loop-sheet-helix motif and two large loops stabilized by a zinc ion) that form the DNA-binding surface [22–24]. Removal of the zinc ion destabilizes the protein and induces the loss of sequence-specific DNA binding activity [25,26]. The DBD binds specifically to double-stranded target DNA (DNA response element). The DNA response

elements (REs) are bound by four DBD in a 4:1 complex [27], and binding affinity depends on RE sequence: typically, p53 binds with high-affinity to REs of genes involved in cell cycle arrest and with low-affinity to REs of genes involved in apoptosis [28,29]. The p53 OD allows the homo-tetramerization (dimers of dimers) that is necessary to bind REs and eventually to activate the transcription of p53 targets [30,31].

The CTD has a regulatory role: it contains a leucine-rich regulatory domain that maintains p53 in an inactive form until phosphorylation or acetylation in this domain activates the protein [32–34]. Moreover, it encodes for a nuclear export signal (NES) and a nuclear localization signal (NLS), which binds to a receptor and allow the selective passage of p53 through the nuclear pores.
Both N-terminal and C-terminal of p53 have a natively unfolded structure [35], which is a typical feature of proteins involved in protein-protein interaction networks [36] because it facilitates binding promiscuity and allows to interact with a large number of different targets proteins [37]. By contrast, the central DBD and the tetramerization domain have a well-defined conformation.

In order to activate the downstream cascade, p53 tetramers shift from a latent to an active form, and to do so they are post-translationally modified through several mechanisms [38–40] (e.g., phosphorylation, glycosylation, acetylation, protein-protein interactions, binding ssDNA, alternative splicing, C-terminal truncation, and N-terminal truncation), which all disrupt the binding between CTD and DBD and eventually make the p53 core domain available to bind DNA REs [14].

1.1.2. Wild-type p53

p53 is a transcription factor, it is the linchpin of a plethora of signaling pathways that regulate proliferation, induce cell cycle arrest and apoptosis in response to stress stimuli (genotoxic damage, oncogene activation, loss of normal cell contacts, hypoxia, nutrient deprivation and telomere erosion) and ultimately maintain the integrity of the human genome [41].
In normal cells, p53 is usually expressed at a very low level cause of Mdm2 binding that ubiquitinates the protein and induces p53 degradation [42–44]. Stress stimuli rapidly

increase p53 protein expression levels, without any effects on *TP53* transcription levels. The increase of p53 protein expression levels can occur both by enhancement of p53 mRNA translation and the stabilization of p53 protein. The latter is due to various post-translational modifications that alter the interaction between p53 and its negative regulator Mdm2, which is also one of p53 transcriptional targets, thus creating a negative feedback loop [45].

p53 acts as tumor suppressor in different ways (Figure 2):

- Promoting the cell cycle arrest in G1/S phase through the transcription of the cyclin-dependent kinase inhibitors (*CDKN1A* and *CDKN2A* that encodes for p21 and p16, respectively). p21 expression is susceptible to even low levels of p53 protein, and this allows cells to safely survive until the damage has been resolved or stress removed [46].
- Promoting the cell cycle arrest in G2/M phase through the transcription of *GADD45* genes. Gadd45 interacts with different proteins involved in cell cycle regulation (i.e., Cdc2 and PCNA) [46].

If DNA damage repair is not possible, p53 activates apoptotic pathways to avoid the proliferation of damaged cells [47]. To do this, p53:

- promotes apoptosis through the activation of PUMA, a member of pro-apoptotic Bcl2- family, that induces the mitochondrial-dependent apoptosis [48].
- Promotes senescence through the expression of plasminogen activator inhibitor 1 (PAI-1) [49,50] and p21 [51].

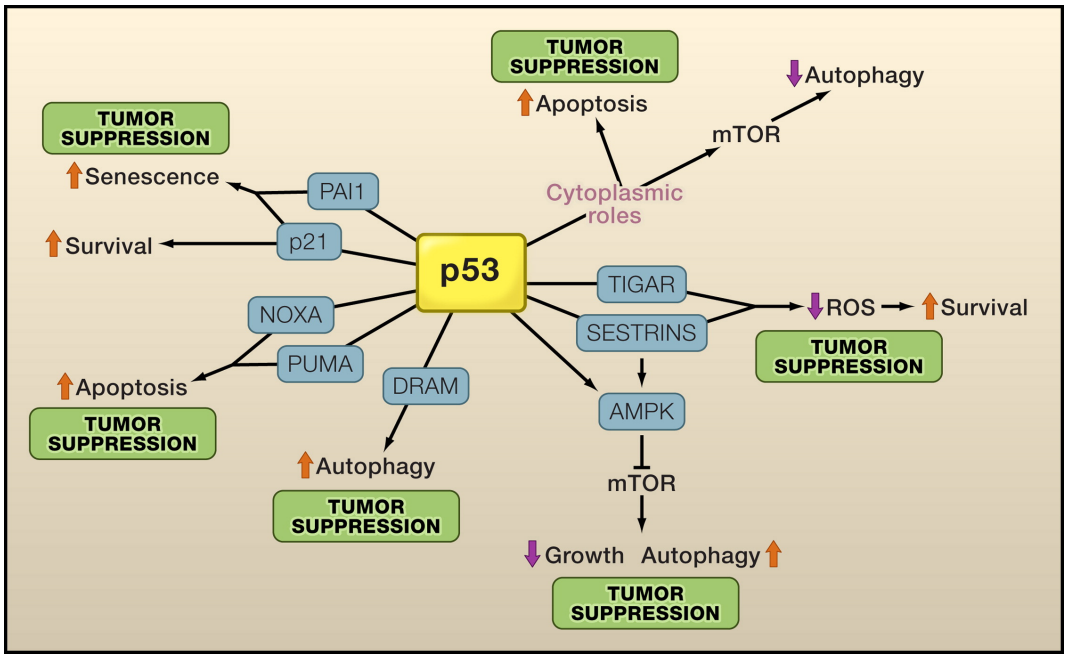

Figure 2: ***p53 tumor suppressor functions****. p53 controls cell survival, proliferation and cell death regulating the expression of different target genes (some of them are reported in blue in this image). Adapted from* [41].

Moreover, p53 protects cells against DNA damage and genome instability using different mechanisms:

- decreasing the levels of intracellular reactive oxygen species [52,53].
- Regulating the metabolism. Indeed, one of the cancer cell features is the ability to survive under adverse conditions (i.e. starvation) [54]. In this situation p53 is activated by AMP-activated prion kinase (AMPK) [55] and negatively regulates the kinase mTOR (mammalian target of rapamycin) which is important in the control of protein synthesis [56,57].
- Regulating autophagy, a membrane trafficking-mediated "self-eating" mechanism that results in lysosomal digestion of cellular components. To do this, p53 induces lysosomal proteins such as DRAM (damage-regulated autophagy modulator) [58] or negative regulates mTOR signaling [59].
- Modulating glucose uptake [60], in particular, dampening glycolysis [61,62] and improved mitochondrial respiration [63], curbing the acquisition of enhanced aerobic glycolysis that is one characteristic metabolic change associated with oncogenesis.
- Promoting antiangiogenic activities that could limit tumor progression [64].

Overall, p53 works as a genome guardian because it avoids the accumulation of cells with oncogenic mutations within the host.

1.1.3. Mutant p53 in cancer

Fifty per cent of all human cancers carry a *TP53* mutation that makes *TP53* the most frequent mutated gene and underlies the importance of p53 in tumor biology [65–67]. Carriers of *TP53* germinal mutations develop the Li-Fraumeni syndrome, which is characterized by the development of malignant tumors by early adulthood (typically breast cancer, sarcomas, brain tumors and adrenocortical carcinomas) [68–71]. Moreover, *TP53* DNA sequence is highly polymorphic both in coding and noncoding regions, and some of these polymorphisms have been shown to increase cancer susceptibility and to modify cancer phenotypes [72].

TP53 mutations are more frequent in the advanced stages or cancer subtypes with aggressive behavior (e.g., triple negative or HER2- amplified breast cancers) [73–75]; whereas, in tumors with low mutation rates, p53 is often inactivated by alternative mechanisms [67].

In contrast to other tumor suppressor genes, most *TP53* mutations in human cancer are missense substitutions (75%); whereas, frameshifts, deletions, amplifications (9%), nonsense (7%) and silent mutations (5%) are rare [76].

Typically, mutations occur in hotspots within the DBD of the protein [77] and in 90% of cases are missense mutations; in contrast, outside DBD, missense mutations are only the 40% and the majority are nonsense or frameshift mutations.

About 25% of the missense mutations are C:G > T:A substitutions that occur in CpG dinucleotides in codons that are essential for the structure and the chemical bond between p53 and DNA REs [78]. CpG dinucleotides are prone to be mutated [79]; indeed, among all residues mutated in the DBD, 3 CpG dinucleotides (175, 248 and 273) represents alone 60% of CpG mutations and another five (196, 213, 245, 282, and 306) residues account for 26% of these variations. Other CpG sites are detected in tumors because substitution at these residues does not generate a dysfunctional protein.

Generally, missense mutations can have two effects on p53 protein: either interfere with the contact between p53 and DNA REs (contact mutant) (e.g., R248 and R273) or alter protein conformation and perturb the structure of the DNA-binding surface (conformation mutant) (e.g., R175, G245, R249 and R282) [22,80].

All *TP53* mutations detected in tumors induce the loss of tumor suppressor function ("loss of function"); in addition, some mutations confer oncogenic features to p53 protein ("gain of function") that contribute to tumor initiation and progression. To sum up, p53 mutations can contribute to cancer progression in three different ways:

1. loss of p53 wild-type (wt_p53) function.
2. Dominant-negative effect (DNE) either on p53 wt allele in case of heterozygous cells or on other p53 family members (p63 and p73) [81]. As previously described, to activate the transcription of its target genes, p53 forms tetramers that are dimers of dimers; mut_p53 together with wt_p53 forms tetramers, which are not functional, thus inhibiting wt_p53 function.
3. Gain of oncogenic functions (GOF). This feature was discovered when the introduction of mut_p53 into p53 null cells give rise to a new phenotype [82]. Moreover, *in vivo* experiments demonstrated that mice expressing mut_p53 display a tumor profile more aggressive (e.g. higher incidence of metastasis) than p53 null or wt_p53 mice [83–86]. GOF confers mut_p53 the ability to interact with other proteins, such as transcription factors (TFs) or chromatin-modifying proteins, that are not partners of wt_p53 [87,88].

   There are several downstream effects of GOF mut_p53: it promotes invasion and motility by enhancing transforming growth factor β (TGF-β) [89], epidermal growth factor receptor (EGFR) [90,91] and MET [92–94] pathways and by enhancing integrin/RCP recycling [93,94]. Mut_p53 regulates apoptosis and autophagy through both cytoplasmic and mitochondrial pathways [95–97]. Mut_p53 also regulates genomic instability [98], chemoresistance [99], metabolic alteration [100], accumulation of reactive oxygen species [101], enhanced cell survival [102] and proliferation.

   Recently, studies identified new activities of mut_p53, such as a role in cell reprogramming [103,104] with the ability to dedifferentiate somatic cells into pluripotent stem cells and thus initiating tumor formation [105,106].

1.1.4. Clinical implications

Different studies have investigated the impact of *TP53* mutations on patient outcome, but the results have been heterogeneous and contradictory. In some studies, *TP53* mutations have been correlated with a shorter survival or a poorer response to treatment [76]; in breast cancer, *TP53* mutations correlated with more aggressive gene expression profiles (e.g. basal) and mutations within the DBD were associated with a worse prognosis compared with mutations outside DBD [107]; however, it was no clear whether *TP53* was an independent prognostic factor, and which specific mutations caused a worse prognosis [108].

From a therapeutic point of view, based on the evidences that mut_p53 confers more aggressive behaviors to tumor cells, mut_p53 is a promising molecular target for newer anti-tumor therapies [109–111], as supported by two studies on transgenic mice models [112,113].

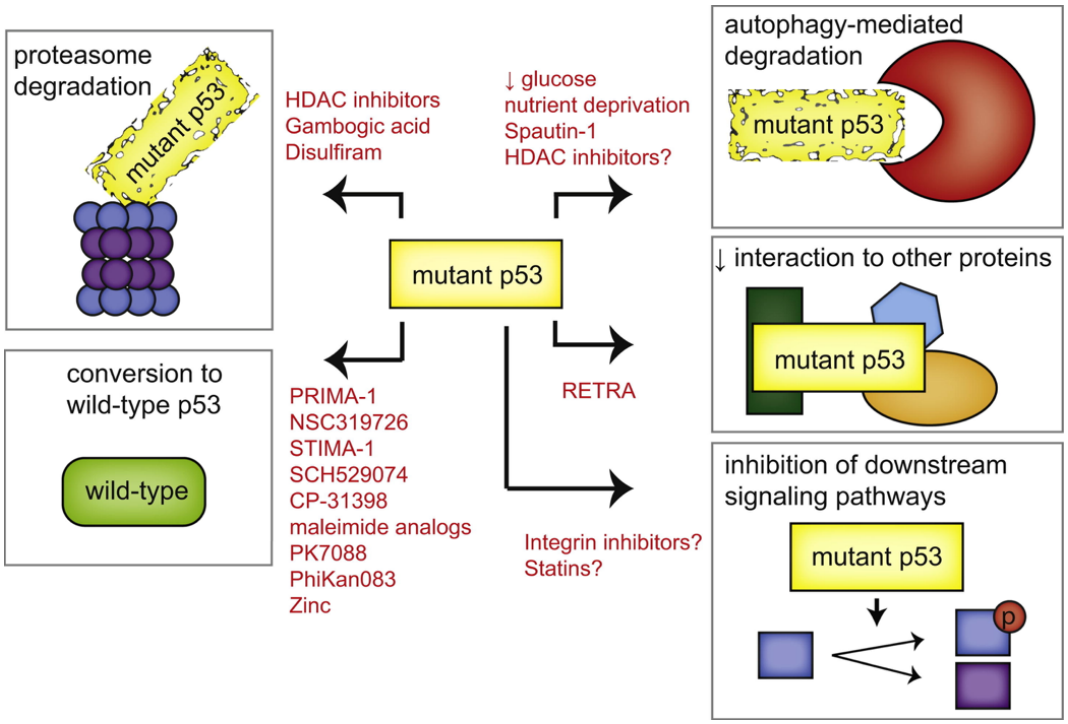

Figure 3: ***Strategies to target mut_p53****. They include promotion of mut_p53 degradation through the proteasome and autophagy pathways, restoration of wt_ p53 activity, interference with the interaction between mut_p53 and other proteins, and interference in signaling pathways downstream of mut_p53. Adapted from* [114].

The second strategy to inhibit mut_p53 activity targets its downstream targets of mut_p53. For instance, RETRA is a small molecule destabilizing p73-mut_p53 interaction, resulting in p73 release and restoration of its anti-tumor suppressor activity [115]. Alternatively, inhibition of cholesterol synthesis [100] or inhibition of EGFR, MET or MAPK pathways [89–91,93], all mut_p53 downstream signaling pathways, can also exert an anti-tumor effect.

The third strategy to inhibit mut_p53 function is to restore wt_p53 protein folding. For example, some compounds (e.g., PRIMA-1, CP-21298, SCH29074) interact with DBD, promote wild-type folding and restoration of p53 function [116–118]. As previously mentioned, the ion Zn(2+) is necessary to wt_p53 folding [26], in some conformational mutants increasing Zn(2+) levels partially restores the wild-type conformation [119,120]. The last example is a class of molecules (e.g., Phikan083, PK7088) designed to target a single conformational mutant, Y220C mut_p53, and able to restore wt_p53 conformation and activity [121,122].

1.2. Non-coding RNAs

Non-coding RNAs (ncRNAs) are RNA molecules that do not encode for proteins. There are two kinds of ncRNAs: infrastructural and regulatory [123]. Infrastructural ones are important for RNA processing and translation: transfer RNAs (tRNAs), ribosomal RNAs (rRNAs), small nuclear RNAs (snRNAs) and small nucleolar RNAs (snoRNAs). The regulatory ncRNAs regulate gene expression at the transcription level, RNA processing or translation: micro RNAs (miRNAs), small interfering RNAs (siRNAs), Piwi-interacting RNAs (piRNAs) and long non-coding RNAs (lncRNAs). Based on their size, ncRNAs could be classified as:

- small ncRNAs: long 20-30 nucleotides (nt);
- long ncRNAs: longer than 200 nt and up to 100 kb [124,125].

Since the discovery of siRNAs, later on of microRNAs, and now with the wave of long ncRNAs, many researchers realized that throughout metazoan evolution, despite a quite constant number of proteins, the size of genomes expanded and the transcribed portion of it, which is 98% in the human genome. Regulatory ncRNAs, but not only [126], seem to have played an important role during human evolution [127]. Without no surprise, ncRNAs not only are involved in evolution and development, but also in diseases, such as cancer and neurodevelopmental disorders [128].

1.2.1. Small ncRNAs

Three main classes of small regulatory RNA exist and they all are processed from longer to shorter mature transcripts (Figure 4).

miRNAs are the most abundant regulatory small RNAs [129], they are about 22nt long, and the most current annotation includes 2588 human miRNAs [130]. miRNA genes are transcribed by RNA polymerase II to generate the primary miRNAs (pri-miRNAs). Like protein coding gens, transcription of miRNAs genes is finely regulated [131–135]; likewise, the maturation from pri-miRNAs to mature miRNA (Figure 4) [136–139] and export from the nucleus to the cytoplasm [140–144]. Mature miRNAs are eventually loaded onto an AGO protein to form the RNA-induced silencing complex (RISC), a ribonucleoprotein complex that mediates all RNA-silencing pathways [145,146]. RISC complex recognizes targets depending on complementarity between mature microRNA and the 3'UTR of target mRNA and reduces translation or induces the degradation of mRNA

transcript, depending on the degree of base-pairing complementarity between the mRNA and the first 5' 8 nucleotides of mature microRNA (seed region) [132]. Since the site of interaction between miRNA and mRNA is long only 6–8 bp, each microRNA has the potential to target multiple different mRNAs [147]; indeed, it has been estimated that overall miRNAs regulate about one-third of human protein-coding genes [148]. miRNAs are typically well conserved throughout evolution and are key regulators of several cellular functions and development, and their misregulation could cause several human diseases, including cancer [149].

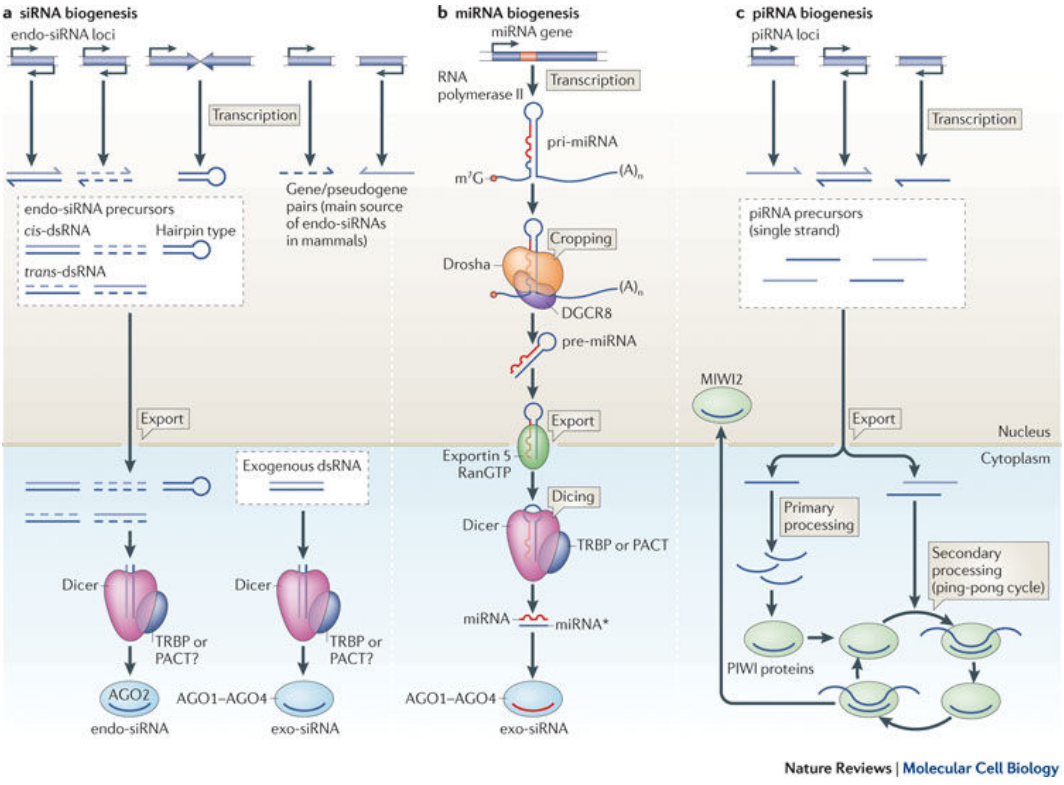

Figure 4: ***Biogenesis of small ncRNAs****. Adapted from* [150].

Piwi-interacting RNAs (piRNAs) are 24-30 nt long, and their primary function is to silence active retrotransposon elements (TEs) in the germline cells [150–152]. Unlike microRNAs, piRNA sequences are not conserved; however, genomic positions of piRNA clusters are conserved in mammals [153–155]. piRNAs are produced through a primary processing pathway, which generates an initial pool of piRNAs, that on its turn is amplified through a ping-pong pathway that amplifies only piRNAs that target active transposons. piRNAs function is not Dicer-dependent [156] but relies on PIWI proteins

to form an active piRNA-induced silencing complex (piRISC) that recognizes and silences complementary TE RNA targets [157–159].

siRNAs are endogenously expressed in plants; whereas, in human there are few examples of endogenous siRNAs. *XIST-TSIX* duplex is processed by Dicer to generate siRNAs which are required for the repressive chromatin modification on the inactive X chromosome [160]. Antisense pseudogene transcripts that pair with cognate gene mRNAs. At the same time, human cells can use miRNA processing and RISC complexes to generate siRNAs when short hairpin RNAs (shRNA) are transfected into the cell, which is a common biotechnology strategy to silence protein expression for research purposes.

1.2.2. LncRNAs

LncRNAs are 200 nt up to 100 kb long [124,125]. The most updated human ENCODE annotation lists more than 28000 different lncRNAs, which are expected to rise even more with the widespread usage of deep sequencing approaches [161]. LncRNAs are transcribed by PolII, they can be either spliced or not, usually polyadenilated, and they are less expressed but in a more tissue-specific manner than the protein coding counterpart or miRNAs [162]. Typically, lncRNAs are present across several species but are poorly conserved [163–166].

Classification of lncRNAs is based on their genomic location relative to protein-coding genes:

1. Intergenic lncRNAs: do not overlap protein-coding genes and have independent transcription units, they are also called long intergenic non-coding RNAs (lincRNAs) [167,168]. They have chromatin signatures of transcribed genes (H3K4me3 at the promoter and H3K36me3 along the transcribed length). They are transcribed by RNA polymerase II, spliced, capped and polyadenylated, and typically they are long 1 kb [169]. They are expressed in a tissue-specific manner more than protein-coding genes [162,170,171] and conserved across multiple vertebrate species [170]. Among lncRNAs, lincRNAs are the most abundant (e.g. *XIST*, *H19* and *MALAT1).*

2. Intronic lncRNAs: although it is well known that introns harbor small ncRNAs (snoRNAs and miRNAs); recently, many lncRNAs have been identified within introns of protein-coding genes.
3. Antisense lncRNAs: are transcripts that intersect any exon of a protein-coding gene but are transcribed in opposite orientation. About 87% of all transcripts (coding and non-coding) overlap with antisense lncRNAs [170], and about 32% of the lncRNAs belong to the antisense subtype. Antisense are mostly enriched around the 5' (promoter), or 3' (terminator) ends of the sense transcripts, typically they are not spliced or polyadenylated.
4. Sense lncRNAs: share any exon of protein-coding genes and are transcribed in the same orientation, but do not encode for proteins [172].

Like miRNAs, lncRNAs are involved in a great variety of biological processes [123,173] (e.g. transcription [174,175], splicing [176,177], translation [178,179], protein localization [180,181], cellular structure integrity [182,183], imprinting [184–186], cell cycle [187,188], apoptosis [189,190], stem cell pluripotency [191] and reprogramming [192] and heat shock response [193–195]); but unlike other ncRNA classes, lncRNAs have several different mechanisms of action [124]. For example, lncRNAs are predominately localized in the cell nucleus and bound to chromatin [162], suggesting a role in regulation of gene transcription. They can work both in *cis*, regulating the expression of genes closed to lncRNA locus, and in *trans*, regulating the expression of distant genes. To this aim, lncRNAs recruit chromatin remodeling complexes (e.g. Polycomb) and guide them to specific genomic loci thus affecting gene expression [196,197]. *XIST* (X inactive-specific transcript) acts in *cis* and is involved in epigenetic X chromosome inactivation [198,199]. It is highly expressed only by the chromosome that will be inactivated, and it coats the chromosome serving as a guide for the recruitment of the Polycomb repressive complex 2 (PRC2), a member of the chromatin-modifying complexes that trimethylates histone H3 at lysine 27, which represses expression of the targeted chromosome [200]. Another example of lncRNAs regulating gene expression happens during body segmentation. Many lncRNAs are transcribed in the intergenic regions between Homeobox transcription factor (*HOX)* genes [175]: *HOTTIP* recruits a protein complex that trimethylates lysine residue 4 (K4) of histone H3 to activate the *HOXA* gene cluster [201]; whereas, *HOTAIR* (HOX antisense intergenic RNA) represses the transcription of *HOXD* in *trans* guiding PRC2 and LSD1,

which is an H3K4 demethylase [202]. Finally, *LincRNA-p21* is located upstream of *CDKN1A* gene, which encodes p21 protein, a known downstream target of wt_p53. *LincRNA-p21* expression is directly regulated by wt_p53 and itself enables wt_p53 machinery to increase *CDKN1A* expression levels [189,203].

LncRNAs can also decoy proteins and RNAs preventing them to act. For instance, *PANDA* sequesters and inhibits the nuclear transcription factor NF-YA, which actives the apoptotic program after DNA damage. Thus, *PANDA* promotes cell survival [204]. Similarly, *Gas5* (growth arrest-specific 5) binds to the DNA-binding domain of the glucocorticoid receptor, inhibiting glucocorticoid-regulated transcription in growth-arrested cells [205]. At the same time, *PTENP1* is *PTEN* pseudogene, it does not encode for Pten protein, but its 3'UTR can bind miRNAs that regulate *PTEN* expression, acting as a miRNA sponge and ultimately increasing Pten expression levels [206]. Similarly, *linc-RoR* (lincRNA regulator of reprogramming) is a sponge of miR-145, which in its turn regulates the expression of Oct4, Sox-2, Nanog, three transcription factors important in cellular reprogramming and the maintenance of pluripotency [192].

Finally, lncRNAs can serve as central scaffold in which multiple proteins assemble. The scaffold archetype is lincRNA NEAT1 (nuclear enriched abundant transcript 1), an essential architectural component of paraspeckles, the nuclear domains implicated in mRNA nuclear retention. NEAT1 participates in PSP1 and p54 dimer formation and localized them to the paraspeckles [207]. Another example is HOTAIR, which binds to two E3 ubiquitin ligases with RNA-binding domains (Dzip3 and Mex3b) and with the relative substrates (Ataxin-1 and Snurportin-1), facilitating their ubiquitination and degradation [208].

1.2.3. LncRNAs and cancer

By genome-wide association studies (GWAS) it has been discovered that 80% of cancer-associated SNPs (single nucleotide polymorphisms) are inside non-coding regions of the genome [209]. Many of these loci may be transcribed into ncRNAs and collaborate to tumorigenesis and metastasis. LncRNAs can be either tumor suppressors or oncogenes. Moreover, next-generation sequencing (NGS) revealed that thousands of lncRNAs are aberrantly expressed or mutated in various cancers [210].

Below, we report some examples of lncRNA involved in human cancers, in particular, focusing on breast and ovarian cancer Figure 5 [211].

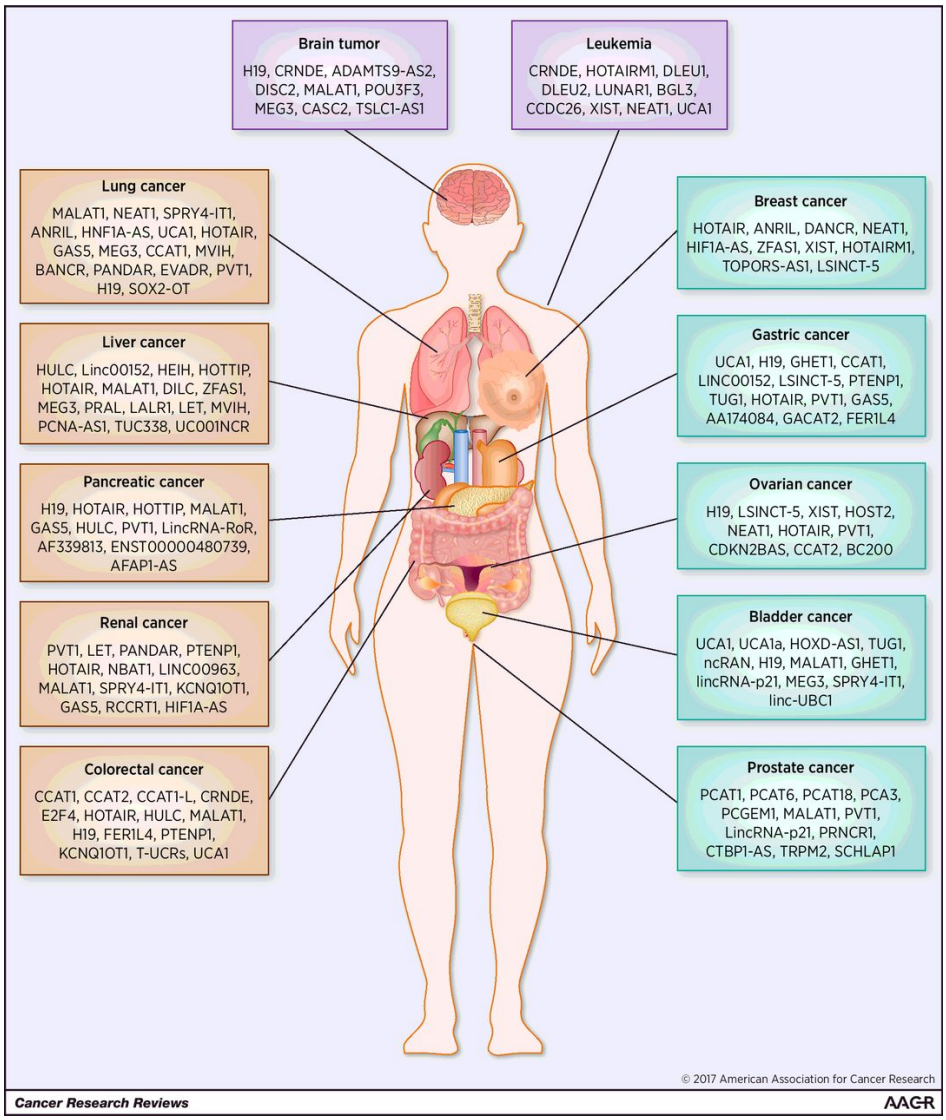

Figure 5: ***LncRNAs associated with cancer.*** *Adapted from* [211].

HOTAIR is frequently overexpressed in human cancer (breast, ovarian, colorectal, hepatocellular, pancreatic, renal, gastrointestinal, non-small cell lung carcinomas) [212–216], it increases tumor invasiveness and metastasis and is associated with poor prognosis in several cancers [217]. As described above, it silences the expression of target genes through the induction of epigenetic modifications and is involved in the assembling of E3-ubiquitin ligases during protein degradation [175]. *HOTAIR* is required for the viability of breast cancer cells and estradiol regulates its expression via the estrogen receptor pathway [218].

ANRIL is upregulated in leukemia, breast and prostate cancers [219]. It is an antisense transcript of *CDKN2B* (cyclin-dependent kinase inhibitor 2B) gene and controls cell

proliferation and senescence via the epigenetic regulation of its neighboring tumor suppressor gene *CDKN2A/B* [220]. It is also required for the repression of tumor suppressors *p15*.

MALAT1 also call *NEAT2* (nuclear enriched abundant transcript 2) is frequently overexpressed in human cancer (lung, bladder, breast, colorectal, liver, prostate and ovarian cancer) [221], correlated with increased cell proliferation and metastasis, by deregulating N-cadherin and E-cadherin expression [222]. It is post-transcriptionally processed to produce a short RNA; whereas, the long form is localized to nuclear speckles where modulates the alternative splicing by regulating the level of phosphorylated splicing-associated serine-arginine (SR) proteins. It is a potential biomarker and therapeutic target.

H19 is one of the first lncRNAs discovered and has a crucial role in embryonic development and tumorigenesis (liver, breast, colorectal, esophageal, lung, pancreatic, gastric, bladder and cervical carcinoma) [223–226]. It is a decoy for miRNAs and interacts with transcriptional repressors to induce the silencing of its target genes. It is the precursor of miR-675, which inhibits p53, which in turn represses H19. It promotes tumorigenesis and metastasis, and it is expressed in response to hypoxic stress and epithelial-to-mesenchymal transition (EMT). Its expression leads to the activation of genes involved in angiogenesis, cell survival, proliferation.

XIST it is overexpressed in leukemia and ovarian cancer and regulates genes expression by interacting with PRC1, PRC2 [227]. Its knockdown results in enhanced sensitivity to Taxol [228].

As described in the first chapter, p53 is among the most important transcription factors and it is finely regulated by several mechanisms that involve transcription, translation, and post-translational modifications. LncRNAs both regulate p53 expression levels and are downstream targets of p53 [229]. Among the lncRANs that regulate p53, we mention *MALAT1* (repressor of *TP53* transcription) and *MEG3* (activator of *TP53* transcription). Among lncRNAs that are p53 effectors, there are *lincRNA-p21*, *PANDA*, *H19*, *loc285184*, and *lncRNA-Ror*.

1.3. Ovarian cancer

1.3.1. Ovarian cancer epidemiology

Ovarian Cancer (OvCa) is a relatively uncommon tumor, accounting for about 1.3% of newly diagnosed tumors in 2017 in the United States; yet, it represents the 5th most common cause of cancer death in women in Western countries and the leading among gynecological cancer [230–232]. Typically, OvCa is diagnosed in postmenopausal age, being the majority (>80%) of cases diagnosed in women over 50 years with a median age at diagnosis of 63 years [230]. Overall survival rate at 5 years is 46,5%, greatly depending on tumor stage; indeed, in the rare case in which OvCa is diagnosed in local stage (localized to the ovary), the 5-years survival is 92.5%, whereas when it has been diagnosed in advanced stage (dissemination outside the ovaries) the survival is only 28.9%. Unfortunately, only the 15% of cases are diagnosed at a local stage (tumor confined to primary site), 20% at regional stage (tumor spread to regional lymph nodes) and the majority (60%) at a distant stage when cancer metastasize [230]. Moreover, death rates increase with age [233] and in the last 30 years, the overall 5-years relative survival rate had only a very modest increase (2%-4%) [234].

Many risk factors have been identified to be associated with OvCa. Among environmental risk factors, the principal is the life-long number of ovulations; indeed, nulliparae have greater risk than multiparare; likewise, longer reproductive life (early menarche and late menopause) increases OvCa risk. On the contrary, the use of oral contraceptive pill, tubal ligation, breastfeeding and suppression of ovulation are all protective against OvCa [235]. Two hypotheses explain the association between number of ovulations and OvCa risk. The first is the "incessant ovulation" hypothesis, which holds that the number of ovulatory cycles increases the rate of cellular division associated with the repair of the surface epithelium after each ovulation, thereby increasing spontaneous mutation [236,237]. The second hypothesis, namely the "gonadotropin hypothesis", focuses on the role of gonadotropins, such as luteinizing hormone and follicle-stimulating hormone, hypnotizing that OvCa develops in response to an excessive stimulation of ovarian tissue by these hormones [238]. Other environmental risk factors are obesity [239–241], endometriosis [242–244], the use of postmenopausal hormone therapy [245–247] and the use of talcum powder [230,235,248,249].

Regarding OvCa genetic risk, the most critical factor is a positive familial history of OvCa; indeed, approximately 20% of OvCa are familial, and women with a first-degree relative with OvCa have a risk to develop OvCa twofold higher than women with no family history [250]. The single most common genetic mutation associated with OvCa is the mutation of *BRCA1* or *2* genes. Both mutations are highly penetrant [251]. In particular, a mutation in *BRCA1* increases the lifetime risk of 15-45% and a *BRCA2* mutation of 10-20%. These women tend to develop the disease earlier (10 years before) than the women with non-hereditary OvCa [235], and their tumors metastasize more frequently to the viscera; whereas, sporadic ovarian cancer remains confined to the peritoneum. At the same time, OvCa risk is also due to low-moderate penetrance variants, which explain about 80% of the familial risk and located in intergenic or in protein coding genes (e.g. *BRIP1* [252] and *RAD51* [253,254]).

1.3.2. Ovarian cancer histology and pathogenesis

OvCa is a highly heterogeneous group of malignant tumors that may arise from germ cells, stromal or epithelial cells, which per se represents 90% of OvCas (Epithelial Ovarian Cancer – EOC). Based on histopathology and molecular genetic alterations, EOCs are divided into five main subtypes [235,255]:

- endometrioid,
- clear cell,
- mucinous
- high-grade serous,
- low-grade serous.

Endometrioid OvCas are about 10% of all OvCas, they are typically diagnosed at early stage and have low grade. Such as colorectal and stomach cancers, also inherited endometrial cancer is commonly associated with Lynch syndrome, a condition caused by germline pathogenic variants in the highly penetrant mismatch repair genes *MLH1*, *MSH2*, *MSH6*, *PMS2*, and *EPCAM* [256]. Both endometrioid cysts and endometrioid OvCas have a mutation in *ARID1A* [257].

Clear cell OvCa account for 5% of OvCas, and it is more frequent in Japanese women. This tumor type is strongly associated with endometriosis and it is frequently mutated in *ARID1A* [257]. Clear cell OvCas frequently develop chemoresistance with a worse patient outcome in advance stages compared to than serous OvCa.

Mucinous OvCa accounts for about 10% of OvCas and have a different natural history from other histologic types in terms of presentation, response to therapy and outcome. Commonly, patients with a mucinous OvCa are diagnosed at early-stage and have an excellent prognosis, whereas when diagnosed in advanced disease the outcome is poor. Mucinous OvCas are characterized by the overexpression of *KRAS*, whereas *BRCA1/BRCA2* and *TP53* typically are not mutated [258], which all suggest that develop along a separate pathway.

Low grade serous OvCa (LGSOC) (<5% of EOC [259,260]) typically arises at younger age and has mild to moderate cytologic atypia and low mitotic rate. LGSOC tends to have a better survival than HGSOC; even though, LGSOC do not respond to traditional chemotherapy [261,262].

The majority of epithelial OvCas (80%) belong to the high-grade serous ovarian carcinoma (HGSOC) subtype, which is the most lethal among the 5 subtypes. HGSOC presents severe nuclear atypia and high mitotic rates. Gene expression profiling identified four HGSOC molecular subtypes of biological and clinical importance: mesenchymal (worse prognosis), proliferative, differentiated and immunoreactive (better prognosis) [263].

Recent findings highlighted that epithelial OvCas do not originate from ovaries, but from other gynecological tissues and involve the ovary secondarily [264]. For example, clear cell and endometrioid OvCas develop from endometriotic cysts associated with endometriosis [235], and mucinous OvCa from transitional cell nests at the tubal-mesothelial junction [265]. Concerning HGSOC, histopathologic examinations of fallopian tubes removed from *BRCA 1* and *2* carriers showed hyperplastic and dysplastic lesions that are characterized by higher expression and mutations of *TP53* (p53 signature) and serous tubal intraepithelial carcinoma (STIC) [266,267]. Evolutionary analyses revealed that p53 signatures and STICs are precursors of OvCas and identified a window of 7 years

between the development of STIC and initiation of ovarian carcinoma, with metastases following rapidly after that [268].

Another classification divides epithelial OvCa into two types [235,269,270], based on their molecular expression profile:

- Type 1 includes: low-grade serous, endometriosis-related subtypes (endometrioid, clear-cell and seromucinous), mucinous and malignant Brenner tumors. They are characterized by a young age at diagnosis, an indolent disease course with a prolonged overall survival time [271] and a relative resistance to standard platinum and Taxol chemotherapy [236]. These tumors show genomic stability and mutations in *KRAS*, *BRAF*, *ERBB2*, *PTEN*, *PIK3CA* and *ARID1A* genes that occur early in the tumorigenesis.
- Type 2 comprises aggressive tumors: high-grade serous, high-grade endometrioid, malignant mixed mesodermal tumors and undifferentiated tumors. These tumors usually present with a symptomatic bulky stage III or IV disease and ascites. They are most prevalent in postmenopausal women, are initially very chemosensitive to platinum chemotherapy, however, they have a poor outcome [236]. They are usually associated with *TP53* mutations (97% of HGSOC have a *TP53* mutation) [272,273], mutations are found in tumors of all stages, suggesting that they were originated in an early event in the progression of the disease [274]. Approximately 20% of these tumors carries a somatic o germline mutation in *BRCA1/2*, amplification of the *AKT2* and the phosphatidylinositol 3-kinase genes [275].

1.3.3. Mechanisms of ovarian cancer metastasis

OvCa cells primarily disseminate within the peritoneal cavity and only rarely spreads through the vasculature [236].

In the first steps of metastasis, OvCa cells undergo to EMT, which loses the attachment of epithelial cells from the basement membrane and neighboring cancer cells. Fundamental in this process is the loss of E-cadherin, a membrane glycoprotein located at cell adherens junctions [276,277]. E-cadherin connects through α- and β- catenin to the actin microfilaments within the cytoplasm, anchoring epithelial cells to each

other. In OvCa, E-cadherin expression in metastatic cancer cells (i.e. ascites and metastatic implants) is lower than in primary tumor [278], and its low expression predicts poor patient survival [279]. During EMT occurs a "cadherin-switch" which consists of E-cadherin downregulation, N-cadherin and P-cadherin up-regulation [280–282]. This situation allows cancer cells to survive under hypoxic conditions [283] and activate mesenchymal signaling by interaction with surrounding stromal cells: on tumor cells, integrins activate matrix metalloproteinase (MMP)-9, which cleaves the E-cadherin ectodomain and contribute to the loosening of cell-cell adhesion thus spreading transformed cells as single cells or spheroids into ascites [284].

In the second step of metastasis, cancer cell spheroids, which detached from the primary tumor, float in the peritoneal fluid. In the spheroids, cancer cells maintain a mesenchymal phenotype [285], keeping repressed E-cadherin and MMP-2; moreover, E-cadherin loss leads to transcriptional up-regulated of fibronectin receptor $\alpha5\beta1$-integrin, facilitating the adhesion of OvCa cells to the secondary site [286].

Once cell spheroids adhere to peritoneum, OvCa cells revert to their epithelial phenotype to respond to paracrine oncogenic growth factor. In particular, OvCa cells invade the mesothelium, a monolayer of mesothelial cells attached to a basement membrane predominantly composed of collagen types I and IV, fibronectin and laminin [287]. Mesothelium covers all organs within the peritoneal cavity [288,289]. Integrins and CD44 (the principal cell surface receptor for hyaluronic acid) are the principal mediators of OvCa metastasis in the mesothelium [290]. When OvCa cells attach to mesothelial cells, cancer cells up-regulate MMP-2, that cleaves fibronectin and vitronectin in smaller fragments, which are even better ligands of $\alpha5\beta1$ and $\alpha V\beta3$ integrins [291–296]. Moreover, a recent study demonstrated that cancer-associated mesothelial cells facilitate initial metastatic colonization of OvCa cells, secreting fibronectin and providing access to the submesothelial extracellular matrix [297].

After OvCa cells implanted on omentum or peritoneum, cells start to replicate and when reaching a certain size, they require new blood vessels to provide nutrients and support their growth. Inflammation and injury stimulate the peritoneal cells and their associated immune and stromal cells to release cytokines such as inteleukin1 (IL)-1, -6 and -8 that subsequently increased the secretion of vascular endothelial growth factor (VEGF) by cancer cells [298]. VEGFs stimulate vascular and lymphatic endothelium to form new blood and lymphatic vessels and regulate their permeability.

Lastly, microarray studies [299,300], comparative genomic hybridization [301] and high-resolution single-nucleotide polymorphism analysis [302] demonstrated similar genetic alterations in primary ovarian tumors and their respective metastases, further supporting the passive mechanism of OvCa metastasis.

1.4. Breast cancer

1.4.1. Breast cancer epidemiology

Breast cancer (BC) represents the most common non-skin malignancy in women, and it is the second cause of cancer mortality. In the United States in 2017, more than 250,000 new BC cases and 40,000 BC-related deaths are estimated [303], indicating that fewer than one out of six women diagnosed with BC die for the disease [304]. In recent years, the mortality rate has decreased, especially in younger age groups, because of improved treatment and earlier detection [234,305]. BC incidence increased after introduction of mammography screening and continues to grow with the aging of the population [306]. Indeed, a 70-years-old woman has a chance of being diagnosed with BC 10 times higher than a 30-years-old woman [307].

Regarding the environmental risk factors, a relevant one is the exposure to estrogen, both endogenous (e.g., nulliparity, early menarche and late menopause, older age at first birth) and exogenous (e.g., use of combination estrogen-progesterone hormones after menopause) [306,308] that increases growth of breast cells, facilitating the development of BC. Other environmental risk factors include, alcohol consumption, obesity and exposure to ionizing radiation during puberty [309].

Concerning the genetic factors, women with family history of BC have an increased risk [310,311]: risk is doubled if a first-degree relative is affected similarly to OvCa, germline mutations of *BRCA* genes are typically occurring in 5-10% of all BC [312–314]. These mutations are high penetrant, with BC diagnosis occurring at a younger age, and with a lifetime risk of 55%-65% and 45%-47% for *BRCA1* and *BRCA2* mutation carriers, respectively [256,315].

1.4.2. Breast cancer histology and pathogenesis

BC is a highly heterogeneous disease in terms of histopathological and biological features and clinical outcome [316].

The histopathological classification is based on the diversity of the morphological features of the tumors. The first major histopatological difference is between *in situ* and invasive (i.e. infiltrating) carcinomas [307,317,318]. *In situ* BC is sub-classified in:

- **Ductal** (DCIS), in which breast epithelial cells that connect the lobules to the nipple have become cancerous, but do not invade the basal membrane. It represents the 83% of *in situ* cases, and even though is nonlethal, it can develop into a deadly invasive form [319,320]. DCIS is frequently identified through mammographic screening programs, and it is usually treated with surgical excision [304].
- **Lobular** (LCIS), in which cancerous cells are found in the breast lobules. It is the 13% of *in situ* cases, and generally is not a precursor of invasive cancer.

The majority of BCs (80%) belong to the invasive type, in which tumors invade the basal lamina and grow into surrounding breast tissue. Invasive BC can be sub-classified in [318]:

- **Infiltrating ductal** (IDC), that is the most common, comprises 70-80% of all cases. Based on the levels of nuclear pleomorphism, glandular/tubule formation, and mitotic index, IDC is further sub-classified as well-differentiated (grade 1), moderately differentiated (grade 2) or poorly differentiated (grade 3) [321,322].
- **Invasive lobular,**
- **Mucinous**,
- **Tubular**,
- **Medullary**,
- **Papillary**.

A more recent classification scheme is based on the immunohistochemical characterization of hormone (estrogen -ER- or progesterone –PR-) receptor status, Her2 protein

overexpression or HER2 gene amplification and the proliferative fraction (Ki-67) [316,323]. Therefore, a tumor can be considered [324]:

- **ER and PR positive,** if it has 1% or more immunoreactive cells. The higher is the number of positive neoplastic cells, and the larger is the expected benefit of endocrine therapies.
- **HER2 positive,** if it overexpresses Her2 in more than 10% of invasive tumor cells, or show HER2 gene amplification. They are candidates for Trastuzumab treatment.
- **Triple negative**, if it is ER, PR and HER2 negative. They are more common in premenopausal women in *BRCA1* mutant carriers [325]. They have the shortest survival, because contain high number of cancer steam cells [326] and also because there are not targeted therapies [327].

Hierarchical clustering analysis of gene expression identified different heterogeneous subtypes of BC with different distinct molecular patterns correlated with a different prognosis [328–331]. Perou et al. identified four major BC subtypes:

- **Luminal**: are hormone receptor-expressing cancers, and their gene expression patterns remind the luminal epithelial component of the breast [328]. In particular, they express luminal cytokeratins 8 and 18, ER and genes associated with ER activation, whereas mutations in *TP53* are rare (<20%) [328–330]. Luminal BCs are often grade I and typically carry a good prognosis. They are treated with hormone therapy since several reports have demonstrated that ER-positive tumors respond poorly to conventional chemotherapy [332]. It represents the most common subtype of BC and is in turn subdivided in:
    - Luminal A: have, in general, higher expression of ER-related genes than luminal B. They are slow-growing and low-aggressive and can be treated with endocrine therapy alone [333,334].
    - Luminal B: have higher expression of proliferative genes and tend to be a higher grade than luminal A, for these reasons patients benefit from chemotherapy added to endocrine therapy [334,335].
- **HER2-enriched**: are hormone receptor-negative (low expression of ER and related genes) and have an overexpression or amplification of HER2 gene [329]. It has a high proportion of *TP53* mutations (40-80%), and since it is typically

high grade and poorly differentiated, this subtype carries a poor prognosis [329]. It can be treated with molecularly targeted agents, such as the anti-HER2 monoclonal antibody Trastuzumab.

- **Basal-like**: it is so-called because the expression pattern mimicked that of the basal epithelial cells [328]. This subtype lacks expression of ER and related genes, low expression of HER2, strong expression of basal cytokeratins 5,6 and 17 and expression of proliferation-related genes. They are typically *BRCA* and *TP53* mutated. Basal-like tumors have aggressive features, are generally high grade and carries a poor prognosis [329,330]. Since they are triple-negative for the receptors (ER, PR, and HER2), conventional targeted therapies are not used, and the unique choice is chemotherapy.

To classify BC samples in these three groups, a gene expression assay has been developed: PAM50 (prediction analysis of microarray) which is a 50-genes signature able to differentiate the molecular subtype using gene expression on FFPE tissue [336].

1.4.1. Mechanisms of breast cancer metastasis

Metastasis is of great importance in BC, because it accounts for the majority of cancer deaths. To metastasize, BC cells have to perform an extraordinarily complex process that comprises a series of sequential steps collectively termed metastatic cascade (Figure 6). All these steps must be executed while tumor cells avoid immunological responses and survive to apoptotic signals [337].

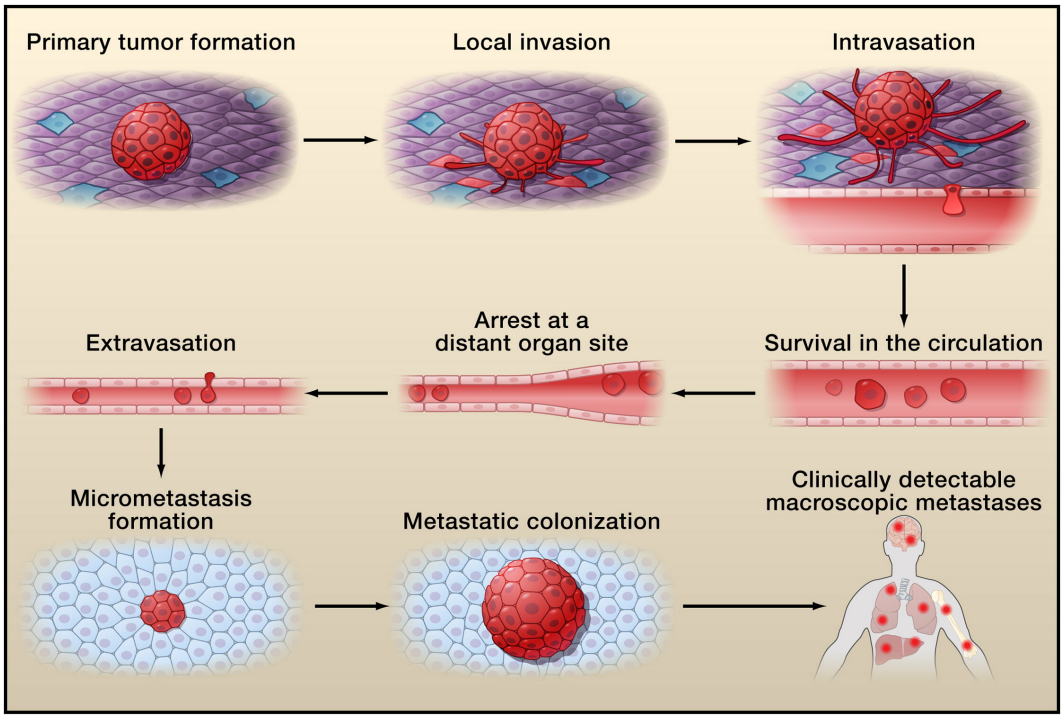

Figure 6: ***The Metastasis Cascade****. During metastatic progression, tumor cells exit from their primary sites of growth (local invasion, intravasation), translocate systemically (survival in the circulation, arrest at a distant organ site, extravasation), and adapt to survive and thrive in the foreign microenvironments of distant tissues (micrometastasis formation, metastatic colonization). Adapted from* [338].

Local invasion: in the first step, BC cells have to separate from the primary tumor and invade the surrounding tumor-associated stroma. To do this, tumor cells must lose their cell-to-cell adhesion and cell-matrix (ECM) contacts. The cadherin family has a predominant role in this step [339]: E-cadherin maintains the cell-cell junctions, and its downregulation determines the outgrowth of metastatic BC cells [340], whereas N-cadherin is closely associated with mesenchymal cells and related to EMT [341]. EMT plays an important role in stroma invasion, because it induces the production of metalloproteinases and other proteolytic enzymes that degrade the ECM [342,343]. Once the BC cells invade the stroma, they adhere to the ECM through the integrins [344] that interact with fibronectin, laminin, collagen, fibrinogen, and vitronectin [339].

Intravasation: during this step, the BC cells enter into the lumina of blood or lymphatic vessels. Intravasation can be facilitated by molecular changes that promote the ability of carcinoma cells to cross the pericyte and endothelial cell barriers that form

the walls of microvessels. For example TGFβ enhances mammary carcinoma intravasation, ostensibly by increasing carcinoma cell penetration of microvessel walls or augmenting invasiveness more generally [345]. This passage is strongly influenced by the structural feature of tumor-associated blood vessels. In contrast to non-cancerous blood vessels, these are tortuous, prone to leakiness and in a state of continuous reconfiguration [346]. Since the interaction between adjacent endothelial cells are weak, and there are not pericyte, the intravasation is facilitated.

Survival into the circulation: once BC cells have intravasated into the lumina of blood vessels, they can disseminate through the circulation as circulating tumor cells (CTCs) [347,348]. They represent "metastatic intermediates" between primary tumors and sites of dissemination.
Inside the hematogenous circulation, CTCs must survive to a variety of stresses, such as the absence of anchorage that stimulates anoikis mechanism [349], toxic conditions (e.g., the high concentration of oxygen), immunological stress and collision with host cells [350,351].

Extravasation: BC cells arrest at distant organ sites and extravasate into the parenchyma of distant tissues. Each tumor type typically metastatize to selected target organs [352], which are for BC: brain, lung, bone, and liver. Once the BC cells lodge in the microvasculature of a distant organ, CTCs may initiate to growth and form a microcolony that can break the walls of the surrounding vessels [353]. In an alternative way, BC cells cross the vessel wall into the tissue parenchyma in the opposite direction of what happened during intravasation.

Colonization: once extravasated, carcinoma cells have to survive in the foreign microenvironment that they encounter in the parenchyma of distant tissues. The cells are called disseminated tumor cells (DTCs) [350]. The microenvironment in the metastatic site is very different from that of the primary tumor and DTCs must overcome these differences to proliferate to eventually generate micrometastasis, macroscopic metastases, which are eventually diagnosed.

2. Aim and strategy

This PhD thesis stems on three central considerations: OvCa and BC share a high rate of *TP53* mutations and high incidence of tumor metastasis; mut_p53 gain of function regulates tumor invasiveness and metastasis, and ncRNAs, particularly lncRNAs, are central players of gene regulation including wt_p53 pathway. However, there are not reports that investigate the role of lncRNAs in the pro-invasive phenotype of mut_p53. Therefore, the overall aim of this project is to investigate whether lncRNAs participate in the mut_p53 gain of function of HGSOC and BC.

Our strategy was first to characterize HGSOC and BC cell models and to choose the best cell lines to investigate mut_p53 phenotypes. Next, we silenced mut_p53 in OvCa and BC cell lines and evaluated changes in invasiveness ability in *in vitro* assays (mesothelial clearance and 3D colony assay). Finally, using RNA deep-sequencing of nuclear long RNAs, we profiled the expression of lncRNAs in *TP53*_silenced cells and validated deep-sequencing results in mutant and wt_p53 cell models. Our future aim will be to modulate candidate lncRNAs gene expression using CRISPR activators and repressors to investigate the impact on pro-invasiveness phenotype of mut_p53.

3. Materials and methods

3.1. Cell lines and cultures

Cells lines used in this project are listed in Table 1. No antibiotics were used for cell culture. Cells were maintained in humidified incubators at 37°C and 5% CO_2 and regularly tested for mycoplasma contamination using MycoAlert detection Kit (Lonza, Germany). Only mycoplasma-negative cells were used for experiments.

Cell line name	Source	Biological source	Medium[#]
Ov90	ATCC (CRL-11732™)	Serous ovarian cancer	MEDIUM 199, NaB, 15% FBS
Cov318	ECACC	Serous ovarian cancer	DMEM, NaP, Gln, 10% FBS
Cov504	ECACC	Serous ovarian cancer	DMEM, NaP, Gln, 10% FBS
Ovcar4	NCI/DCTD	Serous ovarian cancer	RPMI, 10% FBS
Ovcar8	NCI/DCTD	Serous ovarian cancer	RPMI, 10% FBS
Kuramochi	HSRRB	Poorly differentiated ovarian cancer	RPMI, 10% FBS
Ovsaho	HSRRB	Ovarian adenocarcinoma	RPMI, 10% FBS
Cov362	ECACC	Endometrioid ovarian carcinoma	DMEM, NaP, Gln, 10% FBS
Tov112d	ATCC (CRL-11731™)	Endometrioid ovarian carcinoma	RPMI, 10% FBS
MDA-MB-415	ATCC (HTB-128™)	Breast carcinoma	DMEM, 10% FBS
BT474	ATCC (HTB-20™)	Breast carcinoma	RPMI, 10% FBS
T47D	ATCC (HTB-133™)	Breast carcinoma	DMEM, 10% FBS
SKBR3	ATCC (HTB-30™)	Breast carcinoma	DMEM, 10% FBS
SUM149PT	Asterand Bioscience	Breast carcinoma	Ham's F-12, hydrocortisone, insulin, 5% FBS,
MDA-MB-231	ATCC (HTB-26™)	Breast carcinoma	DMEM, 10% FBS
Hs578T	ATCC (HTB-126™)	Breast carcinoma	DMEM, insulin, 10% FBS
BT549	ATCC (HTB-122™)	Breast carcinoma	RPMI, 10% FBS
MCF10a	ATCC (CRL-10317™)	Non-tumorigenic breast epithelial cell line	Mammary Epithelial Cell Growth Medium, SupplementMix
293FT	Thermo Fisher Scientific	Embryonal kidney	DMEM, Gln, NaP, NEAA, 10% FBS
MET-5A	ATCC (CRL-9444™)	Mesothelium	RPMI, EGF, hydrocortisone, insulin, 10% FBS
HCT116	ATCC (CCL-247™)	Colorectal carcinoma	RPMI, 10% FBS

Table 1: ***Cell lines used in this project.***

 # ATCC (http://www.atcc.org/); ECACC (http://www.hpacultures.org.uk/collections/ecacc.jsp); HSRRB (http://www.jhsf.or.jp/English/hsrrb.html); NCI/DCTD (http://dtp.nci.nih.gov/branches/btb/tumor-catalog.pdf).

§ RPMI (RPMI-1640 AQmedia), DMEM (DMEM AQmedia), MEDIUM 199, Ham's F-12, NaB (Sodium Bicarbonate), NaP (Sodium Pyruvate), Gln (Glutamine), NEAA (Non- Essential Amino Acids), Insulin (9.5 - 11.5 μg/ml), Hydrocortisone (500 ng/ml) and EGF (epidermal growth factor) (10 ng/ml) were all from Sigma-Aldrich (St. Louis. MO. USA). FBS (Fetal Bovine Serum) was from Carlo Erba. Cholera toxin 25 ng/ml; Calbiochem. Mammary Epithelial Cell Growth Medium and SupplementMix was from PromoCell.

3.2. Lentivirus production and transduction

Mutant *TP53*_silenced ovarian and breast cancer cell lines were generated by lentivirus transduction. Twenty-four hours before transfection, 293FT cells were plated to be 70-90% confluence the next day. Transfections were performed using Lipofectamine 2000 reagent (Invitrogen, Thermo Fisher Scientific) according to the manufacturer's instructions. The appropriate amount of DNA plasmids (see below) was diluted in Opti-MEM Medium (Gibco, Life Technologies) and added to diluted Lipofectamine 2000 reagent. This mixture was incubated for 5 minutes at room temperature and then the DNA–lipid complex was transferred on cells.

To silence mut_p53, we used two different DNA plasmids pLKO.1 puro vectors encoding *TP53*-shRNAs (TRCN0000003756 or TRCN0000003753 Sigma-Aldrich), as negative control we used a non-target shRNA control (SHC016; Sigma-Aldrich). For all constructs, we used both a stably expressing cassette or an IPTG inducible one. To generate viral particles, 293FT were transfected (as previously described) using one of the pLKO shRNA DNA vector together with ViraPower Lentiviral Packaging Mix (pLP1, pLP2 and pLP/VSV-G) (Invitrogen, Thermo Fisher Scientific, Eugene, OR, USA). Seventy-two hours later, viral supernatants were collected and transducing units per ml of supernatant were determined by limiting dilution titration in HCT116 cells. An MOI (multiplicity of infection) of 5 to 1 (5 transducing viral particles to 1 cell) was used for transducing cells using Polybrene (Sigma-Aldrich) at a final concentration of 8 μg/ml to increase transduction efficiency. Twenty-four hours after transduction, puromycin selection was started and mutant *TP53*_silenced cells were immediately used for *in vitro* experiments, protein and RNA extraction.

Similarly, to generate MET-5A-Tween cell line, we transduced cells with a lentivirus to express Tween and then sorted by FACS.

3.3. Cell treatment

Nutlin-3 (Cayman Chemical) treatment was performed as follows: MCF10a cells plated 24 hours earlier in 10 cm plates were exposed for 24 hours to Nutlin-3 at the final concentration of 10 μM in complete medium.

3.4. Integrin detection

Integrins were measured by FACS using αII (12F1, BD-Bioscience), Integrin α3 (MAB1952Z, Chemicon Int.), Integrin α4 (9F10, BD-Bioscience), Integrin α5 (IIA1, BD-Bioscience), Integrin α9β1 (MAB2078Z, Chemicon Int.), Integrin $\alpha_V\beta3$ (MAB1976X, Chemicon Int.). To this end, cells were detached from culture dishes, pelleted and suspended in 10% FBS at a final concentration 6x10^6 cells/ml. 50 μl of cell suspension was stained on ice with 5 μl of antibody for 30 min. Cells were washed with ice-cold PBS and analyzed using the BD FACScan flow cytometer system.

3.5. Mesothelial clearance assay

To test the ability of OvCa cell lines to invade the peritoneum, we used the *in vitro* mesothelial clearance assay [354]. To form spheroids, 100 ovarian cancer cells stained with DiI (red) were plated in one well of a 96-well U-bottom plate coated with poly-HEMA (poly-2- hydroxyethyl methacrylate, Sigma-Aldrich). polyHEMA is a polymer that forms a hydrogel in water [355] and due to its uniformly nonionic nature, it effectively prevents matrix deposition when used to coat cell culture dishes and so allow the growth in suspension. At the same time, MET-5A-Tween cells were plated on a 6-well dish coated with 5 μg/ml fibronectin (Sigma-Aldrich) to resemble the mesothelium monolayer. After 16 hours, the spheroids were collected and plated on the MET-5A-Tween monolayer. The plate was then transferred to the time-lapse microscope (Leica Time Lapse AF6000LX) interfaced with the Leica Application Suite (LAS) software, where we observed at least 20 spheroids for each treatment over a period of 8 hours, using bright-field and fluorescence filters at 200x magnification. Images were captured every 2 hours and analyzed using ImageJ software by measuring the area of each spheroid at time 0 (t0) and the area of the hole in the MET-5A-Tween monolayer after 8 hours (t8) [356]. Normalized clearance area is defined as the ratio between t8 and t0 according to [354].

3.6. 3D colony assay formation

To test the ability of BC cell lines to invade extracellular matrix, we cultured them in Matrigel. Matrigel matrix (Geltrex® LDEV-Free Reduced Growth Factor Basement Membrane Matrix, Thermo Fisher Scientific) was thawed overnight in ice before use. The day after, 2000 cells were plated with 150 µl of Matrigel matrix in 4 well of a polyHEMA coated 96-plate. The plate has been incubated at 37°C for 30 min to allow the Matrigel matrix to gel, then 120 µl of complete medium were added. After 10 days cells were stained with 2 µg/ml calcein for 30 minutes at 37°C (Life Technologies) and cell morphology was observed using a confocal laser-scanning microscope (TSP2 Leica) interfaced with a Leica DMIRE2 fluorescent.

3.7. Western blotting (WB)

To obtain protein extract, cells were incubated for 20 minutes on ice in NP40 buffer (0.5% NP40, 50 mM HEPES, 250 mM NaCl, 5 mM EDTA, 0.5 mM EGTA, 1 µM DTT) supplemented with Protease Inhibitors (Complete; Roche, Mannheim, Germany) and Phosphatase Inhibitor Cocktail 1 and 2 (P2850 and P5726; Sigma-Aldrich). Cells were vortexed every 5 minutes and then clarified by centrifugation at maximum speed for 20 minutes at 4°C (NP40-soluble fraction). Cell pellets, obtained after clarification, were suspended in SDS lysis buffer (4% SDS, 100 mM Tris-HCl pH 6.8, 20% glycerol) and boiled for 10 minutes at 95°C (NP40-insoluble fraction). The protein concentration of NP40-soluble fraction was quantified by Bradford assay using the Protein Assay Dye Reagent Concentrate (Bio-Rad, Hercules, CA, USA), whereas the concentration of the NP40-insoluble fraction was empirically derived from its corresponding soluble fraction.

For immunoblotting analysis, 40 µg of proteins were boiled in 5X sample buffer (Tris HCl 1M pH 6.8, SDS 10%, glycerol 80%, bromophenol blue 0.4%, β-mercaptoethanol) for 10 minutes, separated using 4-20% SDS-PAGE Criterion TGX Stain-Free Precast Gels (Bio-Rad) and transferred to PVDF or nitrocellulose membranes (Bio-Rad). Membranes were blocked with 5% non-fat dried milk in TBS-Tween20 (20 mM Tris-HCl pH 7.5, 150 mM NaCl, 0,1% Tween 20) or in Odyssey Blocking buffer (Li-cor) for 1 hour at room temperature and then incubated overnight at 4°C with the following antibodies: p53 (sc-126 Santa Cruz), E-cadherin (cat. no.36; BD-Bioscience),

H2AX (cat. no.2595; Cell Signaling, Danvers, MA, USA), Pax8 (10336-1-AP Protein Tech), vimentin (D21H3; Cell Signaling), vinculin (sc-73614; Santa Cruz). Incubation with the secondary antibodies anti-rabbit, anti-mouse or anti-goat linked with horseradish peroxidase (HRP) (GE Healthcare Lifesciences, Little Chalfont, UK) was performed for 1 hour at room temperature at a dilution 1:3000-1:5000. According to signal intensity, secondary antibody detection was performed using either ECL Western Blotting Detection Reagents RPN 2106 (GE Healthcare) or Luminata Forte Western HRP Substrate (Merck Millipore, Darmstadt, Germany) and using Chemidoc MP Imager (Bio-Rad). Band intensities were analyzed and quantified using Image Lab v5.2 (Bio-rad).

3.8. Nucleus/cytoplasmic separation

Cells were collected using a scraper and suspended in ice-cold RSB buffer (10 mM Tris-Cl pH 7.4, 10 mM NaCl, 3 mM $MgCl_2$) with 0,025% or 0,050% NP40 and proteinase inhibitor (cOmplete Protease Inhibitor Tablets, Sigma) and centrifuged at 400g for 15 minutes at 4°C. The supernatant was centrifuged at maximum speed to remove debris, supernatant represents the cytoplasmic enriched fraction. The pellet, containing the intact nuclei, was washed with ice-cold RSB buffer with 0,025% or 0,050% NP40 and spun for 15 minutes at 400g at 4°C to remove cellular debris.

3.9. RNA extraction, cDNA synthesis and Quantitative Real-Time PCR (qRT-PCR)

Total and nuclear RNA was extracted using Isol-RNA Lysis Reagent (5 Prime, Hamburg, Germany), whereas cytoplasmic RNA was isolated from the supernatant using TRIzol LS reagent (Life Technologies), according to protocol instructions. RNA extraction was followed by cleanup with spin columns (RNeasy MinElute Cleanup Kit, Qiagen), DNase digestion (Turbo-DNase, Ambion, Thermo Fisher Scientific). RNA quality was tested by agarose gel electrophoresis after RNA exposure to 70°C for 5 minutes. 1 µg of RNA was reverse transcribed in cDNA using AMV Reverse Transcriptase (Promega) and random primers (Promega). qRT-PCR was performed in duplicate using iQ SYBR Green Mix (Bio-Rad) with the appropriate primers, as reported in Table 2. Primer sequences were designed using Primer 3 Plus [357] and purchased from

Sigma-Aldrich. qRT-PCR reaction was carried out either in 96-well optical reaction plates using Two-Color Real-Time PCR Detection System MyiQ2 (Biorad) or in 384-well optical reaction plates using Applied Biosystems 7900HT Fast Real-Time PCR System (Thermo Fisher Scientific), according to manufacturer 's protocol. To calculate the relative abundance of RNA genes we used the $2-\Delta\Delta Ct$ formula and adopted GAPDH as housekeeping control gene.

Primer name	**Primer 5 sequence (5'-3')**	**Primer 3 sequence (5'-3')**
TP53	GCCGTCCCAGCAATGGATGATTT	TCTGGCATTCTGGGAGCTTCATCT
GAPDH	GAGAGACCCTCACTGCTG	GATGGTACATGACAAGGTGC
PAX8	GCAACCATTCAACCTCCCTA	CTGCTGCTGCTCTGTGAGTC
CDH1	TGCCCAGAAAATGAAAAAGG	GTGTATGTGGCAATGCGTTC
H-VIMENTIN	GAGAACTTTGCCGTTGAAGC	GCTTCCTGTAGGTGGCAATC
CDKN1A	GGACCTGGAGACTCTCA	CCTCTTGGAGAAGATCAG
SLUG	GGGGAGAAGCCTTTTTCTTG	TCCTCATGTTTGTGCAGGAG
BNC2_intr2	TGGGAACAGAATTGCCATAA	CCACCCCCAGCACTATTTTA
SCARNA2	GTGCAGGGTGAGTGTGAGTG	GCAGGAGGAGAGCTTTTCATT
BAIAP2-AS1	GGAAAGTTGAATGGCTGGAA	TTTTCCGGAGAAGCCTACCT
RP11-166D19.1	TGTTCCTTTCAGCTGGTCCT	GCAGAGGAGGTGTCTTCAGG
RP11-244M2.1	GAGCCTTATGTATGTGGTTGAAA	TGCCCAGAGGAAAAATAGTGA
AC034220.3	CTTTGAGGGGTCCATGTGAT	CATGAAGTTGCAGTCAAGCTG
LINC00704	TTTCAGAACCCTGCATTTCC	ACAGGGGTGTGGAGTCAGAG
MALAT1	CAATGAAGAGGCAATGTCCA	AAACGAAACATTGGCACACA
RP11-527N22.2	ACAAGGCGAGGACAAGAAGA	CAGATTCTGCCCTTCGCTAC
LINC01547	CACATCTGCCTCATTCCAGA	TGCGTTTGGCAGACTCATAG
RP11-47A8.5	ATTGGAAGAAGTCGGCAGAA	GATGAGAGTGTTGGGGTTGG
MIR100HG	CGCGTGGATGATTTGAAGAT	AGCATGCCCTAAAAATTTGC
LINC00472	CAGGTACTCCACTGGGCATT	CCACATGGCCCAACTAAGAG
RP11-108P20.2	TGCTAGCAAGCCACATCTTG	GAAAAGCCTCCTGACTGCAC
RP11-362F19.1	TCCTTCTCCACCTCAACCAC	GGGACACATGCTTCTAGTCTTG
RP11-25I15.3	AACATGGCATGATTTCCACA	AGAAATCACCCGCCTTCTG
RMRP	ACTCTGTTCCTCCCCTTTCC	CTAGAGGGAGCTGACGGATG
AC016710.1	AACAGGTCCTCACTGCCCTA	CCATGTTGTTCCCTCCCATA
LINC00621	CCAAGTCTGGTCAACCCAAT	AGCAGCTGGATTGCAGTTTT
AP001628.6	GAGGCTGAGGCAGGATCAC	TATGACCTTGTCCCCTCTCG
RP11-176D17.3	CCAGGTTTAAAGGTGGCTGT	GGATACATAAAGCATCTACCCACA
RP11-7F17.7	TACGGCCAAGACCATAGACC	CTTCCCTCATGGGACAAAAA
TERC	AAGAGTTGGGCTCTGTCAGC	AAGCGAACTGCATGTGTGAG
CDK5	CTTGTGGAGTGGGTGGCTAT	CCACTTGGTGTCCAGAACCT
CDK14	GACCATTGAGGACCTGAGGA	GGCTCTCAATCTGCATCTCC

CDK18	TGGAGCCATTACTTCAAGATCA	TGGCCAGCTCTGTCTCATAC
CDK19	ACTACAGCCACTACTACACGACCAT	GTCTCAAACTTGGTTCGGAAGTC
ACTA1	CTCACTGAGCGTGGCTACTCC	CTTGATGTCGCGCACGATC
ESR1	TGGGCTTACTGACCAACCTG	CCTGATCATGGAGGGTCAAA
ZEB1	CAGGCAGATGAAGCAGGATG	GACCACTGGCTTCTGGTGTG
ZEB2	GCGCTTGACATCACTGAAGG	ACCTGCTCCTTGGGTTAGCA
TWIST	GGAGTCCGCAGTCTTACGAG	TCTGGAGGACCTGGTAGAGG
SOX9	GACCAGTACCCGCACTT	TTCACCGACTTCCTCCG
HAS2	GCCTCATCTGTGGAGATGGT	ATGCACTGAACACACCCAAA

Table 2: ***Primer sequences****.*

3.10. Deep-sequencing Library preparation and sequencing

1 μg of good quality RNA (R.I.N. > 7) nuclear RNA were sent to IGA Technologies (Udine) to perform the deep-sequencing analysis.

For Cov318, 'Ovation RNA-Seq System V2' (NuGEN, San Carlos, CA) has been used for cDNA amplification following the manufacturer's instructions. 10 ng of cDNA was fragmented using Bioraptor (Diagenode, Liége, Belgium) using 15" of "high-mode" fragmentation for 6 cycles. Subsequently 'Ovation Ultralow System V2 1-96' has been used for library preparation following the manufacturer's instructions.

For MDA-MB-231, 'TruSeq Stranded mRNA Sample Prep kit' (Illumina, San Diego, CA) has been used for library preparation following the manufacturer's instructions. The poly-A mRNA was fragmented 3 minutes at 94°C and every purification step has been performed by using 1X Agencourt AMPure XP beads.

cDNA and final libraries were quantified by using the Qubit 2.0 Fluorometer (Invitrogen, Carlsbad, CA) and quality tested by Agilent 2100 Bioanalyzer High Sensitivity or DNA 1000 chip (Agilent technologies, Santa Clara, CA). Libraries were then processed with Illumina cBot for cluster generation on the flowcell, following the manufacturer's instructions and sequenced on single-end mode at the multiplexing level requested on HiSeq2500 (Illumina, San Diego, CA). The CASAVA 1.8.2 version of the Illumina pipeline was used to processed raw data for both format conversion and de-multiplexing.

3.11. Statistical Analysis

Graphs presented in figures were obtained using GraphPad Prism v6.0d software (La Jolla, CA, USA) and statistical analyses were done using JMP v9.0.1 software (Carry, NC, USA). Data were examined using the two-tailed Student's *t*-test assuming unequal variances or one-way ANOVA test when we compared more than two groups at once. Differences were considered significant at $p < 0.05$ and $p < 0.01$ and labeled accordingly (* or **, respectively).

4. Results

4.1. Cell models characterization

4.1.1. Ovarian cancer cell models

To characterize HGSOC ability to metastatize *in vitro*, we first selected 8 commercial EOC cell lines (Table 3) that belong likely or possibly to HGSOC according to Domcke et al. [358]. Domcke et al. classified commercial EOC cell lines based on: histological subtype of tumors from which EOC cell lines were derived according to original publication, number of mutations per million bases, copy number alteration prolife, and mutation in *TP53*, *BRCA1* or *BRCA2, ARID1, RB, PI3K, PTEN, ERBB2, KRAS, BRAF* and *CTNNB1* genes.

Cell line name	**Similarity to HGSOC** [358]	***TP53* status** [21]			
		Exon	**Codon**	**Mutation description**	**Wt → mut codon**
Kuramochi	Likely HGSOC	8	281	c.841G>T missense	GAC → TAC
Ovsaho	Likely HGSOC	10	342	c.1024C>T missense	CGA → Stop codon
Cov362	Likely HGSOC	6	220	c.659A>G missense	TAT → TGT
Ovcar4	Likely HGSOC	5	130	c.388 C > G missense	CTC → GTC
Cov318	Likely HGSOC	6	195	c.583 A > T missense	ATC → TTC
Cov504	Possibly HGSOC	9	322	c.965_966 deletion frameshift	CCA → Stop codon
Ov90	Possibly HGSOC	9	215	c.643A>C missense	AGT → CGT
Tov112D	Endometrioid	5	175	c.524G>A missense	CGC → CAC

Table 3: ***Classification and TP53 mutations in our HGSOC models.***

To confirm the presence of *TP53* mutations and to confirm HGSOC orgin of the 8 cell lines, we sequenced *TP53* and evaluated p53 and Pax8 protein expression by WB. Pax8 is a transcription factor, which regulates organogenesis of Müllerian structures with a critical role in OvCa development [359]. In all cell lines, we identified the expected *TP53* mutation according to IARC TP53 database [21] (Table 3). The protein expression of p53 was absent in Ovsaho and Cov504, which carry a nonsense mutation; whereas, all the other cell lines expressed the mutant protein (Figure 7A). Pax8 protein expression was present in all cell lines except Ov90 (Figure 7C).

Once we confirmed the presence and expression of mutant *TP53* and Pax8, we tested the 8 cell lines, for their ability to clear the mesothelium as described in [354] and in Materials and methods section of this Thesis (Mesothelial clearance assay). All 8 cells proved to be competent to clear mesothelium layer similarly to positive control (Tov112D), having all a median normalized clearance area (area of the hole in the MET-5A-Tween monolayer after 8 hours divided by area of tumor spheroid at time 0) greater than 1; being Cov318, Cov362, Ovcar4 and Cov504 the most efficient ones (Figure 7B).

Since Davidowitz and colleagues demonstrated that OvCa cells clearance capability is directly proportional to the expression of EMT proteins [360], we evaluated by WB and/or qRT-PCR the expression of E-cadherin (epithelial marker), Slug and Vimentin (mesenchymal markers) in our OvCa cell models (Figure 7D and E). E-cadherin is expressed in Ovsaho, Ovcar4, Cov504 and Ov90; whereas, Slug is highly expressed only in Cov504 and Vimentin is highly expressed in Cov362, Kuramochi and Cov504. In our cell models, there was not an evident correlation between EMT markers and intrinsic mesothelial clearance ability.

Furthermore, since it has already demonstrated that OvCa spheroids clear the mesothelium using a α5-integrin-dependent activation of myosin, which on its turn induces a traction force that promotes mesothelial cells displacement [361], we investigated whether the difference that we observed in mesothelial clearance ability could be due to α5-integrin different expression. The results we obtained are not consistent with previous reports [361], indeed in Cov318 (the most competent to clear the monolayer), only a small percentage of cells express α5 (Figure 7F). Therefore, we profiled the expression of other fibronectin-binding integrins in Cov318 cells, and we found that the most expressed integrin is the α3 chain (Figure 7G).

Finally, we decided to use Cov318 and Cov362 for further experiments, because they have good clearance ability, harbor a missense mutation in p53, form stable and compact spheroids and have EMT traits.

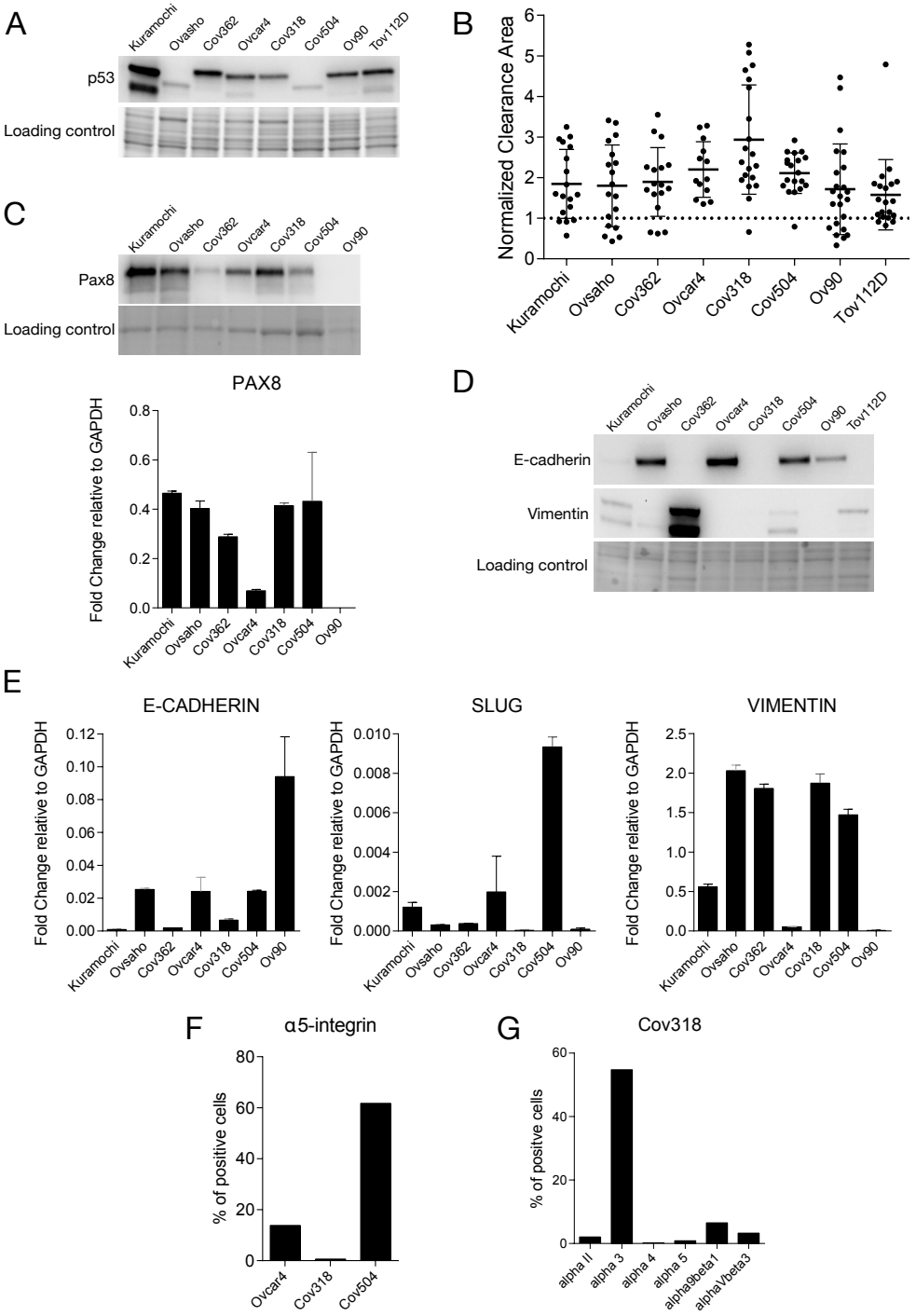

Figure 7: ***HGSOC cell models characterization.*** ***(A)*** *Western Blotting detection of p53 in NP40-insoluble protein extracts from eight OvCa cell lines. Ponceau staining was used as loading control.* ***(B)*** *Quantification of mesothelial clearance ability of eight OvCa cell lines. A total of 20 spheroid were analyzed per cell models. Data are shown as the mean ± standard deviation.* ***(C)*** *Western Blotting detection and qRT-PCR analysis of PAX8. Data are shown as the mean ± standard deviation of two technical replicates.* ***(D)*** *Western Blotting detection of E-cadherin and Vimentin. Ponceau staining was used as loading control.* ***(E)*** *qRT-PCR analysis of E-CADHERIN, SLUG and VIMENTIN. Data are shown as the mean ± standard deviation of two technical replicates.* ***(F)*** *Expression of α5-integrin in three OvCa cell models.* ***(G)*** *A panel of expression of six different integrin in Cov318.*

4.1.2. Breast cancer cell models

As for OvCa, to characterize BC invasiveness ability *in vitro*, we selected 8 commercial BC cell lines which all carry *TP53* mutations (reported in Table 4). Neve and colleagues [362] catalogated BC cell lines for their genomic and molecular proprieties and subdivided into luminal or basal B BC (Table 4).

Cell line name	**Classification** [362]	***TP53* status** [21]			
		Exon	**Codon**	**Mutation description**	**Wt → mut codon**
MDA-MB-415	Luminal	7	236	c.707A>G missense	TAC → TGC
BT474	Luminal	8	285	c.835G>A missense	GAG → AAG
T47D	Luminal	6	194	c.580C>T missense	CTT → TTT
SKBR3	Luminal	5	175	c.524G>A missense	CGC → CAC
MDA-MB-231	Basal B	8	280	c.839G>A missense	AGA → AAA
SUM149PT	Basal B	7	237	c.711G>A missense	ATG → ATA
Hs578T	Basal B	5	157	c.469G>T missense	GTC → TTC
BT549	Basal B	7	249	c.747G>C missense	AGG → AGC

Table 4: ***Classification and TP53 mutations in our BC models.***

To confirm this classification in our own cell models, we evaluated the expression those cytokeratins (CK) that differentiate BC into luminal and basal subtypes according to [362]. As expected by literature, we confirmed the enrichment of luminal CKs (*CK18* and *CK19)* in MDA-MB-415, BT474, T47D and SKBR3 cell models and basal CKs (*CK5* and *CK14)* in MDA-MB-231, SUM149PT, Hs578T and BT549 (Figure 8). Moreover, since basal BC is the most aggressive BC subtype and it is associated with mesenchymal features, we evaluated the expression of several mesenchymal (*ACTA1*, *HAS2, SOX9, SLUG, TWIST, VIMENTIN*, *ZEB1*, *ZEB2*) and epithelial (*CDH1*) markers in these cell models. All the mesenchymal markers were expressed only in the basal cell models, except for *ACTA1* and *SOX9* that were also present in the luminal models. At the same time, we evaluated estrogen receptor (*ESR1*), which was overexpressed in the luminal subtypes (Figure 8). *TP53* mutations are more frequent in basal

BC and MDA-MB-231 was previously used to investigate mut_p53 effect; therefore, we decided use as well this cell line.

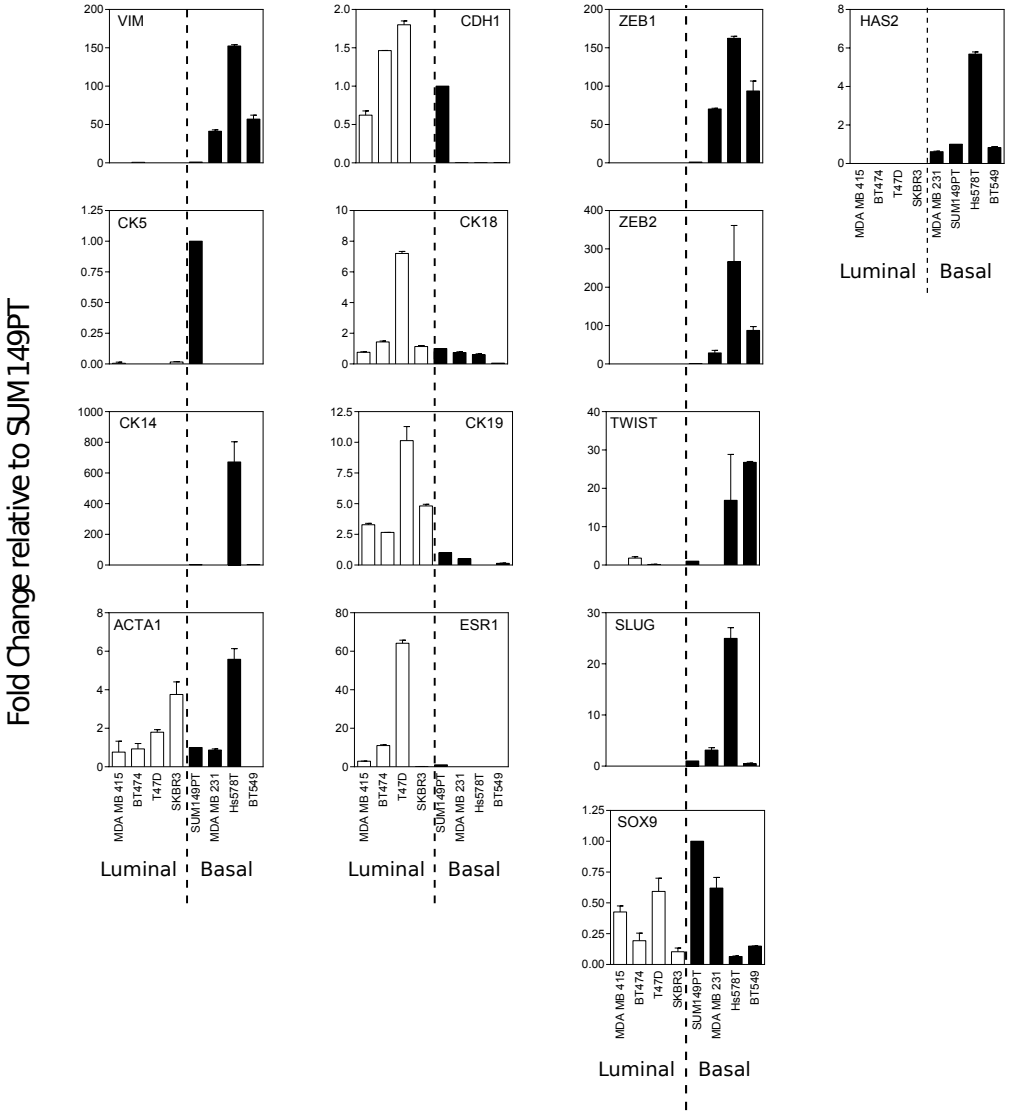

Figure 8: ***BC cell models characterization****. qRT-PCR analysis of several mesenchymal and epithelial genes (VIMENTIN, ACTA1, CDH1, ZEB1, ZEB2, TWIST, SLUG, SOX9, HAS2), basal cytokeratins (CK5. CK14), luminal cytokeratins (CK18, CK19) and estrogen receptor1 (ESR1). Data are shown as the mean ± standard deviation of two technical replicates.*

4.2. Evaluation of mut_p53 in *in vitro* assays

4.2.1. The role of mut_p53 in HGSOC cells mesothelial clearance

To investigate whether mut_p53 drives an invasive advantage in OvCa cells, we engineered Cov318 and Cov362 cell lines to express two inducible shRNAs that target *TP53*. After 4 days of induction with IPTG (Figure 9A and C), we used these cells to perform the mesothelial clearance assay and observed that, in both cell lines, *TP53* silencing caused a significant reduction of their clearance capability compared to control cells (Figure 9B and D).

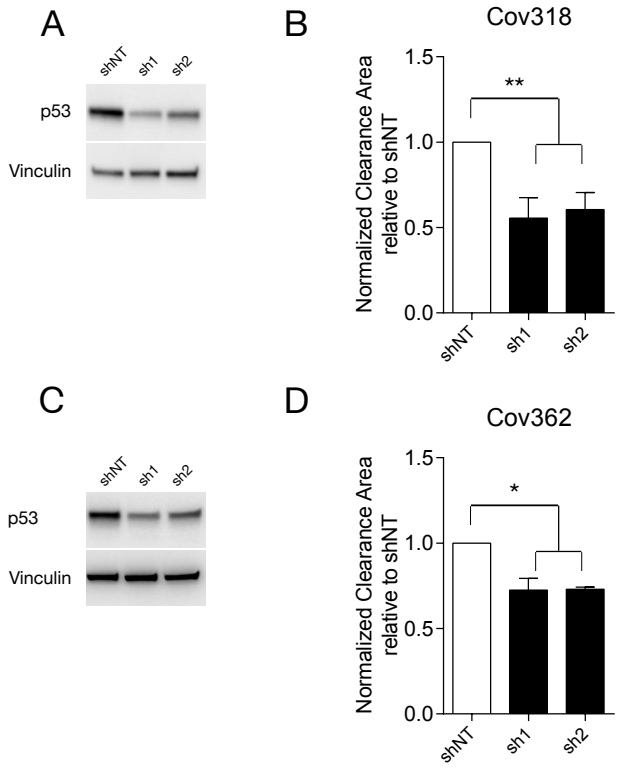

Figure 9: ***Mesothelial clearance assay of Cov318 and Cov362 TP53_silenced.*** *Western Blotting detection of p53 protein reduction after 4 days of cell induction with IPTG in* ***(A)*** *Cov318 and in* ***(C)*** *Cov362.* ***(B)*** *Cov318 and* ***(D)*** *Cov362 quantification of mesothelial clearance assay. The normalized clearance area is obtained by dividing the spheroids area at t=0 for the hole in the mesothelial at 8 hours. These results are the mean of 3 experiments.*

4.2.2. The role of mut_p53 in BC 3D colony formation

To investigate whether mut_p53 confers an invasive advantage to BC cells, we engineered MDA-MB-231 cell line to express two constitutive shRNAs that target *TP53* (Figure 10A) and tested them in 3D colony assay formation. Notably, silenced cells acquired a round shaped morphology and adhered less to cell dishes (data not shown). Four-five days after viral transduction, silenced cells stopped to proliferate (Figure 10B), which is consistent with the oncogenic function of mut_p53 (refer to paragraph Clinical implications); however, 9-10 days later, *TP53*_silenced cells would start growing again. (Figure 10B). Therefore, to avoid the effect of *TP53* silencing on cell proliferation, we decided to test 3D colony formation after 10 days from viral transduction. By these means, we observed that whereas control cells invaded the extracellular matrix and formed star-shaped colonies (Circularity count of Figure 10C), *TP53*_silenced cells despite being able to grow similarly to control cells (Area count of Figure 10C) did not invade the extracellular matrix and formed round-shaped colonies (Circularity count of Figure 10C).

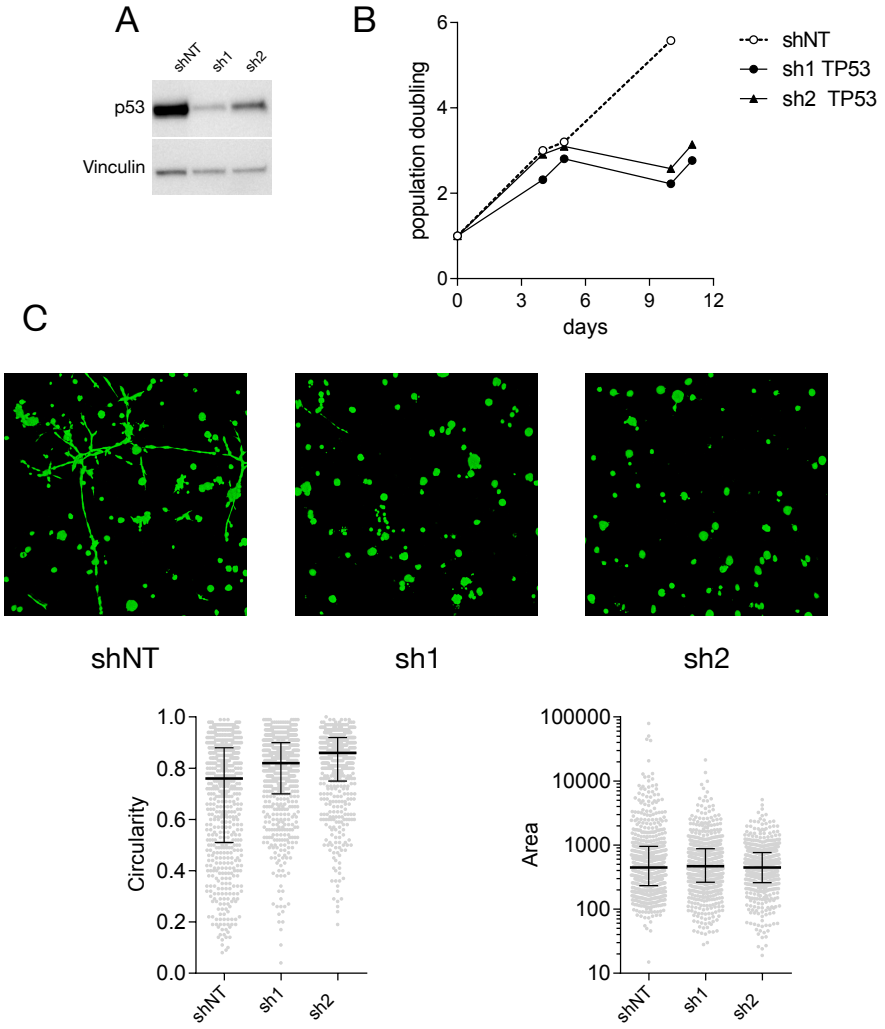

Figure 10: ***3D colony assay of MDA-MB-231 TP53_silenced. (A)*** *Western Blotting detection of p53 protein reduction.* ***(B)*** *Population doubling of MDA-MB-231.* ***(C)*** *Quantification of 3D colony circularity and representation of typical images obtained with fluorescence confocal microscopy after stained with calcein. Images were acquired 10 days after the plating. Circularity were evaluated using ImageJ. ImageJ gives a value 1 to circular colonies, whilst the more spreaded colonies are, the more the values is close to 0. A total of 10 fields were analyzed per conditions. These results are the mean of 2 experiments. Area of the colony 10 days after the plating, measured with ImageJ.*

4.3. Profile the expression of lncRNAs using RNA deep-sequencing analysis

To evaluate whether mut_p53 regulates gene expression of lncRNAs in HGSOC and in BC, we performed a RNA deep-sequencing analysis of Cov318 and MDA-MB-231 *TP53*_silenced cells.

4.3.1. Sample preparation

Because Marchese et al. described that lincRNAs are primarily enriched in the nucleus, where they regulate gene expression [363], we decided to sequence only RNA nuclear fraction. We performed a separation of nuclear and cytoplasmic fractions using the protocol described in Materials and methods section of this Thesis (Nucleus/cytoplasmic separation). To verify the quality of the obtained subcellular fractionation, we measured vinculin and histone 2AX (H2AX) protein expression, which resulted enriched in the cytosolic and nuclear fraction, respectively (Figure 11A and C). Similarly, only for Cov318, we evaluated the nuclear enrichment of one of the introns of *BNC2* protein-coding gene by qRT-PCR (Figure 11B), this analysis was not performed for MDA-MB-231 cells, because they do not express *BNC2*. To identify lncRNA genes that changed after *TP53* silencing, we performed Next Generation Sequencing (NGS) of RNA nuclear fraction in Cov318 and MDA-MB-231 silenced for *TP53* with two different shRNAs and after 11 days from viral transduction (Figure 11A and C). For each cell line, we analyzed two independent biological replicates.

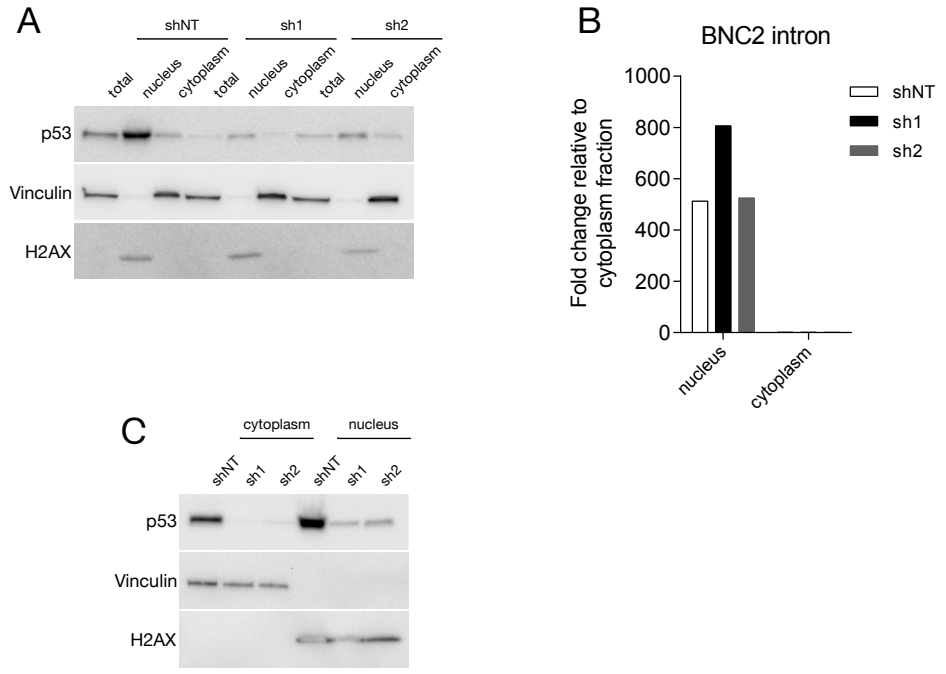

Figure 11: ***Evaluation of the correct nucleus and cytoplasmic fraction separation.*** *Western Blotting detection of vinculin and H2AX in* ***(A)*** *Cov318 and in* ***(C)*** *MDA-MB-231.* ***(B)*** *qRT-PCR analysis of BNC2 intron enrichment in Cov318 nuclear fraction.*

4.3.2. Deep-sequencing output

On average, we obtained 40 millions sequences (125nt long) per sample in Cov318 experiment, and 30 millions sequences (150nt long) per samples in MDA-MB-231 experiment. To check run quality, we used FastQC algorithm on FastQ outputs. In general, MDA-MB-231 sequences had a much better quality than Cov318 samples (Figure 12).

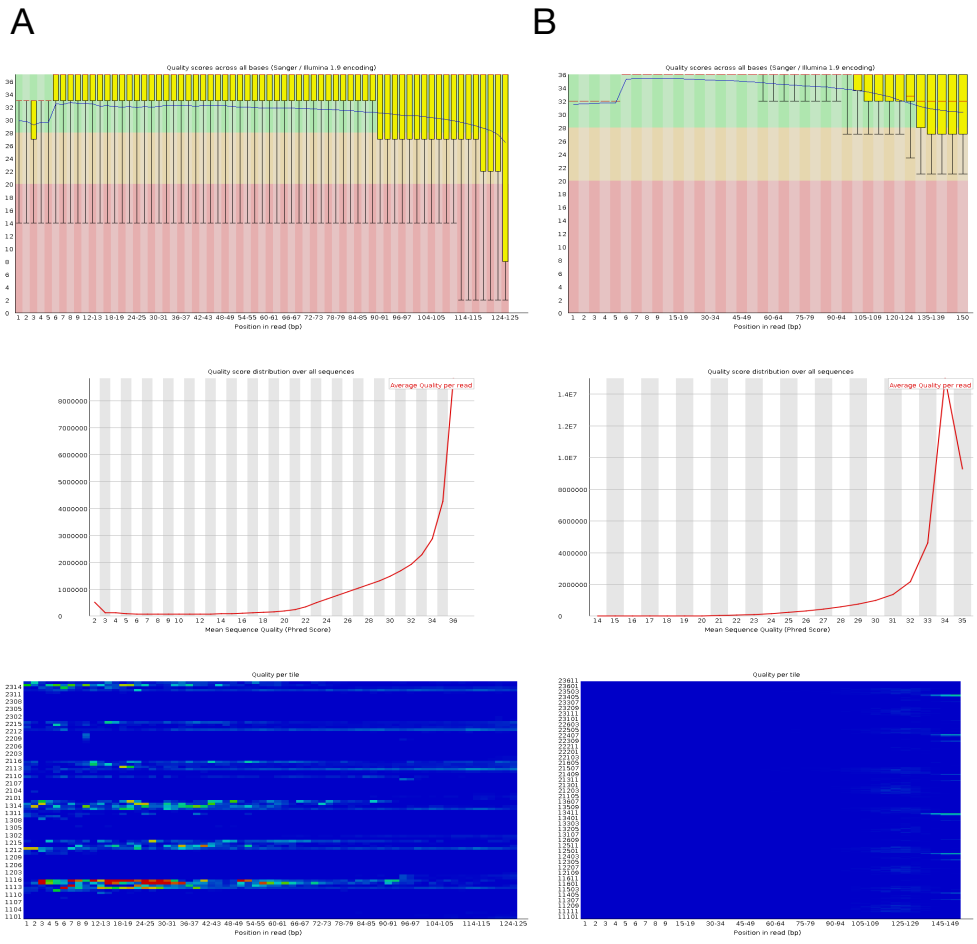

Figure 12: ***FastQ quality****. An example of output of FastQ quality evaluated with FastQC software of* ***(A)*** *Cov318 and* ***(B)*** *MDA-MB-231.*

To analyze data obtained from NGS runs, we used two different strategies: the first analyzed reads based on transcripts (each gene has multiple transcripts that are individually counted), the second analyzed reads according to gene locus (all reads aligned to a gene locus are summed).

4.3.3. Transcript differentially expressed

In this analysis, we used a standard pipeline of RNA deep-sequencing analysis as described in Figure 13. We set a minimum base quality score of 30 and we removed adapter sequences using Trimmomatic [364]. We mapped reads longer than 50nt allowing 2 mismatches to the reference genome (Gencode V25) using the software Salmon [365] . To perform differential expression analysis, we used edgeR package of R [366]. By comparing *TP53* silenced samples to controls in Cov318, we obtained 721 transcripts differentially expressed (FDR ≤ 0.05), among these 361 are annotated as protein-coding transcripts in GencodeV25 and 360 are annotated as ncRNAs (in particular 105 are processed transcripts, 91 retained introns, 48 nonsense-mediated decays and 33 are lincRNAs). Among the 721 transcripts, 292 are downregulated instead 429 are upregulated when mut_p53 is silenced. For MDA-MB-231, we obtained 69 transcripts differentially expressed (FDR ≤ 0.05), among these 56 are annotated as protein-coding transcripts in GencodeV25 and 13 are annotated as ncRNAs (in particular 4 retained introns, 4 are processed transcripts, 3 nonsense-mediated decays and only 1 are lincRNA). Among the 69 transcripts, 3 are downregulated instead 63 are upregulated when mut_p53 is silenced.

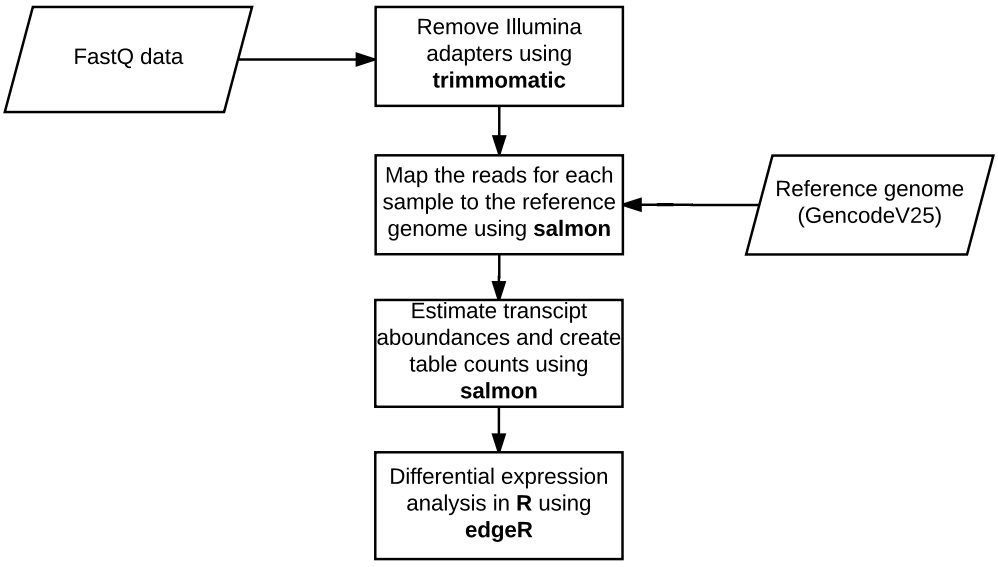

Figure 13: ***Deep-sequencing analysis pipeline to identify transcripts differentially expressed.***

To validate Cov318 and MDA-MB-231 analysis, we selected non_coding transcripts with a FDR less than 0.05 and with an absolute logFC value higher than 1.

We designed qRT-PCR primers for each candidate ncRNA transcript, and tested their gene expression levels on the cytoplasmic and nuclear RNA fraction of Cov318 and MDA-MB_231 cell lines. Unfortunately, we found that all these transcripts except one (*TERC*) were not detectable, so we decided to use a different strategy.

4.3.4. Gene locus differentially expressed analysis

While we analyzed the data based on transcripts, we realized that because we sequenced samples derived from the RNA nuclear fraction, many reads matched to the intronic part of genes (both coding and non-coding), which is certainly expected, because typically introns are retained in the nucleus and soon degraded (Figure 11B). At the same time, intronic reads are still a read-out of gene transcription and regulation; but more importantly, regulatory elements of gene expression (promoters and enhancers) located within or close to gene transcripts generate reads that do not participate to transcript synthesis but are a read-out of the regulatory element activity [367]. Therefore, we reasoned that because we sequenced nuclear RNA), the first transcript-centric approach lost several layers of information; whereas, a gene-centric approach could be more informative. In the gene-centric approach, we considered as gene unit not only the exonic part but also the intronic and the regulatory regions of the gene unit itself. To this aim, we set up a custom pipeline (Figure 14). To generate the library of human gene units, we started from *Homo sapiens* grch37 reference genome, and we merged the genomic intervals of all transcripts annotated to the same gene thus generating the most comprehensive interval for each gene unit. We mapped reads to the gene units library using Hisat2 software [368], assembled the genes and estimated their abundances utilizing the software Featurecounts [369]. To perform differential expression analysis, we used DESeq2 package[370] in R.

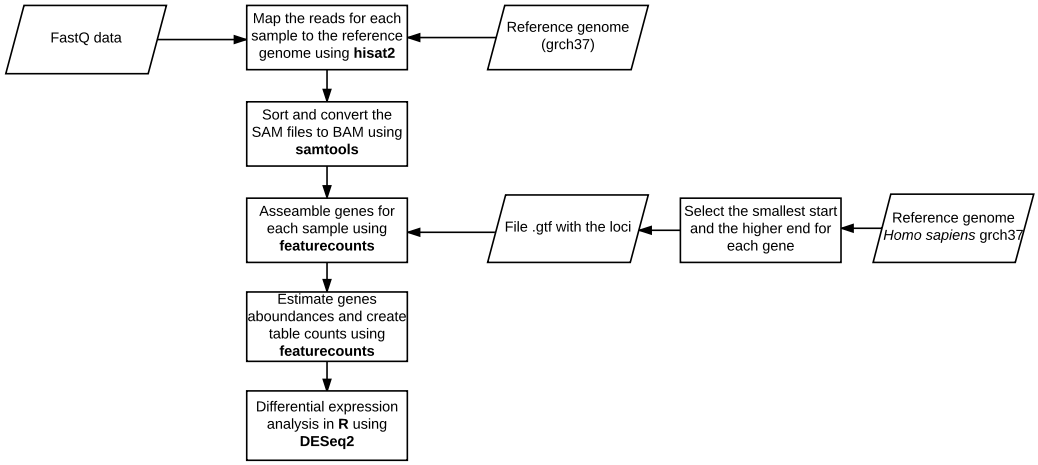

Figure 14: ***Deep-sequencing analysis pipeline to identify genes differentially expressed.***

By comparing *TP53* silenced samples to controls in Cov318, we obtained 806 genes differentially expressed (adj_pvalue ≤ 0.05), among these 680 are annotated as protein-coding genes in GencodeV24 and 126 are annotated as ncRNAs (in particular 62 are lincRNAs and 23 antisense) (Figure 15A). Among the 806 genes, 341 are downregulated whereas 465 are upregulated when *TP53* is silenced. For MDA-MB-231, we found 1820 genes differentially expressed (adj_pvalue ≤ 0.05): 1616 are annotated as protein-coding genes and 204 as ncRNAs (among these 99 as lincRNAs and 38 as antisense) (Figure 15B). Among 1820, 725 are downregulated and 1095 are upregulated when *TP53* is silenced.

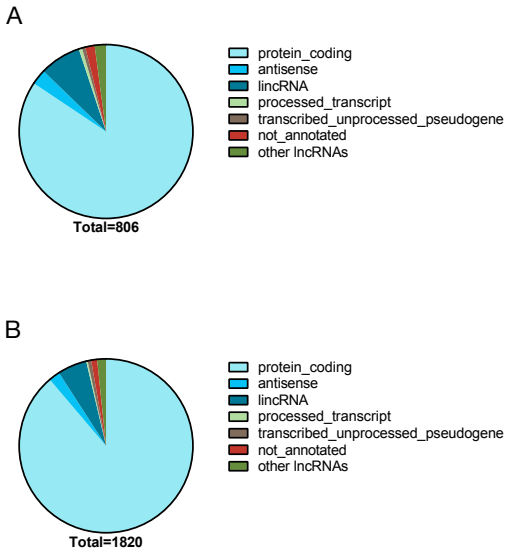

Figure 15: ***Gene types of genes differentially expressed in (A) Cov318 and in (B) M231.***

To validate Cov318 and MDA-MB-231 analysis, for each cell line, we selected the 10 lncRNA transcripts with the lowest adj_pvalue and 2 significant transcripts that changed concordantly in both cell lines. Only gene units with a normalized baseMean read count greater than 20 were included (Table 5 and Table 6).

Gene	Gene_id	GeneType	Log_2FC	padj	qRT-PCR Ct nuclear fraction
RP11-108P20.2	ENSG00000267501	lincRNA	1,365474	0,0000006	28,9
RP11-362F19.1	ENSG00000248810	lincRNA	-0,770444	0,0000055	20,6
RP11-25I15.3	ENSG00000257114	lincRNA	0,826190	0,0000859	22,3
RMRP	ENSG00000269900	lincRNA	0,819893	0,0003735	18,8
AC016710.1	ENSG00000229131	lincRNA	0,894757	0,0013520	26,6
LINC00621	ENSG00000262619	lincRNA	0,540043	0,0027134	22,3
AP001628.6	ENSG00000225218	lincRNA	0,718073	0,0047863	29,7
TERC	ENSG00000270141	lincRNA	0,971149	0,0050568	27,7
RP11-176D17.3	ENSG00000228470	sense_overlapping	0,732544	0,0069626	24,5
RP11-7F17.7	ENSG00000258602	lincRNA	0,885050	0,0077469	24,7
SCARNA2	ENSG00000270066	lincRNA	0,949619	0,0007345	26,1
BAIAP2-AS1	ENSG00000226137	lincRNA	0,818278	0,0253519	25,4

Table 5: ***Genes chose to be validated in Cov318****.*

Gene	Gene_id	GeneType	Log_2FC	padj	qRT-PCR Ct nuclear fraction
RP11-166D19.1	ENSG00000255248	sense_overlapping	-0,826360	0,0000044	20,3
RP11-244M2.1	ENSG00000267374	lincRNA	-0,796658	0,0000055	23,1
AC034220.3	ENSG00000233006	processed_transcript	0,762843	0,0000454	24,5
LINC00704	ENSG00000231298	lincRNA	-0,889951	0,0000459	20,9
MALAT1	ENSG00000251562	lincRNA	0,920520	0,0005078	15,1
RP11-527N22.2	ENSG00000253746	lincRNA	-1,025881	0,0006195	23,6
LINC01547	ENSG00000183250	lincRNA	0,915840	0,0018320	26,2
RP11-47A8.5	ENSG00000272933	lincRNA	1,198957	0,0029381	29,7
MIR100HG	ENSG00000224184	lincRNA	-0,863958	0,0040484	18,7
LINC00472	ENSG00000233237	lincRNA	0,535488	0,0072904	22,6
SCARNA2	ENSG00000270066	lincRNA	0,566727	0,0405347	26,7
BAIAP2-AS1	ENSG00000226137	lincRNA	0,739713	0,0118158	27,1

Table 6: ***Genes chose to be validated in MDA-MB-231****.*

4.3.5. Deep-sequencing validation in mut_p53 cell models

To validate candidate lncRNAs, we first tested their expression through qRT-PCR in the cytoplasmic and nuclear fraction of Cov318 and MDA-MB_231 parental cell lines. To distinguish expressed from not expressed lncRNAs, based on our experience, we set an arbitrary threshold of gene expression of 28 threshold cycles (Ct) in the RNA nuclear fraction that was satisfied by 8 out 10 lncRNAs in Cov318 and by 9 out of 10 in MDA-MB-231 (Table 5 and Table 6). Moreover, we confirmed the enrichment of lncRNA in the nuclear respect to cytoplasmic fraction of Cov318 and MDA-MB_231 parental cell lines (Figure 16A, B and C).

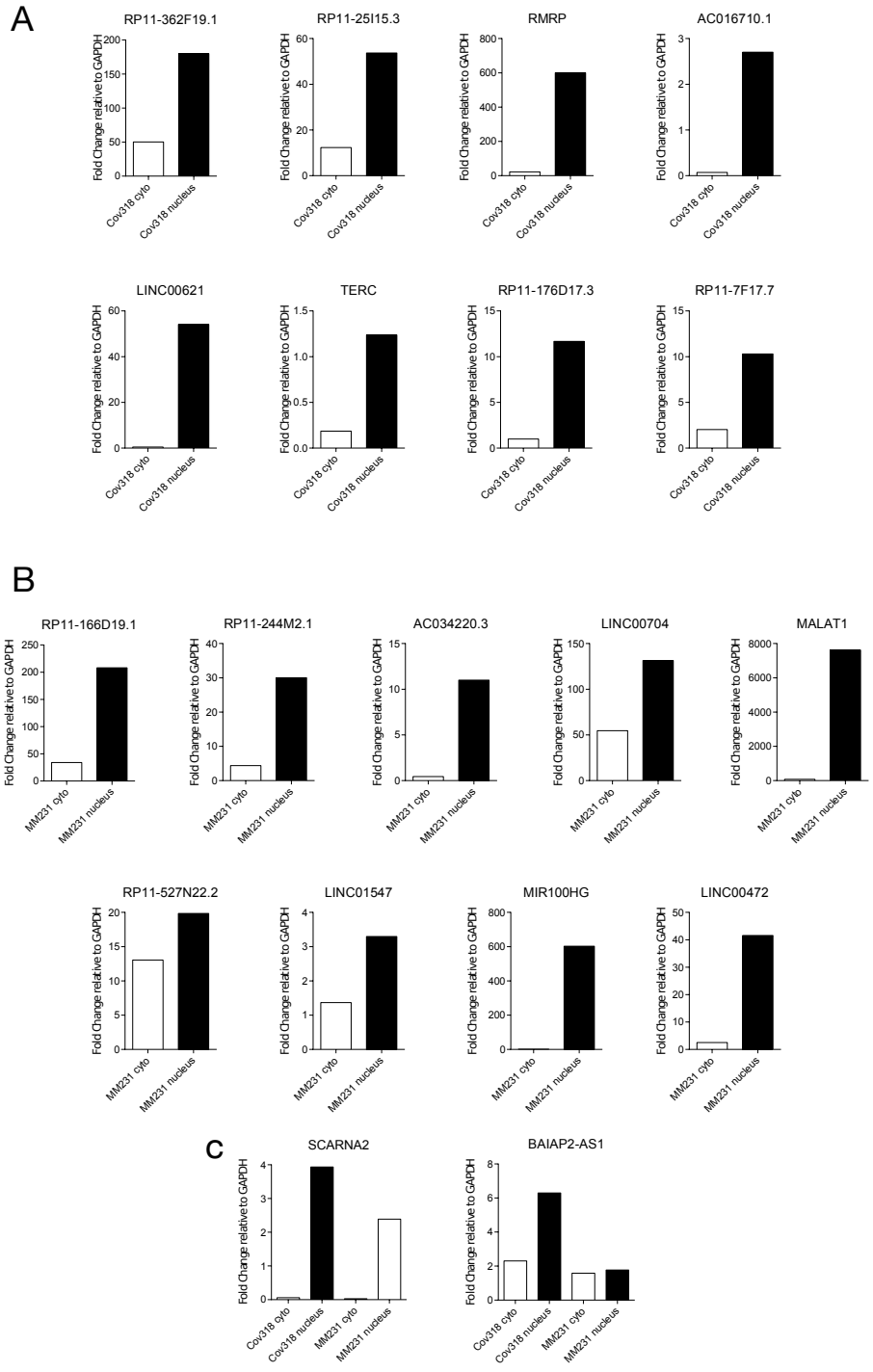

Figure 16: ***Expression of selected genes in cytoplasmic and nuclear fraction****. qRT-PCR analysis of 10 different candidate genes specific for* ***(A)*** *Cov318,* ***(B)*** *MDA-MB-231 and* ***(C)*** *in common among these two cell lines. Gene expressions are evaluated in nuclear and cytoplasmic fraction.*

Next, we investigated gene expression of candidate lncRNAs in *TP53* silenced cells. In Cov318, we found that only two genes changed consistently between NGS and qRT-

PCR data (Figure 17A); in MDA-MB-231, we confirmed 8 out 9 lncRNAs BC-specific candidates (Figure 17B).

Based on the poorer quality of Cov318 runs and poorer confirmation on qRT-PCR tests, we decided to focus only on MDA-MB-231.

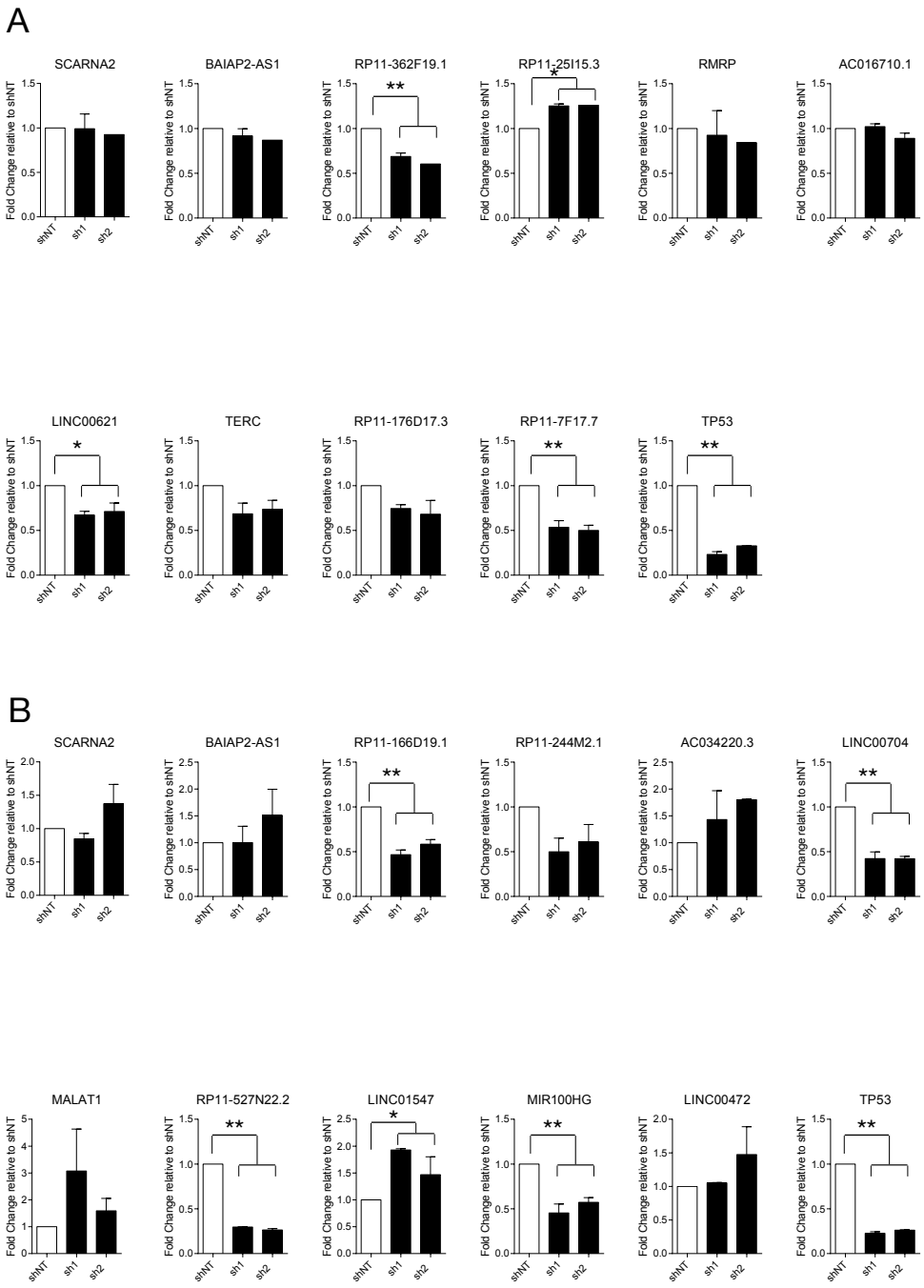

Figure 17: ***Validation of candidate genes.*** *Gene expression are evaluated in the nuclear fraction of* ***(A)*** *Cov318 and* ***(B)*** *MDA-MB-231 TP53_silenced.*

4.3.6. Deep-sequencing validation in wt_p53 cell models

TP53 missense mutants can retain part of wt_p53 transcription activity, which means that activation of wt_p53 and mut_p53 can have equal effect on common targets [371]. To exclude that our candidate BC-specific lncRNAs were common targets of wt_p53 and mut_p53, we evaluated their expression levels in a wt_p53 BC cell line (MCF10a) after exposure to Nutlin-3, a compound that inhibits Mdm2-p53 interaction thus preventing p53 degradation. Nutlin-3 treatment increased expression levels of p53 and *CDKN1A*, a direct target of wt_p53 (Figure 18A). In this same cell model, we discovered that 1 out of 9 lncRNAs was not expressed, that 1 candidate lncRNA was equally regulated by wt_p53 and mut_p53 and 3 lncRNAs were not regulated by wt_p53; whereas the remaining 3 lncRNAs were regulated oppositely by wt_p53 and mut_p53 (Figure 18B).

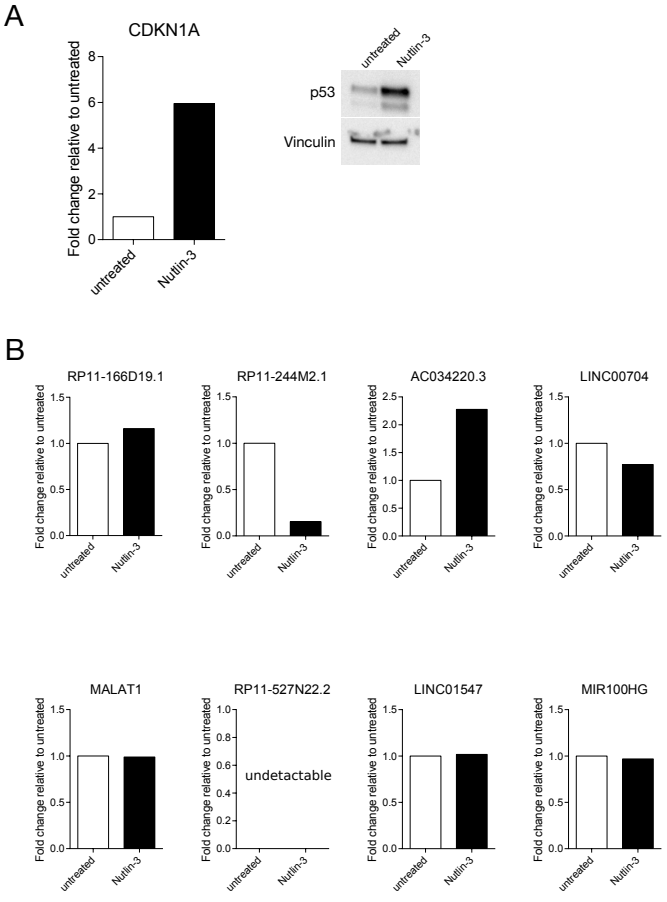

Figure 18: ***Expression of BC candidate genes in wt_p53 BC cell line. (A)*** *qRT-PCR analysis of CDKN1A overexpression (left) and Western Blotting detection of p53 accumulation (right) after treatment with Nutlin-3 for 24 hours in MCF10a.* ***(B)*** *qRT-PCR analysis of candidate genes regulated by mut_p53.*

5. Discussion

Several common features characterize OvCa and BC, among these there are the high rate of mutations in *TP53* and form tumor metastasis. Since several studies have demonstrated that mut_p53 GOF promotes tumor metastasis, but the molecular mechanisms are not fully characterized, we investigate whether lncRNAs participate in mut_p53 GOF. Indeed, some lncRNAs participate in wt_p53 pathway, but little is known about the role of lncRNAs on mut_p53 GOF.

In particular, OvCa metastasizes the peritoneum after tumor cell clusters survived in the ascetic fluid and adhered and invaded the peritoneum. To study the ability of *TP53*_silenced cells to invade the mesothelium, we performed the *in vitro* mesothelial clearance assay [354], that resembles the interaction occurring *in vivo* between OvCa cell spheroids and peritoneum mesothelial cells. We observed that mut_p53 increases the ability of Cov318 and Cov362 OvCa cell lines to invade and spread the peritoneum, in agreement with Iwanicki et al. [372]. Using this assay, Davidowitz and colleagues demonstrated that OvCa cell use an integrin-dependent activation of myosin which induces a traction force to promote mesothelial displacement and integrin α5β1 (a fibronectin receptor) is the most important marker in this process [361]. Nevertheless, we found that Cov318 clearance ability is not integrin α5 dependent, since Cov318 does not express it. At the same time, they found that mesenchymal genes expression (e.g. vimentin) correlates with mesothelial clearance ability; whereas, epithelial genes expression (e.g. E-cadherin, claudin7 and HER3) inversely correlates with clearance ability [360]. However, in our models, we did not find apparent correlation with cells intrinsic mesothelial clearance ability and the expression of EMT genes.

Likewise, we observed that mut_p53 increased MDA-MB-231 ability to invade extracellular matrix when plated in a 3D Matrigel culture. We noticed that 4-5 days after transduction, *TP53*_silenced cells stopped to grow. To avoid this bias, we waited 9-10 days after viral transduction, when cells started growing again, before evaluating the effect of mut_p53 silencing on invasion. Indeed, in the 3D Matrigel colony formation we observed that cell colonies silenced or not for mut_p53 are similar for dimension, but differ for the shape: control colonies were star-shaped, whereas *TP53*_silenced

cells colonies were round-shaped. Round-shape colonies have a typical epithelial morphology and correlate to a less invasive phenotype, whereas the star-shaped colonies are more protrusive and acquired mesenchymal characteristics that indicate a more invasive phenotype.

To investigate whether lncRNAs are involved in mut_p53 GOF, we sequenced the nuclear RNA fraction of Cov318 and MDA_MB_231 after *TP53*_silencing. First, we performed a standard pipeline of RNA deep-sequencing analysis to identify the lncRNA transcripts differentially expressed, but none of the selected transcripts were detectable at qRT-PCR. This can be explained because lncRNA are typically expressed at a very low level and often several transcripts are present for the same gene. Indeed, in this first analysis, significant transcripts were among those less expressed. For this reason, we choose to consider not the transcripts, but the genetic locus that encodes for a lncRNA and we set up a custom pipeline. When we performed this new analysis, we obtained genes detectable at qRT-PCR and we choose to validate the first 10 more differentially expressed and 2 in common between HGSOC and BC cell models.
For Cov318, we were able to confirm through qRT-PCR only 2 lncRNAs obtained by NGS; whereas, in MDA-MB-231, we validated all the BC specific lncRNAs tested. We supposed this difference among Cov318 and MDA-MB-231 could be due to lower quality of Cov318 RNA sequenced or maybe some problems occurred during NGS run, as demonstrated by the FastQC output report. For these reasons, we focused our attention to MDA-MB-231, but we also plan to further investigate also two lncRNAs (RP11-362F19.1 and RP11-25I15.3) differentially expressed in Cov318 *TP53*_silenced. Using a wt_p53 BC cell model (MCF10a) treated with Nutlin-3 (an inhibitor of Mdm2) to overexpress wt_p53, we evaluated the BC-specific lncRNAs to excluded lncRNAs that are regulated both by wt_p53 and mut_p53. We found that 1 out of 9 lncRNAs was not expressed (*RP11-527N22.2*), indicating its expression was cell model specific; 1 lncRNA was regulated both by wt_p53 and mut_p53 (*RP11-166D19.1*), 3 lncRNAs were not regulated by wt_p53 (*MALAT1*, *LINC01547* and *MIR100HG*) and 3 lncRNAs were regulated oppositely by wt_p53 and mut_p53 (*RP11-244M2.1*, *AC034220.3* and *LINC00704*).

Interestingly, *LINC00704* expression predicts BC recurrence [373]. Our data are in agreement with this study, since *LINC00704* is significantly downregulated in *TP53*_silenced BC cell line, indicating a possible oncogenic role.

MIR100HG is a polycistronic miRNA host gene of miR-100, let-7a-2 and miR-125b-1. *MIR100HG*-derived miRNAs and MIR99AHG-derived miRNAs, participate in the pathogenesis of acute megakaryoblastic leukemia [374] and levels of *MIR100HG* are associated with a poor prognosis in cervical cancer [375], whereas its expression is reduced in BC, due to its hypermethylation [376]. Moreover, *MIR100HG* confers cetuximab resistance in colorectal cancer and in head and neck squamous cell cancer cell lines [377].

MALAT1 is one of the first lncRNAs studied, it is involved in several cellular processes (such as alternative splicing, nuclear organization, epigenetic modulation of gene expression) and it is related to several diseases. In cancer, it has been associated with an aggressive phenotype, in terms of cell proliferation and metastasis. It is localized to nuclear speckles, where regulated splicing. A study of Pruszko and et. demonstrates that in BC mut_p53 and the protein ID4 directly or indirectly delocalize *MALAT1* from nuclear speckles promoting its association with chromatin and allowing the formation of a complex with the splicing factor SRSF1. This enables *MALAT1* to control the expression of different isoforms of pre-mRNA [378]. These observations are in disaccord with our data, since we observed an increase of *MALAT1* expression when *TP53* is silenced.

Finally, our future plan is to investigate the impact of candidate lncRNAs on MDA-MB-231 ability to invade and proliferate. Our strategy will be to use CRISPR-Cas9 tool to change lncRNAs expression. Specifically, we will use a nuclease dead Cas9 (dCas9) molecule that cannot cleave target DNA but retains the ability to bind to target DNA based on the gRNA targeting sequence. dCas9 is tagged with transcriptional repressors (e.g. KRAB) or activators (e.g. VP64) and when dCas9 bind the promoter of the target lncRNA, it can repress or activate its transcription.

6. Bibliography

1. Levine, A. J. p53, the cellular gatekeeper for growth and division. *Cell* **88,** 323–331 (1997).
2. Vogelstein, B., Lane, D. & Levine, A. J. Surfing the p53 network. *Nature* **408,** 307–310 (2000).
3. Lane, D. P. Cancer. p53, guardian of the genome. *Nature* **358,** 15–16 (1992).
4. Lane, D. P. & Crawford, L. V. T antigen is bound to a host protein in SV40-transformed cells. *Nature* **278,** 261–263 (1979).
5. Linzer, D. I. H. & Levine, A. J. Characterization of a 54K Dalton cellular SV40 tumor antigen present in SV40-transformed cells and uninfected embryonal carcinoma cells. *Cell* **17,** 43–52 (1979).
6. Finlay, C. A., Hinds, P. W. & Levine, A. J. The p53 proto-oncogene can act as a suppressor of transformation. *Cell* **57,** 1083–1093 (1989).
7. Joerger, A. C. & Fersht, A. R. The tumor suppressor p53: from structures to drug discovery. *Cold Spring Harbor perspectives in biology* **2,** (2010).
8. Cadwell, C. & Zambetti, G. P. The effects of wild-type p53 tumor suppressor activity and mutant p53 gain-of-function on cell growth. *Gene* **277,** 15–30 (2001).
9. Lu, H. & Levine, A. J. Human TAFII31 protein is a transcriptional coactivator of the p53 protein. *Proc. Natl. Acad. Sci. U. S. A.* **92,** 5154–8 (1995).
10. Thut, C. J., Chen, J. L., Klemm, R. & Tjian, R. p53 transcriptional activation mediated by coactivators TAFII40 and TAFII60. *Science* **267,** 100–4 (1995).
11. Seto, E. *et al.* Wild-type p53 binds to the TATA-binding protein and represses transcription. *Proc. Natl. Acad. Sci.* **89,** 12028–12032 (1992).
12. Xiao, H. *et al.* Binding of basal transcription factor TFIIH to the acidic activation domains of VP16 and p53. *Mol. Cell. Biol.* **14,** 7013–7024 (1994).
13. Chao, C. *et al.* p53 transcriptional activity is essential for p53-dependent apoptosis following DNA damage. *EMBO J.* **19,** 4967–75 (2000).
14. Gu, W., Shi, X. L. & Roeder, R. G. Synergistic activation of transcription by CBP and p53. *Nature* **387,** 819–823 (1997).
15. Grossman, S. R. p300/CBP/p53 interaction and regulation of the p53 response. *European Journal of Biochemistry* **268,** 2773–2778 (2001).
16. Lill, N. L., Grossman, S. R., Ginsberg, D., DeCaprio, J. & Livingston, D. M. Binding and modulation of p53 by p300/CBP coactivators. *Nature* **387,** 823–827 (1997).
17. Marine, J. C. *et al.* Keeping p53 in check: Essential and synergistic functions of Mdm2 and Mdm4. *Cell Death and Differentiation* **13,** 927–934 (2006).

18. Toledo, F. & Wahl, G. M. Regulating the p53 pathway: In vitro hypotheses, in vivo veritas. *Nature Reviews Cancer* **6,** 909–923 (2006).
19. Momand, J., Wu, H. H. & Dasgupta, G. MDM2--master regulator of the p53 tumor suppressor protein. *Gene* **242,** 15–29 (2000).
20. Müller-Tiemann, B. F., Halazonetis, T. D. & Elting, J. J. Identification of an additional negative regulatory region for p53 sequence-specific DNA binding. *Proc. Natl. Acad. Sci. U. S. A.* **95,** 6079–6084 (1998).
21. Petitjean, A. *et al.* Impact of mutant p53 functional properties on TP53 mutation patterns and tumor phenotype: Lessons from recent developments in the IARC TP53 database. *Hum. Mutat.* **28,** 622–629 (2007).
22. Cho, Y., Gorina, S., Jeffrey, P. & Pavletich, N. Crystal structure of a p53 tumor suppressor-DNA complex: understanding tumorigenic mutations. *Science (80-.).* **265,** 346–355 (1994).
23. Cañadillas, J. M. P. *et al.* Solution structure of p53 core domain: structural basis for its instability. *Proc. Natl. Acad. Sci. U. S. A.* **103,** 2109–14 (2006).
24. Wang, Y., Rosengarth, A. & Luecke, H. Structure of the human p53 core domain in the absence of DNA. *Acta Crystallogr. Sect. D Biol. Crystallogr.* **63,** 276–281 (2007).
25. Bullock, A. N., Henckel, J. & Fersht, A. R. Quantitative analysis of residual folding and DNA binding in mutant p53 core domain: definition of mutant states for rescue in cancer therapy. *Oncogene* **19,** 1245–1256 (2000).
26. Butler, J. S. & Loh, S. N. Structure, function, and aggregation of the zinc-free form of the p53 DNA binding domain. *Biochemistry* **42,** 2396–2403 (2003).
27. Balagurumoorthy, P. *et al.* Four p53 DNA-binding domain peptides bind natural p53-response elements and bend the DNA (cooperative DNA binding/DNA bending/cyclization). *Biochemistry* **92,** 8591–8595 (1995).
28. Qian, H., Wang, T., Naumovski, L., Lopez, C. D. & Brachmann, R. K. Groups of p53 target genes involved in specific p53 downstream effects cluster into different classes of DNA binding sites. *Oncogene* **21,** 7901–7911 (2002).
29. Weinberg, R. L., Veprintsev, D. B., Bycroft, M. & Fersht, A. R. Comparative binding of p53 to its promoter and DNA recognition elements. *J. Mol. Biol.* **348,** 589–596 (2005).
30. Wang, Y. *et al.* p53 domains: Identification and characterization of two autonomous DNA- binding regions. *Genes Dev.* **7,** 2575–2586 (1993).
31. Friedman, P. N., Chen, X., Bargonetti, J. & Prives, C. The p53 protein is an unusually shaped tetramer that binds directly to DNA. *Proc. Natl. Acad. Sci. U. S. A.* **90,** 3319–3323 (1993).

32. Prives, C. & Manley, J. L. Why is p53 acetylated? *Cell* **107,** 815–818 (2001).
33. Weinberg, R. L., Freund, S. M. V, Veprintsev, D. B., Bycroft, M. & Fersht, A. R. Regulation of DNA binding of p53 by its C-terminal domain. *J. Mol. Biol.* **342,** 801–811 (2004).
34. Friedler, A., Veprintsev, D. B., Freund, S. M. V., Von Glos, K. I. & Fersht, A. R. Modulation of binding of DNA to the C-terminal domain of p53 by acetylation. *Structure* **13,** 629–636 (2005).
35. Bell, S., Klein, C., Müller, L., Hansen, S. & Buchner, J. p53 contains large unstructured regions in its native state. *J. Mol. Biol.* **322,** 917–927 (2002).
36. Liu, J. *et al.* Intrinsic disorder in transcription factors. *Biochemistry* **45,** 6873–6888 (2006).
37. Dunker, A. K., Cortese, M. S., Romero, P., Iakoucheva, L. M. & Uversky, V. N. Flexible nets: The roles of intrinsic disorder in protein interaction networks. *FEBS Journal* **272,** 5129–5148 (2005).
38. Sakaguchi, K. *et al.* Effect of phosphorylation on tetramerization of the tumor suppressor protein p53. in *Journal of Protein Chemistry* **16,** 553–556 (1997).
39. Bode, A. M. & Dong, Z. Post-translational modification of p53 in tumorigenesis. *Nature Reviews Cancer* **4,** 793–805 (2004).
40. Lavin, M. F. & Gueven, N. The complexity of p53 stabilization and activation. *Cell Death and Differentiation* **13,** 941–950 (2006).
41. Vousden, K. H. & Prives, C. Blinded by the Light: The Growing Complexity of p53. *Cell* **137,** 413–431 (2009).
42. Haupt, Y., Maya, R., Kazaz, A. & Oren, M. Mdm2 promotes the rapid degradation of p53. *Nature* **387,** 296–299 (1997).
43. Honda, R., Tanaka, H. & Yasuda, H. Oncoprotein MDM2 is a ubiquitin ligase E3 for tumor suppressor p53. *FEBS Lett.* **420,** 25–27 (1997).
44. Kubbutat, M. H. G., Jones, S. N. & Vousden, K. H. Regulation of p53 stability by Mdm2. *Nature* **387,** 299–303 (1997).
45. Shieh, S. Y., Ikeda, M., Taya, Y. & Prives, C. DNA damage-induced phosphorylation of p53 alleviates inhibition by MDM2. *Cell* **91,** 325–334 (1997).
46. El-Deiry, W. S. Regulation of p53 downstream genes. *Seminars in Cancer Biology* **8,** 345–357 (1998).
47. Bensaad, K. & Vousden, K. H. p53: new roles in metabolism. *Trends in Cell Biology* **17,** 286–291 (2007).
48. Yu, J. & Zhang, L. No PUMA, no death: Implications for p53-dependent apoptosis. *Cancer Cell* **4,** 248–249 (2003).
49. Kortlever, R. M., Higgins, P. J. & Bernards, R. Plasminogen activator inhibitor-1 is a

critical downstream target of p53 in the induction of replicative senescence. *Nat. Cell Biol.* **8,** 878–884 (2006).

50. Leal, J. F. M. *et al.* Cellular senescence bypass screen identifies new putative tumor suppressor genes. *Oncogene* **27,** 1961–1970 (2008).
51. Brown, J. P., Wei, W. & Sedivy, J. M. Bypass of senescenoe after disruption of p21(CIP1)/(WAF1) gene in normal diploid human fibroblasts. *Science (80-.).* **277,** 831–834 (1997).
52. Liu, B., Chen, Y. & St. Clair, D. K. ROS and p53: A versatile partnership. *Free Radical Biology and Medicine* **44,** 1529–1535 (2008).
53. Sablina, A. A. *et al.* The antioxidant function of the p53 tumor suppressor. *Nat. Med.* **11,** 1306–1313 (2005).
54. DeBerardinis, R. J., Lum, J. J., Hatzivassiliou, G. & Thompson, C. B. The Biology of Cancer: Metabolic Reprogramming Fuels Cell Growth and Proliferation. *Cell Metabolism* **7,** 11–20 (2008).
55. Jones, R. G. *et al.* AMP-activated protein kinase induces a p53-dependent metabolic checkpoint. *Mol. Cell* **18,** 283–293 (2005).
56. Budanov, A. V. & Karin, M. p53 Target Genes Sestrin1 and Sestrin2 Connect Genotoxic Stress and mTOR Signaling. *Cell* **134,** 451–460 (2008).
57. Feng, Z. *et al.* The regulation of AMPK B1, TSC2, and PTEN expression by p53: Stress, cell and tissue specificity, and the role of these gene products in modulating the IGF-1-AKT-mTOR pathways. *Cancer Res.* **67,** 3043–3053 (2007).
58. Crighton, D. *et al.* DRAM, a p53-Induced Modulator of Autophagy, Is Critical for Apoptosis. *Cell* **126,** 121–134 (2006).
59. Mathew, R., Karantza-Wadsworth, V. & White, E. Role of autophagy in cancer. *Nat Rev Cancer* **7,** 961–967 (2007).
60. Kawauchi, K., Araki, K., Tobiume, K. & Tanaka, N. p53 regulates glucose metabolism through an IKK-NF-kappaB pathway and inhibits cell transformation. *Nat. Cell Biol.* **10,** 611–618 (2008).
61. Bensaad, K. *et al.* TIGAR, a p53-Inducible Regulator of Glycolysis and Apoptosis. *Cell* **126,** 107–120 (2006).
62. Kondoh, H. *et al.* Glycolytic enzymes can modulate cellular life span. *Cancer Res.* **65,** 177–185 (2005).
63. Ma, W., Sung, H. J., Park, J. Y., Matoba, S. & Hwang, P. M. A pivotal role for p53: Balancing aerobic respiration and glycolysis. *Journal of Bioenergetics and Biomembranes* **39,** 243–246 (2007).
64. Teodoro, J. G., Evans, S. K. & Green, M. R. Inhibition of tumor angiogenesis by p53:

A new role for the guardian of the genome. *Journal of Molecular Medicine* **85,** 1175–1186 (2007).

65. Hollstein, M., Sidransky, D., Vogelstein, B. & Harris, C. C. P53 Mutations in Human Cancers. *Science (80-.).* **253,** 49–53 (1991).
66. Kandoth, C. *et al.* Mutational landscape and significance across 12 major cancer types. *Nature* **502,** 333–339 (2013).
67. Tommasino, M. *et al.* The role of TP53 in cervical carcinogenesis. *Human Mutation* **21,** 307–312 (2003).
68. Wong, P. *et al.* Prevalence of early onset colorectal cancer in 397 patients with classic Li-Fraumeni syndrome. *Gastroenterology* **130,** 73–79 (2006).
69. Li, F. P. *et al.* A Cancer Family Syndrome in Twenty-four Kindreds. *Cancer Res.* **48,** 5358–5362 (1988).
70. Olivier, M. *et al.* Li-Fraumeni and Related Syndromes: Correlation between Tumor Type, Family Structure, and TP53 Genotype. *Cancer Res.* **63,** 6643–6650 (2003).
71. Malkin, D. *et al.* Germ line p53 mutations in a familial syndrome of breast cancer, sarcomas, and other neoplasms. *Science (80-.).* **250,** 1233–1238 (1990).
72. Whibley, C., Pharoah, P. D. P. & Hollstein, M. p53 polymorphisms: Cancer implications. *Nature Reviews Cancer* **9,** 95–107 (2009).
73. Wang, Y. *et al.* TP53 mutations in early-stage ovarian carcinoma, relation to long-term survival. *Br. J. Cancer* **90,** 678–685 (2004).
74. Wang, S. *et al.* Effect of TP53 codon 72 and MDM2 SNP309 polymorphisms on survival of gastric cancer among patients who receiving 5-fluorouracil-based postoperative adjuvant chemotherapy. *Cancer Chemother. Pharmacol.* **71,** 1073–1082 (2013).
75. Langerod, A. AL *et al.* TP53 mutation status and gene expression profiles are powerful prognostic markers of breast cancer. *Breast Cancer Res.* **9,** R30 (2007).
76. Olivier, M., Hollstein, M. & Hainaut, P. TP53 mutations in human cancers: origins, consequences, and clinical use. *Cold Spring Harbor perspectives in biology* **2,** (2010).
77. Olivier, M. *et al.* The IARC TP53 database: New online mutation analysis and recommendations to users. *Human Mutation* **19,** 607–614 (2002).
78. Hainaut, P. & Hollstein, M. p53 and Human Cancer: The First Ten Thousand Mutations. *Adv. Cancer Res.* **77,** 81–137 (1999).
79. Jones, P. A., Rideout, W. M., Shen, J. -C, Spruck, C. H. & Tsai, Y. C. Methylation, mutation and cancer. *BioEssays* **14,** 33–36 (1992).
80. Joerger, A. C. & Fersht, A. R. Structure-function-rescue: The diverse nature of common p53 cancer mutants. *Oncogene* **26,** 2226–2242 (2007).

81. Kern, S. E. *et al.* Oncogenic forms of p53 inhibit p53-regulated gene expression. *Science* **256,** 827–30 (1992).
82. Dittmer, D. *et al.* Gain of function mutations in p53. *Nat. Genet.* **4,** 42–46 (1993).
83. Doyle, B. *et al.* p53 Mutation and loss have different effects on tumourigenesis in a novel mouse model of pleomorphic rhabdomyosarcoma. *J. Pathol.* **222,** 129–137 (2010).
84. Lang, G. A. *et al.* Gain of function of a p53 hot spot mutation in a mouse model of Li-Fraumeni syndrome. *Cell* **119,** 861–872 (2004).
85. Morton, J. P. *et al.* Mutant p53 drives metastasis and overcomes growth arrest/senescence in pancreatic cancer. *Proc. Natl. Acad. Sci.* **107,** 246–251 (2010).
86. Olive, K. P. *et al.* Mutant p53 gain of function in two mouse models of Li-Fraumeni syndrome. *Cell* **119,** 847–860 (2004).
87. Gaiddon, C., Lokshin, M., Ahn, J., Zhang, T. & Prives, C. A Subset of Tumor-Derived Mutant Forms of p53 Down-Regulate p63 and p73 through a Direct Interaction with the p53 Core Domain. *Mol. Cell. Biol.* **21,** 1874–1887 (2001).
88. Strano, S. *et al.* Physical interaction with human tumor-derived p53 mutants inhibits p63 activities. *J. Biol. Chem.* **277,** 18817–18826 (2002).
89. Adorno, M. *et al.* A Mutant-p53/Smad Complex Opposes p63 to Empower TGFβ-Induced Metastasis. *Cell* **137,** 87–98 (2009).
90. Sauer, L., Gitenay, D., Vo, C. & Baron, V. T. Mutant p53 initiates a feedback loop that involves Egr-1/EGF receptor/ERK in prostate cancer cells. *Oncogene* **29,** 2628–2637 (2010).
91. Wang, W., Cheng, B., Miao, L., Me, Y. & Wu, M. Mutant p53-R273H gains new function in sustained activation of EGFR signaling via suppressing miR-27a expression. *Cell Death Dis.* **4,** (2013).
92. Grugan, K. D. *et al.* A common p53 mutation (R175H) activates c-Met receptor tyrosine kinase to enhance tumor cell invasion. *Cancer Biol. Ther.* **14,** 853–859 (2013).
93. Muller, P. A. J. *et al.* Mutant p53 Drives Invasion by Promoting Integrin Recycling. *Cell* **139,** 1327–1341 (2009).
94. Muller, P. A. J. *et al.* Mutant p53 enhances MET trafficking and signalling to drive cell scattering and invasion. *Oncogene* **32,** 1252–65 (2013).
95. Chee, J. L. Y. *et al.* Wild-type and mutant p53 mediate cisplatin resistance through interaction and inhibition of active caspase-9. *Cell Cycle* **12,** 278–288 (2013).
96. Frank, A. K., Pietsch, E. C., Dumont, P., Tao, J. & Murphy, M. E. Wild-type and mutant p53 proteins interact with mitochondrial caspase-3. *Cancer Biol. Ther.* **11,** 740–745 (2011).

97. Morselli, E. *et al.* Mutant p53 protein localized in the cytoplasm inhibits autophagy. *Cell Cycle* **7,** 3056–3061 (2008).

98. Song, H., Hollstein, M. & Xu, Y. p53 gain-of-function cancer mutants induce genetic instability by inactivating ATM. *Nat. Cell Biol.* **9,** 573–580 (2007).

99. Do, P. M. *et al.* Mutant p53 cooperates with ETS2 to promote etoposide resistance. *Genes Dev.* **26,** 830–845 (2012).

100. Freed-Pastor, W. A. *et al.* Mutant p53 disrupts mammary tissue architecture via the mevalonate pathway. *Cell* **148,** 244–258 (2012).

101. Kalo, E. *et al.* Mutant p53R273H attenuates the expression of phase 2 detoxifying enzymes and promotes the survival of cells with high levels of reactive oxygen species. *J Cell Sci* **125,** 5578–5586 (2012).

102. Stambolsky, P. *et al.* Modulation of the Vitamin D3 Response by Cancer-Associated Mutant p53. *Cancer Cell* **17,** 273–285 (2010).

103. Kawamura, T. *et al.* Linking the p53 tumour suppressor pathway to somatic cell reprogramming. *Nature* **460,** 1140–1144 (2009).

104. Marión, R. M. *et al.* A p53-mediated DNA damage response limits reprogramming to ensure iPS cell genomic integrity. *Nature* **460,** 1149–1153 (2009).

105. Sarig, R. *et al.* Mutant p53 facilitates somatic cell reprogramming and augments the malignant potential of reprogrammed cells. *J. Exp. Med.* **207,** 2127–2140 (2010).

106. Yi, L., Lu, C., Hu, W., Sun, Y. & Levine, A. J. Multiple roles of p53-related pathways in somatic cell reprogramming and stem cell differentiation. *Cancer Res.* **72,** 5635–5645 (2012).

107. Olivier, M. *et al.* The clinical value of somatic TP53 gene mutations in 1,794 patients with breast cancer. *Clin. Cancer Res.* **12,** 1157–67 (2006).

108. Petitjean, A., Achatz, M. I. W., Borresen-Dale, A. L., Hainaut, P. & Olivier, M. TP53 mutations in human cancers: functional selection and impact on cancer prognosis and outcomes. *Oncogene* **26,** 2157–2165 (2007).

109. Lehmann, B. D. & Pietenpol, J. A. Targeting mutant p53 in human tumors. *Journal of Clinical Oncology* **30,** 3648–3650 (2012).

110. Maslon, M. M. & Hupp, T. R. Drug discovery and mutant p53. *Trends in Cell Biology* **20,** 542–555 (2010).

111. Wiman, K. G. Pharmacological reactivation of mutant p53: From protein structure to the cancer patient. *Oncogene* **29,** 4245–4252 (2010).

112. Ventura, A. *et al.* Restoration of p53 function leads to tumour regression in vivo. *Nature* **445,** 661–665 (2007).

113. Xue, W. *et al.* Senescence and tumour clearance is triggered by p53 restoration in

murine liver carcinomas. *Nature* **445,** 656–660 (2007).

114. Muller, P. A. J. & Vousden, K. H. Mutant p53 in cancer: New functions and therapeutic opportunities. *Cancer Cell* **25,** 304–317 (2014).
115. Kravchenko, J. E. *et al.* Small-molecule RETRA suppresses mutant p53-bearing cancer cells through a p73-dependent salvage pathway. *Proc. Natl. Acad. Sci.* **105,** 6302–6307 (2008).
116. Bykov, V. J. N. *et al.* Restoration of the tumor suppressor function to mutant p53 by a low-molecular-weight compound. *Nat. Med.* **8,** 282–288 (2002).
117. Demma, M. *et al.* SCH529074, a small molecule activator of mutant p53, which binds p53 DNA Binding Domain (DBD), restores growth-suppressive function to mutant p53 and interrupts HDM2-mediated ubiquitination of wild type p53. *J. Biol. Chem.* **285,** 10198–10212 (2010).
118. Foster, B. A., Coffey, H. A., Morin, M. J. & Rastinejad, F. Pharmacological rescue of mutant p53 conformation and function. *Science (80-.).* **286,** 2507–2510 (1999).
119. Puca, R. *et al.* Restoring wtp53 activity in HIPK2 depleted MCF7 cells by modulating metallothionein and zinc. *Exp. Cell Res.* **315,** 67–75 (2009).
120. Pintus, S. S. *et al.* The substitutions G245C and G245D in the Zn2+-binding pocket of the p53 protein result in differences of conformational flexibility of the DNA-binding domain. in *Journal of Biomolecular Structure and Dynamics* **31,** 78–86 (2013).
121. Boeckler, F. M. *et al.* Targeted rescue of a destabilized mutant of p53 by an in silico screened drug. *Proc. Natl. Acad. Sci. U. S. A.* **105,** 10360–5 (2008).
122. Liu, X. *et al.* Small molecule induced reactivation of mutant p53 in cancer cells. *Nucleic Acids Res.* **41,** 6034–6044 (2013).
123. Ponting, C. P., Oliver, P. L. & Reik, W. Evolution and Functions of Long Noncoding RNAs. *Cell* **136,** 629–641 (2009).
124. Wang, K. C. & Chang, H. Y. Molecular Mechanisms of Long Noncoding RNAs. *Molecular Cell* **43,** 904–914 (2011).
125. Kapranov, P. *et al.* RNA Maps Reveal New and a Possible Classes Pervasive Transcription RNA Function for. *Science (80-.).* **316,** 1486 (2007).
126. Schimmel, P. The emerging complexity of the tRNA world: mammalian tRNAs beyond protein synthesis. *Nat. Rev. Mol. Cell Biol.* (2017). doi:10.1038/nrm.2017.77
127. Pollard, K. S. *et al.* An RNA gene expressed during cortical development evolved rapidly in humans. *Nature* **443,** 167–172 (2006).
128. Doan, R. N. *et al.* Mutations in Human Accelerated Regions Disrupt Cognition and Social Behavior. *Cell* **167,** 341–354.e12 (2016).
129. Griffiths-Jones, S., Saini, H. K., Van Dongen, S. & Enright, A. J. miRBase: Tools for

microRNA genomics. *Nucleic Acids Res.* **36,** (2008).

130. Kozomara, A. & Griffiths-Jones, S. MiRBase: Annotating high confidence microRNAs using deep sequencing data. *Nucleic Acids Res.* **42,** (2014).
131. Kim, V. N., Han, J. & Siomi, M. C. Biogenesis of small RNAs in animals. *Nature Reviews Molecular Cell Biology* **10,** 126–139 (2009).
132. Krol, J., Loedige, I. & Filipowicz, W. The widespread regulation of microRNA biogenesis, function and decay. *Nature Reviews Genetics* **11,** 597–610 (2010).
133. CAI, X. Human microRNAs are processed from capped, polyadenylated transcripts that can also function as mRNAs. *RNA* **10,** 1957–1966 (2004).
134. Lee, Y. *et al.* MicroRNA genes are transcribed by RNA polymerase II. *EMBO J.* **23,** 4051–4060 (2004).
135. Davis-Dusenbery, B. N. & Hata, A. Mechanisms of control of microRNA biogenesis. *Journal of Biochemistry* **148,** 381–392 (2010).
136. Denli, A. M., Tops, B. B. J., Plasterk, R. H. A., Ketting, R. F. & Hannon, G. J. Processing of primary microRNAs by the Microprocessor complex. *Nature* **432,** 231–235 (2004).
137. Gregory, R. I. *et al.* The Microprocessor complex mediates the genesis of microRNAs. *Nature* **432,** 235–240 (2004).
138. Han, J. *et al.* The Drosha-DGCR8 complex in primary microRNA processing. *Genes Dev.* **18,** 3016–3027 (2004).
139. Lee, Y. *et al.* The nuclear RNase III Drosha initiates microRNA processing. *Nature* **425,** 415–419 (2003).
140. BOHNSACK, M. T. Exportin 5 is a RanGTP-dependent dsRNA-binding protein that mediates nuclear export of pre-miRNAs. *RNA* **10,** 185–191 (2004).
141. Lee, Y., Jeon, K., Lee, J. T., Kim, S. & Kim, V. N. MicroRNA maturation: Stepwise processing and subcellular localization. *EMBO J.* **21,** 4663–4670 (2002).
142. Yi, R., Qin, Y., Macara, I. G. & Cullen, B. R. Exportin-5 mediates the nuclear export of pre-microRNAs and short hairpin RNAs. *Genes Dev.* **17,** 3011–3016 (2003).
143. Bernstein, E., Caudy, A. A., Hammond, S. M. & Hannon, G. J. Role for a bidentate ribonuclease in the initiation step of RNA interference. *Nature* **409,** 363–366 (2001).
144. Hutvágner, G. *et al.* A cellular function for the RNA-interference enzyme dicer in the maturation of the let-7 small temporal RNA. *Science (80-.).* **293,** 834–838 (2001).
145. Hammond, S. M., Boettcher, S., Caudy, A. A., Kobayashi, R. & Hannon, G. J. Argonaute2, a link between genetic and biochemical analyses of RNAi. *Science (80-.).* **293,** 1146–1150 (2001).
146. Mourelatos, Z. *et al.* miRNPs: A novel class of ribonucleoproteins containing

numerous microRNAs. *Genes Dev.* **16,** 720–728 (2002).

147. Hayes, J., Peruzzi, P. P. & Lawler, S. MicroRNAs in cancer: Biomarkers, functions and therapy. *Trends in Molecular Medicine* **20,** 460–469 (2014).
148. Du, T. microPrimer: the biogenesis and function of microRNA. *Development* **132,** 4645–4652 (2005).
149. Croce, C. M. Causes and consequences of microRNA dysregulation in cancer. *Nature Reviews Genetics* **10,** 704–714 (2009).
150. Siomi, M. C., Sato, K., Pezic, D. & Aravin, A. A. PIWI-interacting small RNAs: The vanguard of genome defence. *Nature Reviews Molecular Cell Biology* **12,** 246–258 (2011).
151. Lin, H. piRNAs in the germ line. *Science* **316,** 397 (2007).
152. Kazazian, H. H. Mobile Elements: Drivers of Genome Evolution. *Science* **303,** 1626–1632 (2004).
153. Aravin, A. *et al.* A novel class of small RNAs bind to MILI protein in mouse testes. *Nature* **442,** 203–207 (2006).
154. Girard, A., Sachidanandam, R., Hannon, G. J. & Carmell, M. A. A germline-specific class of small RNAs binds mammalian Piwi proteins. *Nature* **442,** 199–202 (2006).
155. Brennecke, J. *et al.* Discrete Small RNA-Generating Loci as Master Regulators of Transposon Activity in Drosophila. *Cell* **128,** 1089–1103 (2007).
156. Vagin, V. V. *et al.* A distinct small RNA pathway silences selfish genetic elements in the germline. *Science (80-.).* **313,** 320–324 (2006).
157. Ishizu, H., Siomi, H. & Siomi, M. C. Biology of Piwi-interacting RNAs: New insights into biogenesis and function inside and outside of germlines. *Genes and Development* **26,** 2361–2373 (2012).
158. Ipsaro, J. J., Haase, A. D., Knott, S. R., Joshua-Tor, L. & Hannon, G. J. The structural biochemistry of Zucchini implicates it as a nuclease in piRNA biogenesis. *Nature* **491,** 279–282 (2012).
159. Nishimasu, H. *et al.* Structure and function of Zucchini endoribonuclease in piRNA biogenesis. *Nature* **491,** 284–287 (2012).
160. Ogawa, Y., Sun, B. K. & Lee, J. T. Intersection of the RNA interference and X-inactivation pathways. *Science (80-.).* **320,** 1336–1341 (2008).
161. Tragante, V., Moore, J. H. & Asselbergs, F. W. The ENCODE project and perspectives on pathways. *Genetic Epidemiology* **38,** 275–280 (2014).
162. Derrien, T. *et al.* The GENCODE v7 catalog of human long noncoding RNAs: Analysis of their gene structure, evolution, and expression. *Genome Res.* **22,** 1775–1789 (2012).
163. Church, D. M. *et al.* Lineage-specific biology revealed by a finished genome assembly

of the mouse. *PLoS Biol.* **7,** (2009).

164. Cabili, M. *et al.* Integrative annotation of human large intergenic noncoding RNAs reveals global properties and specific subclasses. *Genes Dev.* **25,** 1915–1927 (2011).
165. Pang, K. C., Frith, M. C. & Mattick, J. S. Rapid evolution of noncoding RNAs: Lack of conservation does not mean lack of function. *Trends in Genetics* **22,** 1–5 (2006).
166. Wang, J. *et al.* Mouse transcriptome: Neutral evolution of 'non-coding' complementary DNAs. *Nature* **431,** (2004).
167. Consortium, I. H. G. S. Initial sequencing and analysis of the human genome. *Nature* **409,** 860–921 (2001).
168. Venter, J. C. *et al.* The sequence of the human genome. *Science* **291,** 1304–51 (2001).
169. Guttman, M. *et al.* Chromatin signature reveals over a thousand highly conserved large non-coding RNAs in mammals. *Nature* **458,** 223–227 (2009).
170. Arrial, R. T., Togawa, R. C., & Brigido, M. de M. (2009). Screening non-coding RNAs in transcriptomes from neglected species using PORTRAIT: case study of the pathogenic fungus Paracoccidioides brasiliensis. BMC Bioinformatics, 10, 239. doi:10.1186/1471-2105-10-239 *et al.* Extensive and coordinated transcription of noncoding RNAs within cell-cycle promoters. *Nat. Genet.* **43,** 621–629 (2011).
171. Guttman, M. *et al.* Ab initio reconstruction of cell type-specific transcriptomes in mouse reveals the conserved multi-exonic structure of lincRNAs. *Nat. Biotechnol.* **28,** 503–510 (2010).
172. Harrow, J. *et al.* GENCODE: The reference human genome annotation for the ENCODE project. *Genome Res.* **22,** 1760–1774 (2012).
173. Clark, M. B. & Mattick, J. S. Long noncoding RNAs in cell biology. *Seminars in Cell and Developmental Biology* **22,** 366–376 (2011).
174. Martianov, I., Ramadass, A., Serra Barros, A., Chow, N. & Akoulitchev, A. Repression of the human dihydrofolate reductase gene by a non-coding interfering transcript. *Nature* **445,** 666–670 (2007).
175. Rinn, J. L. *et al.* Functional Demarcation of Active and Silent Chromatin Domains in Human HOX Loci by Noncoding RNAs. *Cell* **129,** 1311–1323 (2007).
176. Rintala-Maki, N. D. & Sutherland, L. C. Identification and characterisation of a novel antisense non-coding RNA from the RBM5 gene locus. *Gene* **445,** 7–16 (2009).
177. Tripathi, V. *et al.* The nuclear-retained noncoding RNA MALAT1 regulates alternative splicing by modulating SR splicing factor phosphorylation. *Mol. Cell* **39,** 925–938 (2010).
178. Muddashetty, R. S. *et al.* Poly(A)-binding protein is associated with neuronal BC1 and BC200 ribonucleoprotein particles. *J. Mol. Biol.* **321,** 433–445 (2002).

179. Beltran, M. *et al.* A natural antisense transcript regulates Zeb2/Sip1 gene expression during Snail1-induced epithelial-mesenchymal transition. *Genes Dev.* **22,** 756–769 (2008).

180. Watanabe, Y. & Yamamoto, M. S. pombe mei2+ encodes an RNA-binding protein essential for premeiotic DNA synthesis and meiosis I, which cooperates with a novel RNA species meiRNA. *Cell* **78,** 487–498 (1994).

181. Campalans, A. Enod40, a Short Open Reading Frame-Containing mRNA, Induces Cytoplasmic Localization of a Nuclear RNA Binding Protein in Medicago truncatula. *PLANT CELL ONLINE* **16,** 1047–1059 (2004).

182. Kloc, M. *et al.* Potential structural role of non-coding and coding RNAs in the organization of the cytoskeleton at the vegetal cortex of Xenopus oocytes. *Development* **132,** 3445–57 (2005).

183. Sunwoo, H. *et al.* Men ??/?? nuclear-retained non-coding RNAs are up-regulated upon muscle differentiation and are essential components of paraspeckles. *Genome Res.* **19,** 347–359 (2009).

184. Brockdorff, N. *et al.* Conservation of position and exclusive expression of mouse Xist from the inactive X chromosome. *Nature* **351,** 329–331 (1991).

185. Brown, C. J. *et al.* A gene from the region of the human X inactivation centre is expressed exclusively from the inactive X chromosome. *Nature* **349,** 38–44 (1991).

186. Sur, I. & Taipale, J. Parental imprinting of the mouse H19 gene. *Nat Rev. Cancer* **351,** 153–155 (2016).

187. Ginger, M. R. *et al.* A noncoding RNA is a potential marker of cell fate during mammary gland development. *Proc. Natl. Acad. Sci. U. S. A.* **103,** 5781–5786 (2006).

188. Mourtada-Maarabouni, M., Hedge, V. L., Kirkham, L., Farzaneh, F. & Williams, G. T. Growth arrest in human T-cells is controlled by the non-coding RNA growth-arrest-specific transcript 5 (GAS5). *J. Cell Sci.* **123,** 1181–1181 (2010).

189. Huarte, M. *et al.* A large intergenic noncoding RNA induced by p53 mediates global gene repression in the p53 response. *Cell* **142,** 409–419 (2010).

190. Reeves, M. B., Davies, A. A., McSharry, B. P., Wilkinson, G. W. & Sinclair, J. H. Complex I binding by a virally encoded RNA regulates mitochondria-induced cell death. *Science (80-.).* **316,** 1345–1348 (2007).

191. Sheik Mohamed, J., Gaughwin, P. M., Lim, B., Robson, P. & Lipovich, L. Conserved long noncoding RNAs transcriptionally regulated by Oct4 and Nanog modulate pluripotency in mouse embryonic stem cells. *RNA* **16,** 324–337 (2010).

192. Loewer, S. *et al.* Large intergenic non-coding RNA-RoR modulates reprogramming of human induced pluripotent stem cells. *Nat. Genet.* **42,** 1113–1117 (2010).

193. Shamovsky, I., Ivannikov, M., Kandel, E. S., Gershon, D. & Nudler, E. RNA-mediated response to heat shock in mammalian cells. *Nature* **440,** 556–560 (2006).

194. Espinoza, C. A., Allen, T. A., Hieb, A. R., Kugel, J. F. & Goodrich, J. A. B2 RNA binds directly to RNA polymerase II to repress transcript synthesis. *Nat. Struct. Mol. Biol.* **11,** 822–829 (2004).

195. Ma, L., Bajic, V. B. & Zhang, Z. On the classification of long non-coding RNAs. *RNA Biology* **10,** 924–933 (2013).

196. Khalil, A. M. *et al.* Many human large intergenic noncoding RNAs associate with chromatin-modifying complexes and affect gene expression. *Proc. Natl. Acad. Sci.* **106,** 11667–11672 (2009).

197. Zhao, J. *et al.* Genome-wide Identification of Polycomb-Associated RNAs by RIP-seq. *Mol. Cell* **40,** 939–953 (2010).

198. Brown, C. J. *et al.* The human XIST gene: Analysis of a 17 kb inactive X-specific RNA that contains conserved repeats and is highly localized within the nucleus. *Cell* **71,** 527–542 (1992).

199. Brockdorff, N. *et al.* The product of the mouse Xist gene is a 15 kb inactive X-specific transcript containing no conserved ORF and located in the nucleus. *Cell* **71,** 515–526 (1992).

200. Zhao, J., Sun, B.K., Erwin, J.A., Song, J.J., and Lee, J. T. Polycomb proteins targeted by a short repeat RNA to the mouse X chromosome. *Science (80-.).* **322,** 750–756 (2008).

201. Wang, K. C. *et al.* A long noncoding RNA maintains active chromatin to coordinate homeotic gene expression. *Nature* **472,** 120–126 (2011).

202. Arrial, R. T., Togawa, R. C., & Brigido, M. de M. (2009). Screening non-coding RNAs in transcriptomes from neglected species using PORTRAIT: case study of the pathogenic fungus Paracoccidioides brasiliensis. BMC Bioinformatics, 10, 239. doi:10.1186/1471-2105-10-239 *et al.* Long noncoding RNA as modular scaffold of histone modification complexes. *Science* **329,** 689–693 (2010).

203. Dimitrova, N. *et al.* LincRNA-p21 Activates p21 In cis to Promote Polycomb Target Gene Expression and to Enforce the G1/S Checkpoint. *Mol. Cell* **54,** 777–790 (2014).

204. Hung, T. *et al.* Extensive and coordinated transcription of noncoding RNAs within cell-cycle promoters. in *Nature Genetics* **43,** 621–629 (2011).

205. Kino, M., Hur, D. E., Ichijo, T., Nader, N. & Chrousos, G. P. Noncoding RNA Gas5 Is a Growth Arrest and Starvation- Associated Repressor of the Glucocorticoid Receptor. *Sci. Signal.* **3,** 1–16 (2010).

206. Poliseno, L. *et al.* A coding-independent function of gene and pseudogene mRNAs

regulates tumour biology. *Nature* **465,** 1033–1038 (2010).

207. Clemson, C. M. *et al.* An Architectural Role for a Nuclear Noncoding RNA: NEAT1 RNA Is Essential for the Structure of Paraspeckles. *Mol. Cell* **33,** 717–726 (2009).
208. Yoon, J. H. *et al.* Scaffold function of long non-coding RNA HOTAIR in protein ubiquitination. *Nat. Commun.* **4,** (2013).
209. Hindorff, L. A. *et al.* Potential etiologic and functional implications of genome-wide association loci for human diseases and traits. *Proc. Natl. Acad. Sci.* **106,** 9362–9367 (2009).
210. Bhan, A. & Mandal, S. S. Long noncoding RNAs: emerging stars in gene regulation, epigenetics and human disease. *ChemMedChem* **9,** 1932–1956 (2014).
211. Bhan, A., Soleimani, M. & Mandal, S. S. Long noncoding RNA and cancer: A new paradigm. *Cancer Research* **77,** 3965–3981 (2017).
212. Geng, Y., Xie, S., Li, Q., Ma, J. & Wang, G. Large Intervening Non-Coding RNA HOTAIR is Associated with Hepatocellular Carcinoma Progression. *J. Int. Med. Res.* **39,** 2119–2128 (2011).
213. Kim, K. *et al.* HOTAIR is a negative prognostic factor and exhibits pro-oncogenic activity in pancreatic cancer. *Oncogene* **32,** 1616–1625 (2013).
214. Li, D. *et al.* Long intergenic noncoding RNA HOTAIR is overexpressed and regulates PTEN methylation in laryngeal squamous cell carcinoma. *Am. J. Pathol.* **182,** 64–70 (2013).
215. Nakagawa, T. *et al.* Large noncoding RNA HOTAIR enhances aggressive biological behavior and is associated with short disease-free survival in human non-small cell lung cancer. *Biochem. Biophys. Res. Commun.* **436,** 319–324 (2013).
216. Yang, Z. *et al.* Overexpression of Long Non-coding RNA HOTAIR Predicts Tumor Recurrence in Hepatocellular Carcinoma Patients Following Liver Transplantation. *Ann. Surg. Oncol.* **18,** 1243–1250 (2011).
217. Bhan, A. & Mandal, S. S. LncRNA HOTAIR: A master regulator of chromatin dynamics and cancer. *Biochimica et Biophysica Acta - Reviews on Cancer* **1856,** 151–164 (2015).
218. Bhan, A. *et al.* Antisense transcript long noncoding RNA (lncRNA) HOTAIR is transcriptionally induced by estradiol. *J. Mol. Biol.* **425,** 3707–3722 (2013).
219. Huarte, M. The emerging role of lncRNAs in cancer. *Nature Medicine* **21,** 1253–1261 (2015).
220. Aguilo, F., Zhou, M. M. & Walsh, M. J. Long noncoding RNA, polycomb, and the ghosts haunting INK4b-ARF-INK4a expression. *Cancer Research* **71,** 5365–5369 (2011).
221. Gutschner, T. *et al.* The noncoding RNA MALAT1 is a critical regulator of the

metastasis phenotype of lung cancer cells. *Cancer Res.* **73,** 1180–1189 (2013).

222. Arun, G. *et al.* Differentiation of mammary tumors and reduction in metastasis upon Malat1 lncRNA loss. *Genes Dev.* **30,** 34–51 (2016).
223. Matouk, I. J. *et al.* The H19 non-coding RNA is essential for human tumor growth. *PLoS One* **2,** (2007).
224. Kondo, M. *et al.* Frequent loss of imprinting of the H19 gene is often associated with its overexpression in human lung cancers. *Oncogene* **10,** 1193–8 (1995).
225. Hibi, K. *et al.* Loss of H19 imprinting in esophageal cancer. *Cancer Res.* **56,** 480–482 (1996).
226. Hashimoto, K. *et al.* Loss of H19 imprinting and up-regulation of H19 and SNRPN in a case with malignant mixed Mullerian tumor of the uterus. *Hum. Pathol.* **28,** 862–865 (1997).
227. Cerase, A., Pintacuda, G., Tattermusch, A. & Avner, P. Xist localization and function: New insights from multiple levels. *Genome Biology* **16,** (2015).
228. Huang, K.-C. *et al.* Relationship of XIST expression and responses of ovarian cancer to chemotherapy. *Mol. Cancer Ther.* **1,** 769–76 (2002).
229. Zhang, A., Xu, M. & Mo, Y. Y. Role of the lncRNA-p53 regulatory network in cancer. *Journal of Molecular Cell Biology* **6,** 181–191 (2014).
230. PDQ Adult Treatment Editorial Board, P. A. T. E. *Ovarian Epithelial, Fallopian Tube, and Primary Peritoneal Cancer Treatment (PDQ®): Health Professional Version*. *PDQ Cancer Information Summaries* (2002).
231. American Cancer Society. Cancer Facts & Figures 2016. *Cancer Facts Fig. 2016* 1–9 (2016). doi:10.1097/01.NNR.0000289503.22414.79
232. Feuer EJ, C. K. (eds) H. N. N. A. K. M. G. J. M. D. A. S. K. C. Y. M. R. J. T. Z. M. A. L. D. C. H. National Cancer Institute SEER Cancer Statistics Review 1975-2012. *Natl. Cancer Inst.* **103,** 1975–2012 (2015).
233. Howlader N, Noone AM, Krapcho M, Miller D, Bishop K, Kosary CL, Yu M, Ruhl J, Tatalovich Z, Mariotto A, Lewis DR, Chen HS, Feuer EJ, C. K. (eds). Cancer Statistics Review, 1975-2014 - SEER Statistics. *SEER Cancer Statistics Review, 1975-2014* (2016). Available at: https://seer.cancer.gov/csr/1975_2014/.
234. Allemani, C. *et al.* Global surveillance of cancer survival 1995-2009: analysis of individual data for 25,676,887 patients from 279 population-based registries in 67 countries (CONCORD-2). *Lancet* **385,** 977–1010 (2015).
235. Ledermann, J. A. *et al.* Newly diagnosed and relapsed epithelial ovarian carcinoma: ESMO clinical practice guidelines for diagnosis, treatment and follow-up. *Ann. Oncol.* **24,** (2013).

236. Lengyel, E. Ovarian Cancer Development and Metastasis. *Am. J. Pathol.* **177,** 1053–1064 (2010).

237. Fathalla, M. F. INCESSANT OVULATION-A FACTOR IN OVARIAN NEOPLASIA ? *The Lancet* **298,** 163 (1971).

238. Choi, J. H., Wong, A. S. T., Huang, H. F. & Leung, P. C. K. Gonadotropins and ovarian cancer. *Endocrine Reviews* **28,** 440–461 (2007).

239. Calle, E. E., Rodriguez, C., Walker-Thurmond, K. & Thun, M. J. Overweight, Obesity, and Mortality from Cancer in a Prospectively Studied Cohort of U.S. Adults. *N. Engl. J. Med.* **348,** 1625–1638 (2003).

240. Schouten, L. J. Height, Weight, Weight Change, and Ovarian Cancer Risk in the Netherlands Cohort Study on Diet and Cancer. *Am. J. Epidemiol.* **157,** 424–433 (2003).

241. Engeland, A., Tretli, S. & Bjorge, T. Height, Body Mass Index, and Ovarian Cancer: A Follow-Up of 1.1 Million Norwegian Women. *JNCI J. Natl. Cancer Inst.* **95,** 1244–1248 (2003).

242. Poole, E. M. *et al.* Endometriosis and risk of ovarian and endometrial cancers in a large prospective cohort of U.S. nurses. *Cancer Causes Control* **28,** 437–445 (2017).

243. Pearce, C. L. *et al.* Association between endometriosis and risk of histological subtypes of ovarian cancer: A pooled analysis of case-control studies. *Lancet Oncol.* **13,** 385–394 (2012).

244. Mogensen, J. B., Kjær, S. K., Mellemkjær, L. & Jensen, A. Endometriosis and risks for ovarian, endometrial and breast cancers: A nationwide cohort study. *Gynecol. Oncol.* **143,** 87–92 (2016).

245. Lacey, J. V. *et al.* Menopausal hormone therapy and ovarian cancer risk in the National Institutes of Health-AARP Diet and Health Study Cohort. *J. Natl. Cancer Inst.* **98,** 1397–1405 (2006).

246. Trabert, B. *et al.* Ovarian cancer and menopausal hormone therapy in the NIH-AARP diet and health study. *Br. J. Cancer* **107,** 1181–1187 (2012).

247. Lahmann, P. H. *et al.* Anthropometric measures and epithelial ovarian cancer risk in the European Prospective Investigation into Cancer and Nutrition. *Int. J. Cancer* **126,** 2404–2415 (2010).

248. Huncharek, M., Geschwind, J. F. & Kupelnick, B. Perineal application of cosmetic talc and risk of invasive epithelial ovarian cancer: A meta-analysis of 11, 933 subjects from sixteen observational studies. *Anticancer Res.* **23,** 1955–1960 (2003).

249. Terry, K. L. *et al.* Genital powder use and risk of ovarian cancer: A pooled analysis of 8,525 cases and 9,859 controls. *Cancer Prev. Res.* **6,** 811–821 (2013).

250. Kar SP, Berchuck A, Gayther SA, Goode EL, Moysich KB, Pearce CL, Ramus SJ,

Schildkraut JM, Sellers TA, P. P. Common Genetic Variation and Susceptibility to Ovarian Cancer: Current Insights and Future Directions. *Cancer Epidemiol Biomarkers Prev* (2017).

251. Alsop, K. *et al.* BRCA mutation frequency and patterns of treatment response in BRCA mutation-positive women with ovarian cancer: a report from the Australian Ovarian Cancer Study Group. *J. Clin. Oncol.* **30,** 2654–63 (2012).
252. Ramus, S. J. *et al.* Germline mutations in the BRIP1, BARD1, PALB2, and NBN genes in women with ovarian cancer. *J. Natl. Cancer Inst.* **107,** (2015).
253. Pelttari, L. M. *et al.* RAD51C is a susceptibility gene for ovarian cancer. *Hum. Mol. Genet.* **20,** 3278–3288 (2011).
254. Loveday, C. *et al.* Germline mutations in RAD51D confer susceptibility to ovarian cancer. *Nat. Genet.* **43,** 879–882 (2011).
255. Prat, J. Ovarian carcinomas: Five distinct diseases with different origins, genetic alterations, and clinicopathological features. *Virchows Archiv* **460,** 237–249 (2012).
256. PDQ Cancer Genetics Editorial Board. Genetics of Breast and Gynecologic Cancers (PDQ®): Health Professional Version. *PDQ Cancer Inf. Summ.* 1–49 (2002). doi:http://www.cancer.gov/types/breast/hp/breast-ovarian-genetics-pdq#section/_88
257. Wiegand, K. C. *et al. ARID1A* Mutations in Endometriosis-Associated Ovarian Carcinomas. *N. Engl. J. Med.* **363,** 1532–1543 (2010).
258. Harrison, M. L., Jameson, C. & Gore, M. E. Mucinous ovarian cancer. *International Journal of Gynecological Cancer* **18,** 209–214 (2008).
259. Vang, R., Shih, I.-M. & Kurman, R. J. Ovarian low-grade and high-grade serous carcinoma: pathogenesis, clinicopathologic and molecular biologic features, and diagnostic problems. *Adv. Anat. Pathol.* **16,** 267–82 (2009).
260. Bonome, T. *et al.* Expression profiling of serous low malignant potential, low-grade, and high-grade tumors of the ovary. *Cancer Res.* **65,** 10602–10612 (2005).
261. Diaz-Padilla, I. *et al.* Ovarian low-grade serous carcinoma: A comprehensive update. *Gynecologic Oncology* **126,** 279–285 (2012).
262. Schmeler, K. M. *et al.* Neoadjuvant chemotherapy for low-grade serous carcinoma of the ovary or peritoneum. *Gynecol. Oncol.* **108,** 510–514 (2008).
263. Tothill, R. W. *et al.* Novel molecular subtypes of serous and endometrioid ovarian cancer linked to clinical outcome. *Clin. Cancer Res.* **14,** 5198–5208 (2008).
264. Dubeau, L. & Drapkin, R. Coming into focus: The nonovarian origins of ovarian cancer. *Ann. Oncol.* **24,** (2013).
265. Kurman, R. J. & Shih, I. M. The origin and pathogenesis of epithelial ovarian cancer:

A proposed unifying theory. *Am. J. Surg. Pathol.* **34,** 433–443 (2010).

266. Vang, R., Shih, I. M. & Kurman, R. J. Fallopian tube precursors of ovarian low- and high-grade serous neoplasms. *Histopathology* **62,** 44–58 (2013).
267. Carlson, J. W. *et al.* Serous tubal intraepithelial carcinoma: Its potential role in primary peritoneal serous carcinoma and serous cancer prevention. *J. Clin. Oncol.* **26,** 4160–4165 (2008).
268. Labidi-Galy, S. I. *et al.* High grade serous ovarian carcinomas originate in the fallopian tube. *Nat. Commun.* **8,** (2017).
269. McCluggage, W. G. Morphological subtypes of ovarian carcinoma: a review with emphasis on new developments and pathogenesis. *Pathology* **43,** 420–432 (2011).
270. Kurman, R. J. & Shih, I. M. The dualistic model of ovarian carcinogenesis revisited, revised, and expanded. *Am. J. Pathol.* **186,** 733–747 (2016).
271. Gershenson, D. M. *et al.* Clinical behavior of stage II-IV low-grade serous carcinoma of the ovary. *Obstet. Gynecol.* **108,** 361–368 (2006).
272. Kohler, M. F. *et al.* Spectrum of mutation and frequency of allelic deletion of the p53 gene in ovarian cancer. *J. Natl. Cancer Inst.* **85,** 1513–1519 (1993).
273. Singer, G. *et al.* Patterns of p53 mutations separate ovarian serous borderline tumors and low- and high-grade carcinomas and provide support for a new model of ovarian carcinogenesis: A mutational analysis with immunohistochemical correlation. *Am. J. Surg. Pathol.* **29,** 218–224 (2005).
274. Milner, B. J. *et al.* p53 Mutation Is a Common Genetic Event in Ovarian Carcinoma. *Cancer Res.* **53,** 2128–2132 (1993).
275. Bell, D. *et al.* Integrated genomic analyses of ovarian carcinoma. *Nature* **474,** 609–615 (2011).
276. Cavallaro, U. & Christofori, G. Cell adhesion and signalling by cadherins and Ig-CAMs in cancer. *Nat. Rev. Cancer* **4,** 118–132 (2004).
277. Huber, M. A., Kraut, N. & Beug, H. Molecular requirements for epithelial-mesenchymal transition during tumor progression. *Current Opinion in Cell Biology* **17,** 548–558 (2005).
278. Veatch, A. L., Carson, L. F. & Ramakrishnan, S. Differential expression of the cell???cell adhesion molecule E???cadherin in ascites and solid human ovarian tumor cells. *Int. J. Cancer* **58,** 393–399 (1994).
279. Daraï, E. *et al.* Expression of cadherins in benign, borderline, and malignant ovarian epithelial tumors: A clinicopathologic study of 60 cases. *Hum. Pathol.* **28,** 922–928 (1997).
280. Ahmed, N., Thompson, E. W. & Quinn, M. A. Epithelial-mesenchymal

interconversions in normal ovarian surface epithelium and ovarian carcinomas: An exception to the norm. *Journal of Cellular Physiology* **213,** 581–588 (2007).

281. Hudson, L. G., Zeineldin, R. & Stack, M. S. Phenotypic plasticity of neoplastic ovarian epithelium: Unique cadherin profiles in tumor progression. *Clinical and Experimental Metastasis* **25,** 643–655 (2008).
282. Patel, I. S., Madan, P., Getsios, S., Bertrand, M. A. & MacCalman, C. D. Cadherin switching in ovarian cancer progression. *Int. J. Cancer* **106,** 172–177 (2003).
283. Imai, T. *et al.* Hypoxia attenuates the expression of E-cadherin via up-regulation of SNAIL in ovarian carcinoma cells. *Am. J. Pathol.* **163,** 1437–1447 (2003).
284. Symowicz, J. *et al.* Engagement of collagen-binding integrins promotes matrix metalloproteinase-9-dependent E-cadherin ectodomain shedding in ovarian carcinoma cells. *Cancer Res.* **67,** 2030–2039 (2007).
285. Burleson, K. M., Hansen, L. K. & Skubitz, A. P. N. Ovarian carcinoma spheroids disaggregate on type I collagen and invade live human mesothelial cell monolayers. *Clin. Exp. Metastasis* **21,** 685–697 (2005).
286. Sawada, K. *et al.* c-Met overexpression is a prognostic factor in ovarian cancer and an effective target for inhibition of peritoneal dissemination and invasion. *Cancer Res.* **67,** 1670–1679 (2007).
287. Witz CA, Montoya-Rodriguez I, Cho S, Centonze V, Bonewald L, S. R. Composition of the extracellular matrix of the peritoneum. *J Soc Gynecol Investig* **8,** 299–304 (2001).
288. Kenny, H. A., Krausz, T., Yamada, S. D. & Lengyel, E. Use of a novel 3D culture model to elucidate the role of mesothelial cells, fibroblasts and extra-cellular matrices on adhesion and invasion of ovarian cancer cells to the omentum. *Int. J. Cancer* **121,** 1463–1472 (2007).
289. Daya, D, McCaughy, W. Pathology of the peritoneum: a review of selected topics. *Semin Diagn Pathol* **8,** 277–289 (1991).
290. Cannistra, S. A. *et al.* Binding of Ovarian Cancer Cells to Peritoneal Mesothelium in Vitro Is Partly Mediated by CD44H. *Cancer Res.* **53,** 3830–3838 (1993).
291. Kenny, H. A., Kaur, S., Coussens, L. M. & Lengyel, E. The initial steps of ovarian cancer cell metastasis are mediated by MMP-2 cleavage of vitronectin and fibronectin. *J. Clin. Invest.* **118,** 1367–1379 (2008).
292. Strobel, T. & Cannistra, S. A. β1-integrins partly mediate binding of ovarian cancer cells to peritoneal mesothelium in vitro. *Gynecol. Oncol.* **73,** 362–367 (1999).
293. Cannistra, S. A., Ottensmeier, C., Niloff, J., Orta, B. & DiCarlo, J. Expression and function of beta 1 and alpha v beta 3 integrins in ovarian cancer. *Gynecologic oncology* **58,** 216–25 (1995).

294. Lössner, D., Abou-Ajram, C., Benge, A. & Reuning, U. Integrin alphavbeta3 mediates upregulation of epidermal growth-factor receptor expression and activity in human ovarian cancer cells. *Int. J. Biochem. Cell Biol.* **40,** 2746–61 (2008).

295. Kaur, S. *et al.* {Beta}3-Integrin Expression on Tumor Cells Inhibits Tumor Progression, Reduces Metastasis, and Is Associated With a Favorable Prognosis in Patients With Ovarian Cancer. *Am. J. Pathol.* **175,** 2184–96 (2009).

296. Kenny, H. A. & Lengyel, E. MMP-2 functions as an early response protein in ovarian cancer metastasis. *Cell Cycle* **8,** 683–688 (2009).

297. Kenny, H. A. *et al.* Mesothelial cells promote early Ovarian cancer metastasis through fibronectin secretion. *J. Clin. Invest.* **124,** 4614–4628 (2014).

298. Freedman, R. S., Deavers, M., Liu, J. & Wang, E. Peritoneal inflammation - A microenvironment for epithelial ovarian cancer (EOC). *Journal of Translational Medicine* **2,** (2004).

299. Adib, T. R. *et al.* Predicting biomarkers for ovarian cancer using gene-expression microarrays. *Br. J. Cancer* **90,** 686–692 (2004).

300. Hibbs, K. *et al.* Differential gene expression in ovarian carcinoma: identification of potential biomarkers. *Am. J. Pathol.* **165,** 397–414 (2004).

301. Israeli, O. *et al.* Genomic analyses of primary and metastatic serous epithelial ovarian cancer. *Cancer Genet. Cytogenet.* **154,** 16–21 (2004).

302. Haverty, P. M., Hon, L. S., Kaminker, J. S., Chant, J. & Zhang, Z. High-resolution analysis of copy number alterations and associated expression changes in ovarian tumors. *BMC Med Genomics* **2,** 21 (2009).

303. American Cancer Society. Cancer Facts and Figures 2017. *Genes Dev.* **21,** 2525–2538 (2017).

304. PDQ Adult Treatment Editorial Board, P. A. T. E. *Breast Cancer Treatment (PDQ®): Health Professional Version*. *PDQ Cancer Information Summaries* (2002).

305. Autier, P. *et al.* Disparities in breast cancer mortality trends between 30 European countries: Retrospective trend analysis of WHO mortality database. *BMJ* **341,** 335 (2010).

306. Senkus, E. *et al.* Primary breast cancer: ESMO Clinical Practice Guidelines for diagnosis, treatment and follow-up. *Ann. Oncol.* **26,** v8–v30 (2015).

307. American Cancer Society. *Breast Cancer Facts & Figures 2017-2018*. (2017).

308. McTiernan, A. Behavioral risk factors in breast cancer: Can risk be modified? *Oncologist* **8,** 326–334 (2003).

309. Tamimi, R. M. *et al.* Population attributable risk of modifiable and nonmodifiable breast cancer risk factors in postmenopausal breast cancer. *Am. J. Epidemiol.* **184,** 884–

893 (2016).

310. Colditz, G. A., Kaphingst, K. A., Hankinson, S. E. & Rosner, B. Family history and risk of breast cancer: Nurses' health study. *Breast Cancer Res. Treat.* **133,** 1097–1104 (2012).

311. Collaborative Group on Hormonal Factors in Breast Cancer. Familial breast cancer: collaborative reanalysis of individual data from 52 epidemiological studies including 58,209 women with breast cancer and 101,986 women without the disease. *Lancet (London, England)* **358,** 1389–99 (2001).

312. Goodwin, P. J. *et al.* Breast cancer prognosis in BRCA1 and BRCA2 mutation carriers: an International Prospective Breast Cancer Family Registry population-based cohort study. *J. Clin. Oncol.* **30,** 19–26 (2012).

313. Mavaddat, N. *et al.* Pathology of breast and ovarian cancers among BRCA1 and BRCA2 mutation carriers: Results from the consortium of investigators of modifiers of BRCA1/2 (CIMBA). *Cancer Epidemiol. Biomarkers Prev.* **21,** 134–147 (2012).

314. Blackwood, M. A. & Weber, B. L. BRCA1 and BRCA2: from molecular genetics to clinical medicine. *J. Clin. Oncol.* **16,** 1969–77 (1998).

315. Chen, S. & Parmigiani, G. Meta-analysis of BRCA1 and BRCA2 penetrance. *J. Clin. Oncol.* **25,** 1329–1333 (2007).

316. Viale, G. The current state of breast cancer classification. *Ann. Oncol.* **23,** (2012).

317. Ellis, I. ., Schnitt, S. J., Bussalati, G. & Tavassoli, F. . CHAPTER 1 WHO histological classification of tumours of the breast. *Pathol. Genet. Breast Female Genit. Organs* 432 (2003).

318. Malhotra, G. K., Zhao, X., Band, H. & Band, V. Histological, molecular and functional subtypes of breast cancers. *Cancer Biol. Ther.* **10,** 955–60 (2010).

319. Allred, D. C. Ductal carcinoma in situ: Terminology, classification, and natural history. *J. Natl. Cancer Inst. - Monogr.* 134–138 (2010). doi:10.1093/jncimonographs/lgq035

320. Erbas, B., Provenzano, E., Armes, J. & Gertig, D. The natural history of ductal carcinoma in situ of the breast: A review. *Breast Cancer Research and Treatment* **97,** 135–144 (2006).

321. Li, C. I., Uribe, D. J. & Daling, J. R. Clinical characteristics of different histologic types of breast cancer. *Br. J. Cancer* **93,** 1046–1052 (2005).

322. Shikha Bose, Yunn-Yi Chen, James L. Connolly, Monica E. de Baca, Patrick L. Fitzgibbons, Daniel F. Hayes, Kalisha A. Hill, Celina Kleer, Frances P. O'Malley, David L. Page, Barbara L. Smith, Lee K. Tan, Donald L. Weaver, Eric Winer, J. F. S. Protocol for the Examination of Specimens from Patients with Carcinoma of the Vulva Protocol applies to all invasive carcinomas of the vulva . *Cap* 1–14 (2012).

323. Gerdes, J., Schwab, U., Lemke, H. & Stein, H. Production of a mouse monoclonal antibody reactive with a human nuclear antigen associated with cell proliferation. *Int J Cancer* **31,** 13–20 (1983).

324. Goldhirsch, A. *et al.* Thresholds for therapies: Highlights of the St Gallen international expert consensus on the primary therapy of early breast cancer 2009. in *Annals of Oncology* **20,** 1319–1329 (2009).

325. Perou, C. M. & Borresen-Dale, A. L. Systems biology and genomics of breast cancer. *Cold Spring Harb. Perspect. Biol.* **3,** 1–17 (2011).

326. Park, S. Y. *et al.* Heterogeneity for stem cell-related markers according to tumor subtype and histologic stage in breast cancer. *Clin. Cancer Res.* **16,** 876–887 (2010).

327. Bianchini, G., Balko, J. M., Mayer, I. A., Sanders, M. E. & Gianni, L. Triple-negative breast cancer: Challenges and opportunities of a heterogeneous disease. *Nature Reviews Clinical Oncology* **13,** 674–690 (2016).

328. Perou, C. M. *et al.* Molecular portraits of human breast tumours. *Nature* **406,** 747–752 (2000).

329. Sorlie, T. *et al.* Gene expression patterns of breast carcinomas distinguish tumor subclasses with clinical implications. *Proc. Natl. Acad. Sci. U. S. A.* **98,** 10869–10874 (2001).

330. Sotiriou, C. *et al.* Breast cancer classification and prognosis based on gene expression profiles from a population-based study. *Proc. Natl. Acad. Sci. U. S. A.* **100,** 10393–10398 (2003).

331. Brenton, J. D., Carey, L. A., Ahmed, A. & Caldas, C. Molecular classification and molecular forecasting of breast cancer: Ready for clinical application? *Journal of Clinical Oncology* **23,** 7350–7360 (2005).

332. Rouzier R, Anderson K, Hess KR, et al. *Basal and luminal types of breast cancer defined by gene expression patterns respond differently to neoadjuvant chemotherapy. San Antonio Breast Cancer Symposium. San Antonio, TX.* (2004).

333. Blows, F. M. *et al.* Subtyping of breast cancer by immunohistochemistry to investigate a relationship between subtype and short and long term survival: A collaborative analysis of data for 10,159 cases from 12 studies. *PLoS Med.* **7,** (2010).

334. Haque, R. *et al.* Impact of breast cancer subtypes and treatment on survival: an analysis spanning two decades. *Cancer Epidemiol. Biomarkers Prev.* **21,** 1848–55 (2012).

335. Sorlie, T. *et al.* Repeated observation of breast tumor subtypes in independent gene expression data sets. *Proc. Natl. Acad. Sci.* **100,** 8418–8423 (2003).

336. Bernard, P. S. *et al.* Supervised risk predictor of breast cancer based on intrinsic subtypes. *J. Clin. Oncol.* **27,** 1160–1167 (2009).

337. Scully, O. J., Bay, B.-H., Yip, G. & Yu, Y. Breast cancer metastasis. *Cancer Genomics Proteomics* **9,** 311–20 (2012).

338. Valastyan, S. & Weinberg, R. A. Tumor metastasis: Molecular insights and evolving paradigms. *Cell* **147,** 275–292 (2011).

339. Li, D.-M. & Feng, Y.-M. Signaling mechanism of cell adhesion molecules in breast cancer metastasis: potential therapeutic targets. *Breast Cancer Res. Treat.* **128,** 7–21 (2011).

340. Wendt, M. K., Taylor, M. A., Schiemann, B. J. & Schiemann, W. P. Down-regulation of epithelial cadherin is required to initiate metastatic outgrowth of breast cancer. *Mol. Biol. Cell* **22,** 2423–2435 (2011).

341. Kotb, A. M., Hierholzer, A. & Kemler, R. Replacement of E-cadherin by N-cadherin in the mammary gland leads to fibrocystic changes and tumor formation. *Breast Cancer Res.* **13,** (2011).

342. Bonnomet, A. *et al.* Epithelial-to-mesenchymal transitions and circulating tumor cells. *Journal of Mammary Gland Biology and Neoplasia* **15,** 261–273 (2010).

343. Ota, I., Li, X. Y., Hu, Y. & Weiss, S. J. Induction of a MT1-MMP and MT2-MMP-dependent basement membrane transmigration program in cancer cells by Snail1. *Proc. Natl. Acad. Sci. U. S. A.* **106,** 20318–20323 (2009).

344. Mego, M., Mani, S. A. & Cristofanilli, M. Molecular mechanisms of metastasis in breast cancer-clinical applications. *Nature Reviews Clinical Oncology* **7,** 693–701 (2010).

345. Giampieri, S. *et al.* Localized and reversible TGFbeta signalling switches breast cancer cells from cohesive to single cell motility. *Nat Cell Biol* **11,** 1287–1296 (2009).

346. Carmeliet, P. & Jain, R. K. Principles and mechanisms of vessel normalization for cancer and other angiogenic diseases. *Nature Reviews Drug Discovery* **10,** 417–427 (2011).

347. Nagrath, S. *et al.* Isolation of rare circulating tumour cells in cancer patients by microchip technology. *Nature* **450,** 1235–1239 (2007).

348. Pantel, K., Brakenhoff, R. H. & Brandt, B. Detection, clinical relevance and specific biological properties of disseminating tumour cells. *Nature Reviews Cancer* **8,** 329–340 (2008).

349. Guo, W. & Giancotti, F. G. Integrin signalling during tumour progression. *Nature Reviews Molecular Cell Biology* **5,** 816–826 (2004).

350. Leber, M. F. & Efferth, T. Molecular principles of cancer invasion and metastasis (Review). *International Journal of Oncology* **34,** 881–895 (2009).

351. Wirtz, D., Konstantopoulos, K. & Searson, P. C. The physics of cancer: The role of physical interactions and mechanical forces in metastasis. *Nature Reviews Cancer* **11,** 512–522 (2011).

352. Fidler, I. J. The pathogenesis of cancer metastasis: The 'seed and soil' hypothesis revisited. *Nature Reviews Cancer* **3,** 453–458 (2003).

353. Al-Mehdi, A. B. *et al.* Intravascular origin of metastasis from the proliferation of endothelium-attached tumor cells: A new model for metastasis. *Nat. Med.* **6,** 100–102 (2000).

354. Davidowitz, R. A., Iwanicki, M. P. & Brugge, J. S. In vitro Mesothelial Clearance Assay that Models the Early Steps of Ovarian Cancer Metastasis. *J. Vis. Exp.* 1–7 (2012). doi:10.3791/3888

355. Liu, F., Zhou, X., Cui, F. & Jia, D. Synthesis and properties of poly(hydroxyethyl methacrylate) hydrogel for IOL materials. *Sheng Wu Yi Xue Gong Cheng Xue Za Zhi* **24,** 595–598 (2007).

356. Schneider, C. a, Rasband, W. S. & Eliceiri, K. W. NIH Image to ImageJ: 25 years of image analysis. *Nat. Methods* **9,** 671–675 (2012).

357. Untergasser, A. *et al.* Primer3Plus, an enhanced web interface to Primer3. *Nucleic Acids Res.* **35,** (2007).

358. Domcke, S., Sinha, R., Levine, D. a, Sander, C. & Schultz, N. Evaluating cell lines as tumour models by comparison of genomic profiles. *Nat. Commun.* **4,** 2126 (2013).

359. Di Palma, T., Lucci, V., de Cristofaro, T., Filippone, M. G. & Zannini, M. A role for PAX8 in the tumorigenic phenotype of ovarian cancer cells. *BMC Cancer* **14,** 292 (2014).

360. Davidowitz, R. A. *et al.* Mesenchymal gene program-expressing ovarian cancer spheroids exhibit enhanced mesothelial clearance. *J. Clin. Invest.* **124,** 2611–2625 (2014).

361. Iwanicki, M. P. *et al.* Ovarian cancer spheroids use myosin-generated force to clear the mesothelium. *Cancer Discov.* **1,** 144–157 (2011).

362. Neve, R. M. *et al.* A collection of breast cancer cell lines for the study of functionally distinct cancer subtypes. *Cancer Cell* **10,** 515–527 (2006).

363. Marchese, F. P. & Huarte, M. Long non-coding RNAs and chromatin modifiers: Their place in the epigenetic code. *Epigenetics* **9,** 21–26 (2014).

364. Bolger, A. M., Lohse, M. & Usadel, B. Trimmomatic: A flexible trimmer for Illumina sequence data. *Bioinformatics* **30,** 2114–2120 (2014).

365. Patro, R., Duggal, G., Love, M. I., Irizarry, R. A. & Kingsford, C. Salmon provides fast and bias-aware quantification of transcript expression. *Nature Methods* (2017). doi:10.1038/nmeth.4197

366. Robinson, M. D., McCarthy, D. J. & Smyth, G. K. edgeR: a Bioconductor package for differential expression analysis of digital gene expression data. *Bioinformatics* **26,** 139–40 (2010).

367. Melo, C. A. *et al.* ERNAs Are Required for p53-Dependent Enhancer Activity and Gene Transcription. *Mol. Cell* **49,** 524–535 (2013).

368. Kim, D., Langmead, B. & Salzberg, S. L. HISAT: A fast spliced aligner with low memory requirements. *Nat. Methods* **12,** 357–360 (2015).

369. Liao, Y., Smyth, G. K. & Shi, W. The Subread aligner: Fast, accurate and scalable read mapping by seed-and-vote. *Nucleic Acids Res.* **41,** (2013).

370. Love, M. I., Huber, W. & Anders, S. Moderated estimation of fold change and dispersion for RNA-seq data with DESeq2. *Genome Biol.* **15,** 550 (2014).

371. Bouaoun, L. *et al.* TP53 Variations in Human Cancers: New Lessons from the IARC TP53 Database and Genomics Data. *Hum. Mutat.* **37,** 865–876 (2016).

372. Iwanicki, M. P. *et al.* Mutant p53 regulates ovarian cancer transformed phenotypes through autocrine matrix deposition. *JCI Insight* **1,** 1–20 (2016).

373. Liu, H. *et al.* Long non-coding RNAs as prognostic markers in human breast cancer. *Oncotarget* **7,** 20584 (2016).

374. Emmrich, S. *et al.* LincRNAs MONC and MIR100HG act as oncogenes in acute megakaryoblastic leukemia. *Mol. Cancer* **13,** (2014).

375. Shang, C. *et al.* Characterization of long non-coding RNA expression profiles in lymph node metastasis of early-stage cervical cancer. *Oncol. Rep.* **35,** 3185–3197 (2016).

376. Chen, D. *et al.* miR-100 Induces Epithelial-Mesenchymal Transition but Suppresses Tumorigenesis, Migration and Invasion. *PLoS Genet.* **10,** (2014).

377. Lu, Y. *et al.* LncRNA MIR100HG-derived miR-100 and miR-125b mediate cetuximab resistance via Wnt/β-catenin signaling. *Nat. Med.* **23,** 1331–1341 (2017).

378. Pruszko, M. *et al.* The mutant p53-ID4 complex controls VEGFA isoforms by recruiting lncRNA MALAT1. *EMBO Rep.* **18,** 1331–1351 (2017).